LATVIJAS UNIVERSITĀTE

FOTONIKA-LV

LATVIJAS UNIVERISTĀTES NACIONĀLĀ ZINĀTNES PLATFORMA

The 4th International Conference

Quantum Optics and Photonics 2021

organised by the
ERA Chair Project and NSP FOTONIKA-LV of the University of Latvia

Riga, 22–23 April 2021

BOOK OF ABSTRACTS

LATVIJAS UNIVERSITĀTE

FOTONIKA-LV
LATVIJAS UNIVERISTĀTES NACIONĀLĀ ZINĀTNES PLATFORMA

The 4th International Conference

Quantum Optics and Photonics 2021

Riga, 22–23 April 2021

BOOK OF ABSTRACTS

Riga, 2021

The 4th International Conference "Quantum Optics and Photonics 2021", 22–23 April 2021, Riga, University of Latvia. Book of Abstracts. P. 104.

Organised by the ERA Chair Project and NSP FOTONIKA-LV of the University of Latvia

The conference was supported by ERDF project No. 1.1.1.5/19/A/003 "The Development of Quantum Optics and Photonics at the University of Latvia"

The Scientific Committee of the Conference

Rashid A. Ganeev – Conference Chair
Aigars Atvars – Coordinator of the ERAChair project
Arnolds Ūbelis – Scientific secretary of the NSP FOTONIKA-LV

The Secretariat of the Conference

Dina Bērziņa – Head of the Secretariat of the Conference

Editors

Dina Bērziņa, Rashid A. Ganeev, Ojārs Balcers

https://doi.org/10.22364/qoph.ul.2021
ISBN 978-9934-18-707-0
ISBN 978-9934-18-708-7 (PDF)

Contents

PLENARY SESSIONS

THEMATIC SESSIONS

POSTER SESSIONS

ADDITIONAL CONTRIBUTIONS

AUTHOR INDEX

Plenary Sessions

NSP FOTONIKA-LV on the Upwards Track

Arnolds Ūbelis

National Science Platform FOTONIKA-LV, University of Latvia, Latvia
arnolds.ubelis@lu.lv

The Association of Research Institutes of the University, FOTONIKA-LV, formed on 24 April 2010 was designated the National Science Platform FOTONIKA-LV in quantum sciences, space sciences and related technologies by the decree of the University of Latvia No. 1/215 on 18 June 2018. In early spring, just 11 years ago, the directors of three institutes signed an agreement unique in the history of Latvian science, to create a framework where research communities while continuing to keep responsibility in relevant areas on an historically based national scale, joined forces to undertake larger cross-disciplinary research projects under the umbrella of photonics – the driving technology of the 21st century. FOTONIKA-LV received a special notice in the report of international evaluators of Latvian science led by the TECHNOPOLIS group:1 "In April 2010, three institutions of the University of Latvia (Atomic Physics and Spectroscopy, Astronomy and Geodesy and Geoinformatics) established the association FOTONIKA-LV with the aim of taking responsibility for sustainable advancement in the sector of photonics in Latvia. The association submitted an ambitious FP7 project of basic and applied research in the traditional and innovative fields of photonics: REGPOT-2011-1 which was eventually granted € 3.8 million. Other laboratories should follow this example".

Seven years have passed since the report was published, but the NSP FOTONIKA-LV is still a unique phenomenon in the research landscape of Latvia, is open for new partnerships and is prepared to expand across the borders of the University of Latvia.

NSP FOTONIKA-LV face problems typical to the whole research community in Latvia, precisely highlighted in the already cited TECHNOPOLIS report from 2014:

- an acute shortage of institutional funding (see page #27[2]) is also the case in 2021;
- evidence shows that the *low political priority of innovation and research*[3] in Latvia is going to be a problem for years to come.

Nevertheless, NSP FOTONIKA-LV in 2021 is on a difficult, but convincingly upward, promising track, scaling up fundamental and applied research activities and cooperation with industry on a national level, inside the European Research Area and worldwide.

The foundation of the Association FOTONIKA-LV followed by the NSP FOTONIKA-LV, evidently, was a strategically decisive step and structural change, granting survival of the national research community within the frame of photonics despite exclusively

---

1 Arnold, E., Knee, P., Angelis, J., Giarraca, F., Griniece, E., Jávorka, Z., Reid, A. (2014). Latvia – Innovation System Review and Research Assessment Exercise: Final Report. TECHNOPOLIS, 20 April. DOI 10.13140/RG.2.2.21960.52489. https://www.researchgate.net/publication/312593088_Latvia_Innovation_System_Review_and_Research_Assessment_Exercise

2 Only 17% of research funding is institutional (ERAWATCH Country Report, 2011), making Latvia's one of the most highly 'contested' systems in the world. While there is no clear international benchmark for what the proportion of institutional funding should be, there is some consensus that 50% is the minimal viable level. The Finnish Research and Innovation Council recently observed that the share of competitive funding in the university research system has recently approached that value and that to do any more would be dangerous, citation from page 27.

3 The difficult financial climate, short-term planning within the state, insufficient administrative capacity and the low political priority of innovation and research and a heavily bureaucratic tradition all make it hard to implement research and innovation policy in Latvia, citation from page 38.

unfavourable context to RTD and innovation policy in Latvia. The idea was inherited in the outstanding achievements of researchers and the collective intellectual capital of the laboratories and observatories currently forming NSP FOTONIKA-LV at the University since the early 1960s in the following fields:

- Quantum optics, laser spectroscopy, VUV, UV and visible light spectroscopy;
- Atomic, molecular and optical physics, molecular beam and ion beam physics; ICP plasma devices;
- Optical fibres technologies, in particular UV fibre optics;
- Vacuum-sputtering, quartz, glass, and vacuum technologies;
- Atmosphere physics and photochemistry; development of atmospheric remote sensing devices;
- Observational astronomy and astrophysics of galactic carbon stars, research on late evolution stars (MS, S type);
- Observation, and monitoring of small objects (asteroids) of the Solar System and Near-Earth Objects with a wide field Ø 1.2 metres Schmidt type telescope in Baldone (Code 0.69);
- Terrestrial geodesy and geodynamics measurements with the world class laser telescope LS-105 with which Latvian astronomers have served for decades as a node of the International Laser Ranging Service (ILRS code name RIGL-1884, Riga);
- Advancement of satellite laser ranging (SLR) instruments, including software and hardware components;
- During the last decade, contributions in various areas of applied research is on the agenda based on cooperation with research driven SMEs in Latvia and looking forward across the national borders.

Isolation from the international research community came to an end when the "iron curtain" was removed in 1990. a lot of various strategic international partnerships emerged due to a very supportive attitude of the international research community to recognised researchers in Latvia (the Baltic country which restored its independence after 50 years of Soviet occupation).

Incorporation in the European Research Area via association with EU Framework Research programmes and participation in the implementation of FP5, FP6, FP7 and HORIZON 2020 EU Framework programmes for RTD and innovation was an exclusive chance for the survival of the FOTONIKA-LV research community when national funding was cut drastically. The availability of resources coming from EU Regional development funds when Latvia joined the EU was another valuable asset despite the awful bureaucratic burden, wasting time and suppressing creativity.

Fig. 1 provides an insight into the budget dynamics since 2001 of the research community from which NSP FOTONIKA-LV emerged. The budget is the result of an intensive project life. National budget funding (institutional funding) formed for years only 10% of the sum needed to sustain full scale research activities.

The unique ERA Chair project is the best one from the point of view of "academic freedom" available to five highly qualified researchers which means new opportunities to be successful with new project proposals up to the level of Future Emerging Technologies projects and European Research Council grants in the Horizon Europe programme (2021–2027) and to attract experienced researchers and students from the diaspora and to recruit researchers from abroad via Marie Skłodowska-Curie fellowships, Post Doc Grants and ERASMUS fellowships.

The absence of institutional funding "de facto" is still a very painful problem, but now the research community NSP FOTONIKA-LV has the capacity to influence and to change RTD policy in Latvia via the authority of the recruited ERA Chair supported by the International Scientific Council of FOTONIKA-LV representing a strategic partnership with institutions in the European Research Area.

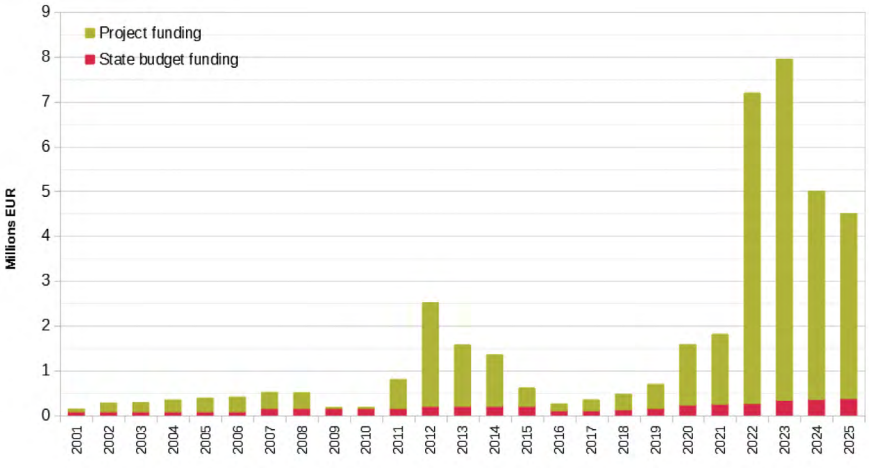

Fig. 1. *Financial history and project life since 2001 of the research institutes and researchers' community related to NSP FOTONIKA-LV*

The Progress of the ERDF Project "The Development of Quantum Optics and Photonics at the University of Latvia" (refinanced Horizon 2020 ERA Chairs project)

Aigars Atvars[1], Rashid A. Ganeev[1], Dina Bērziņa[2]

[1] Institute of Astronomy, University of Latvia, Latvia
[2] Institute of Atomic Physics and Spectroscopy, University of Latvia, Latvia
aigars.atvars@lu.lv

The University of Latvia (UL) is implementing European Regional Development Fund Project No. 1.1.1.5/19/A/003 "The Development of Quantum Optics and Photonics in the University of Latvia" (Project) [1]. The realisation period of the project's activities is 01.05.2019–30.11.2023. The budget of the Project is EUR 2.5 million (85% covered by the European Regional Development Fund and 15% covered by the State budget). The Project was initially submitted to the Horizon 2020 call "WIDESPREAD-04-2019: ERA Chairs" and was scored above the threshold.

The objective of the Project is to attract a high-level research leader (ERA Chair) who will develop quantum optics and photonics at the University of Latvia and thus will raise the research quality and international recognition of the UL. The project has the following work packages: WP1. Selection and Recruitment of an ERA Chair; WP2. Selection, recruitment, and personnel management of an ERA Chair's research team; WP3. Research activities of an ERA Chair and his/her team; WP4. Preparation of competitive project proposals; WP5. Strategy development and implementation of structural changes; WP6. Communication, Networking, and Dissemination; WP7. Management. The main expected results of the Project and their achievements so far are summarised in Tab. 1.

Tab. 1. *The main expected results of Project No. 1.1.1.5/19/A/003 and the achievements as of 31.05.2021*

Expected result	**To be achieved during the Project, by 30.11.2023**	**Achieved till 31.05.2021**	**Achieved till 31.05.2021, %**	**Planned to be achieved by the end of 2021**
ERA Chair holder recruited (agreement)	1	1	100%	1
ERA Chair scientific group recruited (agreements)	4	4	100%	4
Publications submitted	24	9 (8 published)	33%	> 20
Project proposals submitted	6	5 (1 funded)	83%	> 7
Patents applied	2	0 in progress	0%	0 in progress

Expected result	To be achieved during the Project, by 30.11.2023	Achieved till 31.05.2021	Achieved till 31.05.2021, %	Planned to be achieved by the end of 2021
Lecture course prepared	1	0 in progress	0%	0 draft version prepared
Human Resources Strategy for Researchers prepared	1	0 in progress	0%	0 in progress
Strategy for the Development of Quantum Optics and Photonics at the University of Latvia prepared	1	0 in progress	0%	0 draft version prepared
International conferences organised	2	1	50%	1

The Project has an international Advisory Board which, within a Selection Committee, launched an open international competition for the ERA Chair position [2] and evaluated the candidates. Finally, Dr. Rashid Ganeev was selected and recruited as the ERA Chair in Quantum Optics and Photonics at the University of Latvia. R. Ganeev is a highly productive researcher with a total number of publications (SCOPUS) 504 and H-index (SCOPUS) 47. He is the author of eight monographs. His research topics cover quantum optics and photonics, including research on resonance-induced processes of single high-order harmonic enhancement in different metal plasmas, time-resolved plasma characterisation with spectral, morphological, and harmonic issues, studies of the nonlinear refraction, and nonlinear absorption in nanoparticles suspensions. The ERA Chair's main tasks are to develop quantum optics and photonics at the UL, lead the ERA Chair research group, prepare new project proposals, develop Strategies, and implement structural changes at the UL to achieve excellence on a sustainable basis. To implement R. Ganeev's research activities, a Laboratory of Nonlinear Optics at the Institute of Astronomy, UL was established.

The core research team of the ERA Chair has been selected in an international competition and is formed by Jānis Alnis (Latvia; whispering gallery mode resonator sensors), Uldis Bērziņš (Latvia; atomic spectroscopy), Javed Iqbal (Canada, Pakistan; laser-produced plasma), and Vyacheslav Kim (United Arab Emirates, Uzbekistan; high-order harmonic generation). R. Ganeev leads this research group and supports the career development of its members.

During the Project, various new project proposals have been prepared. In 2020, two project proposals were submitted to Horizon 2020 FET Open and RISE calls, two project proposals to the Latvian Council of Science call, and one project proposal for

ERDF Activity 1.1.1.1. call. The previously submitted project No. 1.1.1.1/20/A/070 "Next generational technology for high purity crystal growth using MHD pseudo levitation" was approved for funding. In 2021, an ERC Advanced grant proposal is being prepared by R. Ganeev (submission deadline August 2021), Horizon EUROPE Teaming project (expected submission deadline Fall 2021), and Latvian Council of Science projects (submission deadline August 2021) are under preparation. Horizon EUROPE Teaming Project (6 years, 15 million EUR from the European Commission + 15 million EUR from National funding) is considered as a proper continuation of an ERA Chair project.

The Project aims to implement structural changes at the UL that will allow to form and keep research excellence on a sustainable basis. For this, the "Strategy for the Development of Quantum Optics and Photonics at the University of Latvia" and "Human Resource Strategy" will be developed. Project members are involved in working groups to prepare a "Strategy of the University of Latvia 2021–2027". R. Ganeev is providing his competence on research article preparation. Actions have been taken to mobilise the research community of the UL in the field of quantum optics and photonics. Joint research seminars in the House of Science of the UL will be launched. New partnerships with foreign research institutions – the Center for Soft Nanoscience, University of Münster (Germany), and Sapienza University of Rome (Italy) – were created for joint research and project preparation.

R. Ganeev is preparing a lecture course "Nonlinear Optics of Plasmas" for physics students of the UL. It is expected that this course, together with other publicity activities of the ERA Chair, will raise the attractivity of quantum optics and photonics, and will grow human resources in this field for the benefit of research and industry. The National Science Platform (NSP) FOTONIKA-LV as an initiator of the Project, holds a network of photonics companies in Latvia. This network will be employed to launch industry-driven research topics and new technologies.

Actual information is on the Project web page – https://www.erachair.lu.lv.

References

[1] Atvars, A. (2019). ERA Chair in Quantum Optics and Photonics. Project proposal to H2020-WIDESPREAD-2019-4 call. In: Abstract book. The 3rd International Conference FOTONIKA-LV "Achievements and Future Prospects", Riga, Latvia, 24–25 April, pp. 46–48. https://www.lu.lv/fileadmin/user_upload/lu_portal/projekti/fotonika-lv/ERA_Chair/2015_Conference_FOTONIKA-LV.pdf

[2] EURAXESS announcement "Principal investigator – ERA Chair in Quantum Optics and Photonics". https://euraxess.ec.europa.eu/jobs/442744 (1st competition), https://euraxess.ec.europa.eu/jobs/536042 (2nd competition).

Laser Spectroscopy Applied to the Environmental, Ecological and Agricultural Areas

Sune Svanberg

South China Academy of Advanced Optoelectronics, South China Normal University, China
Department of Physics, Lund University, Sweden
sune.svanberg@fysik.lth.se

An overview of the possibilities of laser spectroscopy applied to the environmental, ecological, and agricultural areas is given, based on the experience of the author within these fields at the University of Latvia, Lund University, and the South China Normal University.

Optical probing of the atmosphere using active remote sensing techniques of the laser-radar type will be discussed, but also some passive techniques employing ambient radiation. Atmospheric objects of quite varying sizes can be studied. Mercury is the only pollutant in atomic form in the atmosphere, while other pollutants are either molecular or in particle form. Light detection and ranging (Lidar) techniques provides three-dimensional mapping of such constituents. Recently, the techniques have been extended to the ecological field. Monitoring of flying insects and birds is of considerable interest, and several projects have been pursued in collaboration with biologists.

Fluorescence lidar also allows remote monitoring of vegetation and historical building facades. In agricultural applications, e.g., the fertilisation levels of crops can be assessed. Drone-based techniques are now also augmenting the possibilities of fluorescence mapping of the environment.

Laser spectroscopy also allows for non-intrusive quality control of pharmaceutical preparations and foods, now mostly employing the gas in the scattering media absorption spectroscopy (GASMAS) technique.

The talk emphasizes the value of cross-disciplinary work to help solve important societal issues. Some background material is provided as Refs [1–10].

Acknowledgements

The author is very grateful to numerous students and colleagues who contributed to this work. Financially, it was supported by many Swedish funding sources, and by the Science and Technology Program of Guangzhou (No. 2019050001), and the Guangdong Provincial Key Laboratory of Optical Information Materials and Technology (No. 2017B030301007).

References

[1] Svanberg, S. (2013). Gas in Scattering Media Absorption Spectroscopy – from Basic Studies to Biomedical Applications. Lasers and Photonics Reviews 7, 779.

[2] Li, T. Q., Lin, H. Y., Zhang, H., Svanberg, K., & Svanberg, S. (2017). Application of Tunable Diode Laser Spectroscopy in Assessment of Food Quality. Appl. Spectroscopy 71, 929.

[3] Zhu, S. M., Malmqvist, E., Li, W. S., Jansson, S., Li, Y. Y., Duan, Z., Svanberg, K., Feng, H. Q., Song, Z. W., Zhao, G. Y., Brydegaard, M., Svanberg, S. (2017). Insect Abundance over Chinese Rice Fields in Relation to Environmental Parameters, Studied with a Polarization-sensitive CW Near-IR Lidar System. Appl. Phys. B 123, 211.

[4] Zhao, G. Y., Lian, M., Li, Y. Y., Duan, Z., Zhu, S. M., Mei, L., & Svanberg, S. (2017). Mobile Lidar System for Environmental Monitoring. Applied Optics 65, 1506.

[5] Li, Y., Li, W. S., Hu, L. N., Svanberg, K., & Svanberg, S. (2018). Non-intrusive Studies of Gas Contents and Gas Diffusion in Hen Eggs. Biomed. Optics Express 10, 83.

[6] Brydegaard, M., & Svanberg, S. (2018). Photonic Monitoring of Atmospheric and Aquatic Fauna. Lasers and Photonics Review. DOI 10.1002/lpor.201800135.
[7] Duan, Z., Ying, Li, Wang, J. L., Zhao, G. Y., & Svanberg, S. (2019). Aquatic Environment Monitoring using a Drone-Based Fluorosensor. Appl. Phys. B 125, 108.
[8] Zhao, G. Y., Zhang, W. X., Duan, Z., Lian, M., Hou, N. B., Li, Y. Y., Zhu, S. M., & Svanberg, S. (2020). Mercury as a geophysical tracer gas – Emissions from the Emperor Qin tomb in Xi´an studied by laser radar. Scientific Reports 10, 10414.
[9] Duan, Z., Yuan, Y., Lu, J. C., Wang, J. L., Li, Y., Svanberg, S., & Zhao, G. Y. (2020). Under-water Spatially, Spectrally, and Temporally Resolved Optical Monitoring of Aquatic Fauna. Optics Express. DOI 10.1364/OE.383061.
[10] Song, Z. W., Zhang, B. X., Feng, H. Q., Zhu, S. M., Hu, L. N., Brydegaard, M., Li, Y. Y., Jansson, S., Svanberg, K., Zhao, G. Y., Bood, J., Svanberg, S., & Li, D. S. (2020). Application of Lidar Remote Sensing of Insects in Agricultural Entomology on the Chinese Scene. J. Appl. Entomology 144, 161.

Quantum Silicon Photonics

Lorenzo Pavesi

Nanoscience Laboratory, Department of Physics, University of Trento, Italy
lorenzo.pavesi@unitn.it

We are at the dawn of the second quantum revolution, where single particles, quantum superposition and quantum entanglement are used to enable new technologies and devices [1]. In this talk, I will review a few devices, which are based on these concepts. In addition, I will show that Silicon Photonics is the proper platform to integrate quantum photonics [2]. Indeed, Silicon Photonics is the technology to fabricate photonics devices with standard silicon microelectronics processing [3]. By using Silicon Photonics, I will discuss:

1) a tiny, low cost, high performance fully silicon device to generate random numbers for security applications [4–8];
2) a source of single photon entanglement which can be used as a resource for quantum information applications such as quantum key distribution or as a certified quantum random number generator [9–12];
3) a heralded single photon source which works in the MIR and can be used for ghost imaging or undetected photon spectroscopy [13–17];
4) a near-ideal spontaneous photon source in silicon quantum photonics which could enable a silicon quantum computer [18].

Acknowledgements

I thank all my collaborators who are listed in the references. This work was supported by the EC through the Horizon 2020 program (projects QRANGE and EPIQUS) and by Provincia Autonoma Trentino through the project SIQURO.

References

[1] https://qt.eu/

[2] Bonneau, D., Silverstone, J. W., & Thompson M. G. (2016). Silicon Quantum Photonics. In: Silicon Photonics III: Systems and Applications. L. Pavesi, and D. J. Lockwood (eds.). Topics in Applied Physics. Springer vol. 122. Berlin: Springer Verlag, p. 41.

[3] Handbook of Silicon Photonics (2013). L. Vivien, and L. Pavesi (eds.). CRC Press (Taylor and Francis group, April), p. 849. ISBN 978-1-4398-3610-1.

[4] Bisadi, Z., Fontana, G., Moser, E., Pucker, G., & Pavesi, L. (2017). Robust Quantum Random Number Generation with Silicon Nanocrystals Light Source. IEEE/OSA Journal of Lightwave Technology 35 (1 May), 1588–1594.

[5] Bisadi, Z., Acerbi, F., Fontana, G., Zorzi, N., Piemonte, C., Pucker, G., & Pavesi, L. (2018). Compact Quantum Random Number Generator with Silicon Nanocrystals Light Emitting Device Coupled to a Silicon Photomultiplier. Frontiers in Physics: Optics & Photonics 6, 9.

[6] Acerbi, F., Bisadi, Z., Fontana, G., Zorzi, N., Piemonte, C., & Pavesi, L. (2018). a Robust Quantum Random Number Generator Based on An Integrated Emitter-Photodetector Structure. IEEE Journal of Selected Topics in Quantum Electronics 24, 6101107.

[7] Acerbi, F., Massari, N., Gasparini, L., Tomasi, A., Zorzi, N., Fontana, G., Pavesi, L., & Gola, A. (2020). Structures and methods for fully-integrated quantum random number generators. IEEE Journal of Selected Topics in Quantum Electronics 26, 9200116.

[8] Leone, N., Rusca, D., Azzini, S., Fontana, G., Acerbi, F., Gola, A., Tontini, A., Massari, N., Zbinden, H., & Pavesi, L. (2020). An optical chip for self-testing quantum random number generation. APL Photonics 5, 101301.

[9] Azzini, S., Mazzucchi, S., Moretti, V., Pastorello, D., & Pavesi, L. (2020). Single-Particle Entanglement. Invited review Advanced Quantum Technologies 3, 2000014.
[10] Pasini, M., Leone, N., Mazzucchi, S., Moretti, V., Pastorello, D., & Pavesi, L. (2020). Bell inequality violation by entangled single photon states generated from a laser, a led, or a halogen lamp. Physical Review A102, 063708.
[11] Leone, N., Azzini, S., Mazzucchi, S., Moretti, V., & Pavesi, L. Certified quantum random numbers based on single-photon entanglement. arXiv:2104.04452.
[12] Mazzucchi, S., Leone, N., Azzini, S., Pavesi, L., & Moretti, V. Entropy certification of a realistic QRNG based on single-particle entanglement. arXiv:2104.06092.
[13] Signorini, S., & Pavesi, L. (2020). On-chip heralded single photon sources. Invited review AVS Quantum Science 2, 041701.
[14] Signorini, S., Mancinelli, M., Borghi, M., Bernard, M., Ghulinyan, M., Pucker, & Pavesi, L. (2018). Intermodal Four Wave Mixing in Silicon waveguides. Photonics Research 6, 805–814.
[15] Signorini, S., Finazzer, M., Bernard, M., Ghulinyan, M., Pucker, G., & Pavesi, L. (2019). Silicon photonics chip for inter-modal Four Wave Mixing on a broad wavelength Range. Frontiers in Physics, section Optics and Photonics 7, 128.
[16] Signorini, S., Piccione, S., Ghulinyan, M., Pucker, G., & Pavesi, L. (2018). Are on-chip heralded single photon sources possible by intermodal four wave mixing in silicon waveguides? Proc. SPIE 10733, Quantum Photonic Devices 2018 (11 September), 107330G.
[17] Signorini, S., Sanna, M., Piccione, S., Ghulinyan, M., Tidemand-Lichtenberg, P., Pedersen, Ch., & Pavesi, L. (2021). a silicon source of heralded single photons in the mid infrared. APL Photonics.
[18] Paesani, S., Borghi, M., Signorini, S., Mainos, A., Pavesi, L., & Laing, A. (2020). Near-ideal spontaneous photon sources in silicon quantum photonics. Nature Communications 11, 2505.

High-Accuracy Laboratory Atomic Astrophysics

Henrik Hartman

Department of Materials Science and Applied Mathematics, Malmö University, Sweden
henrik.hartman@mau.se

Analyses of astronomical spectra rely on detailed knowledge of the structure of the atomic species involved. Furthermore, the line strengths must be accurately known to use astronomical spectra for quantitative analyses, such as the determination of stellar and nebular temperature, density, or ultimately chemical abundance. The near-infrared wavelength region, 1–5 μm, is becoming more important thanks to its smaller interstellar extinction and several spectrographs are coming online matching these needs, e.g., the CRIRES+ at VLT and the APOGEE survey. The planned European Extremely Large Telescope (E-ELT) will observe predominantly in the infrared domain, and the lack of data will also appear significant in this case. In addition, the optical region surveys are dependent on accurate atomic transitional data to fully exploit the expensive observations.

Our research program on Laboratory Atomic Astrophysics focuses on meeting the needs for infrared atomic data, both line identification and measurements of intrinsic line strengths, the oscillator strengths.

We will review the branching fraction and lifetime technique to measure line strengths, using the high-resolution Fourier spectrometer at Edlen Laboratory, in combination with radiative lifetimes. The measurements are combined with calculations using the GRASP and ATSP2k codes, providing a high-accuracy data set for astrophysical analysis. We participate in observational programs to identify the relevant problems and priorities in the need for atomic data.

In the present contribution, we will discuss infrared transitions from an atomic structure point of view and as a base for the astronomical analysis as well as for laboratory and theoretical priorities. Furthermore, we will discuss the effect of hyperfine structure on the astrophysical analysis. Examples are given from recent and ongoing studies on e.g., Sc I, Mg I, Si I and La I.

New areas include the radiative data for nuclear capture elements and kilonova spectroscopy, which are not available with the existing techniques. We will discuss new developments to measure lifetimes for these important elements and a recent collaboration with the group of Lead researcher Uldis Bērziņš (University of Latvia) around light sources to access the spectrum of additional elements for spectroscopic analysis.

Thematic Sessions

Laser Spectroscopy to Meet Some Challenges in Medicine

Katarina Svanberg

South China Academy of Advanced Optoelectronics, South China Normal University, China
Department of Clinical Sciences, Lund University, Sweden
katarina.svanberg@med.lu.se

There are a lot of unmet needs in medicine, such as reliable tools for early tumor detection, objective guidance in therapy decisions in infectious diseases avoiding the alarming development of antibiotic resistance, too few minimally invasive surgical procedures among other challenges. Laser spectroscopy has been shown to be a valuable tool, both in the detection and the therapy of human malignancies. The most important prognostic factor for cancer patients is early tumor discovery. If malignant tumors are detected during the non-invasive stage, most tumors show a high cure rate of more than 90%. Even though there are many conventional diagnostic modalities, very early tumors may be difficult to discover. Laser-induced fluorescence (LIF) for tissue characterisation is a technique that can be used for monitoring the biomolecular changes in tissue under transformation from normal to dysplastic and cancer tissue before structural tissue changes are seen at a later stage. The technique is based on UV or near-UV illumination for fluorescence excitation. The fluorescence from endogenous chromophores in the tissue alone or enhanced by exogenously administered tumor seeking substances can be utilised. The technique is non-invasive and gives results in real-time. LIF can be applied for point monitoring or in an imaging mode for larger areas, such as the vocal cords or the portio of the cervical area.

Photodynamic therapy is a selective treatment technique for human malignancies. To overcome the limited light penetration in superficial illumination interstitial delivery (IPDT) with the light transmitted to the tumor via optical fibers has been developed. Interactive feed-back dosimetry is of importance for optimizing this modality and such a concept has been developed. The technique has special interest for tumors where there are no other options, such as for recurrent prostate cancer after ionizing radiation. For correct dosimetry it is important to assess the optical properties of the tissue; this can be done by time resolving propagation techniques.

Another technique which has been developed for medical application is based on gas in scattering media absorption spectroscopy (GASMAS). The technique is used to detect free gas (e.g., oxygen and water vapor) in hollow organs in the human body and has been applied to the detection of the human sinus cavities in the facial skeleton. The GASMAS technique might also be used for the surveillance of prematurely born infants. As the organs are not fully developed there is a risk of morbidity. In particular, the lung function is limited, and the babies may develop respiratory distress syndrome resulting in decreased oxygen saturation affecting risk organs, such as the brain. GASMAS may also be developed for the detection of other diseases, such as middle ear infection in small children. a certain proportion of these infections are virally induced and in these cases no antibiotics should be prescribed. GASMAS has the potential to discriminate the origin of the disease and thus guide in the decision of appropriate therapy, trying to fight the global problem of antibiotic resistance. Many of these techniques can also be applied to study other organic materials, e.g., foods.

A few references, illustrating laser spectroscopy applied to the medical area, are given in [1–10].

Acknowledgements

Colleagues and numerous students have collaborated in this work and are greatly acknowledged, and the author is very grateful for their contributions. Financially, the work was supported by numerous Swedish funding sources, and by the Science and Technology Program of Guangzhou (No. 2019050001), and the Guangdong Provincial Key Laboratory of Optical Information Materials and Technology (No. 2017B030301007).

References

[1] Thompson, M. S., Johansson, T., Pålsson, S., Andersson-Engels, S., Svanberg, S., Bendsoe, N., Stenram, U., Svanberg, K., Spigulis, J., Derjabo, A., & Kapostins, J. (2006). Photodynamic Therapy of Basal Cell Carcinoma with Multi-Fibre Contact Light Delivery. J. Envir. Path. Toxic. Onc. 25, 411.

[2] Pålsson, S., Stenram, U., Thompson, M. S., Vaitkuviene, A., Puskiene, V., Ziobakiene, R., Oyama, J., Gustafsson, U., DeWeert, M. J., Bendsoe, N., Andersson-Engels, S., Svanberg, S., & Svanberg, K. (2006). Methods for Detailed Histopathological Investigation and Localisation of Cervical Biopsies to Improve the Interpretation of Autofluorescence Data. J. Envir. Path. Toxic. Onc. 25, 321.

[3] Svanberg, K., Bendsoe, N., Axelsson, J., Andersson-Engels, S., & Svanberg, S. (2010). Photodynamic Therapy – Superficial and Interstitial Illumination in Skin and Prostate Cancer. J. Biomed. Optics 15, 041502.

[4] Lundin, P., Krite Svanberg, E., Cocola, L., Lewander Xu, M., Somesfalean, G., Andersson-Engels, S., Jahr, J., Fellman, V., Svanberg, K., & Svanberg, S. (2013). Non-invasive Monitoring of Gas in the Lungs and Intestines of Newborn Infants using Diode Lasers: Feasibility Study. J. Biomedical Optics 18, 127005.

[5] Huang, J., Zhang, H., Li, T. Q., Lin, H. Y., Svanberg, K., & Svanberg, S. (2015). Assessment of Human Sinus Cavity Air Volume using Tunable Diode Laser Spectroscopy, with Application to Sinusitis Diagnostics. J. Biophotonics 8, 985.

[6] Svanberg, K., & Svanberg, S. (2015). Monitoring of Free Gas In-Situ for Medical Diagnostics using Laser Spectroscopic Techniques. In: Frontiers in Biophotonics for Translational Medicine. U. S. Dimish, and M. Olivo (eds.). Singapore: Springer, pp. 307–321.

[7] Krite Svanberg, E., Lundin, P., Larsson, M., Åkesson, J., Svanberg, K., Svanberg, S., Andersson-Engels, S., & Fellman, V. (2016). Noninvasive monitoring of oxygen in the lungs of newborn infants by diode laser spectroscopy. Pediatric Research 79, 621.

[8] Li, W. S., Lin, H. Y., Zhang, H., Svanberg, K., & Svanberg, S. (2017). Detection of Free Oxygen and Water Vapor in Fertilized and Unfertilized Eggs by Diode Laser Spectroscopy – Exploration of Diagnostics Possibilities. J. Biophotonics. DOI 10.1002/jbio.201700154.

[9] Hu, L. N., Li, W. S., Lin, H. Y., Li, Y., Zhang, H., Svanberg, K., & Svanberg, S. (2019). Towards an Optical Diagnostic System for Otitis Media using a Combination of Otoscopy and Spectroscopy. J. Biophotonics. DOI org/10.1002/jbio.201800305.

[10] Lin, X. B., Zhang, H., Hu, L. N., Zhao, G. Y., Svanberg, S., & Svanberg, K. (2020). Ripening of Avocado Fruits Studied by Spectroscopic Techniques. Journal of Biophotonics. DOI org/10.102.jbio.202000076.

Nanotechnology in Optics, Electronics and Biomedicine: Advantages of the Optical Materials Surface Structuration with the Carbon Nanotubes

Natalia V. Kamanina

Vavilov State Optical Institute, Russian Academy of Sciences
Saint Petersburg Electrotechnical University
Kurchatov Institute – Nuclear Physics Institute
nvkamanina@mail.ru

It is well known that at present the nanotechnology approach has been used by different scientific and technical teams in order to optimise the basic physical-chemical properties of the materials. In the current research the comparative study of the spectral parameters, wetting phenomena, as well as of the micro hardness improvement for the large groups of the model optical materials such as: KCl, KBr, LiF, MgF2, BaF2, CaF2, Si, ZnS, Sc, ITO, and others have been shown via surface structuration. The carbon nanotubes have been chosen as specific and effective nano-objects, which permits the modification of the materials' physical-chemical characteristics with good advantage. The laser-oriented deposition (LOD) technique with an additional procedure to use the surface electromagnetic waves (SEWs) has been shown. The CO_2-laser has been used in this case. Some special accent has been given to postulate the nano-structurisation process advantage to modify the ITO conducting coatings and the PVA thin-film polarisers. The resistivity and refractivity change of the ITO coatings have been presented; the improvement of the transmittance of the parallel component of the electromagnetic wave for the PVA polarisers has been shown and explained. Analytical and quantum-chemical simulations have supported the experimental results.

Furthermore, additional data have been received and discussed for the nanostructured organic conjugated materials (polymers, monomers and the liquid crystal ones) via a change of their refractive parameters. The fullerenes, shungites, graphene oxides, etc. nano-sensitisers have been used. Nd-pulsed laser has been applied in this case. The area of the structured materials application can be extended from optoelectronics to biomedicine.

Some previously obtained results have been shown in papers [1–3].

References

[1] Kamanina, N. V., Likhomanova, S. V., & Kuzhakov, P. V. (2018). Advantages of the Surface Structuration of KBr Materials for Spectrometry and Sensors. MDPI in Sensors 18(9). DOI 10.3390/s18093013. https://www.scilit.net/article/6d1a040dd26a2081fe82eb58565844fc

[2] Kamanina, N. V. (2019). Nanoparticles doping influence on the organics surface relief. Journal of Molecular Liquids 283, 65–68. https://doi.org/10.1016/j.molliq.2019.03.043

[3] Kamanina, N., Kuzhakov, P., & Kvashnin, D. (2020). Novel Perspective Coatings for the Optoelectronic Elements: Features of the Carbon Nanotubes to Modify the Surface Relief of BaF2 Materials. Coatings, MDPI 10, 661, p. 10. DOI 10.3390/coatings1007066.

Testing Quantum Mechanics Foundations with a Laser Field

Emilio Fiordilino

Department of Physics and Chemistry, University of Palermo, Italy
fiordilino@unipa.it

Our communication presents a systematic theoretical test of the fundamental laws of Quantum Mechanics by means of a laser field that has been demonstrated to be a powerful tool for the investigation of the behaviour of atoms, molecules, and nanoparticles because of its versatility to be tuned – In intensity, frequency and duration – according to the requirements of the designed experiment. One important feature is the possibility of setting the laser angular frequency ω_L to resonance with a Bohr transition of a quantum object; in this way the wave function of the object undergoes rapid oscillations and introduces a wealth of effects that would, otherwise, be difficult to observe. Moreover, quantum objects driven by a laser field become the source of new electromagnetic radiation the spectrum of which contains a large plateau of odd harmonics of ω_L. The diffused radiation carries information on the nature and comportment of the objects; it can be detected and unveil microscopic properties otherwise not observable.

Quantum Physics is based upon postulates which can be checked in their validity by slightly changing the form of the Schrödinger equations and by observing the sort of modifications that are produced by the new form. In this communication we present investigations on two issues: 1. the *linearity* of Quantum Mechanics and 2. the *constancy* of physical constants.

1. Linearity is a basic axiom of Quantum Mechanics which has been the object of investigation [1]. We have introduced, in the form of the Schrödinger equation describing an atom-radiation interaction, a tiny nonlinearity and observed that under opportune conditions the dynamics of the object presents traits of non-predictability of a chaotic nature. In fact, the population of the quantum states in the non-linear case is very sensitive on the initial atomic state and this fact is a flag of Chaos in the realm of Classical Physics.
2. Since Dirac's [2] hypothesis that Newton's gravitational constant *G* is time dependent, a fervid debate has been carried out on the possibility that other constants – dimensionless or not – may be variable. Experimental evidence, although not universally accepted, suggests that the fine structure constant α and Plank's constant might be time [3] or space dependent [4, 5]. We introduce a general form of the Schrödinger equation and two experimental protocols to investigate the behaviour of an atom driven by a laser field under the hypothesis that $\hbar$ is not constant. The form of the new Schrödinger equation assumes a particular simple form if we define a new time standard $\tau = \int_0^t \hbar(t')\, dt'$ that substitutes for ordinary time. The first protocol requires two observations of the time evolution of the population of the ground state of an atom at different moments separated by a gap of one hour. The second one requires the measurement of the harmonic spectrum emitted by the atom. Both experiments are well inside today's state of the art. We again observe modified chaotic evolution of the atomic dynamics and a redshift of the emitted harmonic lines. The results permit the setting of constraints on the value of $\Delta\hbar/\hbar$ which considerably improve the experimental constraints presented up to now. In Fig. 1 we show the harmonic spectrum emitted by an atom driven by a laser pulse. The spectrum contains hyper-Raman lines which are always predicted

but never detected and odd order lines; these are slightly redshifted because of the assumed inconstancy of $\hbar$.

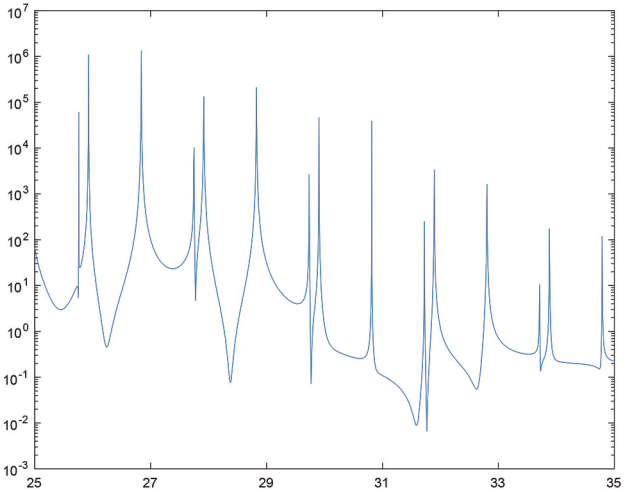

Fig. 1. *Spectrum emitted by an atom driven by a laser field when the Planck constant is dependent upon the coordinates. It is evident a small redshift of the odd order harmonics. The redshift can be measurable*

References

[1] Weinberg, S. (1989). Precision Tests of Quantum Mechanics. Phys. Rev. Lett. 62(485).
[2] Dirac, P. A. M. (1938). a New Basis for Cosmology. Proc. Roy. Soc. Lon., Ser. A. 165(199).
[3] Martins, C. J. A. P. (2017). The Status of Varying constants: a Review of the Physics, Search and Implications. Rep. Prog. Phys. 80(126902).
[4] Kentosh, J., & Mohageg, M. (2012). Global Positioning System Test of the Local Position Invariance of Plank's Constant. Phys. Rev. Lett. 108(110801).
[5] Hutchin, R. A. (2016). Experimental Evidence for a Variability in Planck's constant. Opt. Phot. J. 6(124).

Photodetachment Studies of Negative Ions

Dag Hanstorp

Department of Physics, University of Gothenburg, Sweden
dag.hanstorp@gu.se

The extra electron in a negative ion does not experience the Coulomb force from the nucleus at large distances. Instead, core polarisation induced by the extra electron stabilizes the ion. The correlated motion of the electrons requires theoretical models that go beyond the independent particle approximation. Experimental investigations of the structure and dynamics of negative ions can hence lead to an increased understanding of many-electron effects.

I will review various laboratory experiments of negative ions. First, photo detachment experiments at the negative ion beam facility GUNILLA in Sweden and at the ISOLDE facility at CERN, revealing structural properties of various atomic negative ions, will be presented. Thereafter, I will show how the dynamics of negative can be studied using femtosecond laser pulses in combination with a velocity map imaging (VMI) spectrometer in order to visualise the electronic motion in the ground state of an atom. It will also be demonstrated how the 2-dimensional VMI technique can be used to produce a complete 3-dimensional image using a tomographic technique. Third, experimental investigations of the lifetimes of an excited state in negative ions using the cryogenic electrostatic double storage ring DESIREE will be presented. Finally, possible experiments using the GRIBA facility, located at the University of Latvia, will be discussed.

Chalcogenide Colloidal Quantum Dots of Lead and Mercury for Near/mid-IR-applications

Ivan A. Shuklov

Moscow Institute for Physics and Technology, Russia
ivan.shuklov@gmx.de

The use of colloidal quantum dots (CQDs) offers an interesting alternative to the expensive epitaxially-grown structures for the production of low-cost infrared detectors. Technologies based on near-/mid-IR CQDs are not as mature as the application of CQDs visible spectral range. Near-IR energies could be achieved with a lead chalcogenide CQD. The long wavelength could not be accessed with these CQD due to their bulk band gap. So PbS possess the band gap in bulk (0.41 eV) and the lowest band gap in bulk among lead chalcogenides observed for PbSe (0.28 eV). Semimetals, such as HgTe or HgSe show the most promising properties for the creation of CQD devices for the mid wavelength infrared (MWIR).

Significant effort has been invested in the development methods for the synthesis of chalcogenide CQD of lead and mercury [1]. Particular interest was paid to the development of the production of CQDs with narrow size distribution and good stability [2, 3]. Nevertheless, even for the most developed lead sulphide CQD it is rather difficult to get the broad range of nanocrystal sizes and the narrow size distribution by a single method of PbS synthesis. Another acute problem is the lack of understanding of the chemistry involved in the synthesis of chalcogenide quantum dots, that hampers developing efficient methods of chalcogenide CQD production.

Controlled aging of PbS

The joint-application of the lead oleate in oleic acid as a lead precursor with a sulphur-oleylamine reagent was developed for the synthesis of PbS CQDs [4], and the influence of temperature and Pb/S-ratio was studied in detail. The innovative controlled aging approach to the quantum dots of PbS will be described. The combination of this approach with the described synthetic method allows one to produce the PbS colloidal quantum dots with a first excitonic peak from 1100 to 2050 nanometres. Our controlled aging approach is designed to utilize larger PbS QDs as a starting material for smaller QDs, and therefore significantly increase the range of accessible QDs.

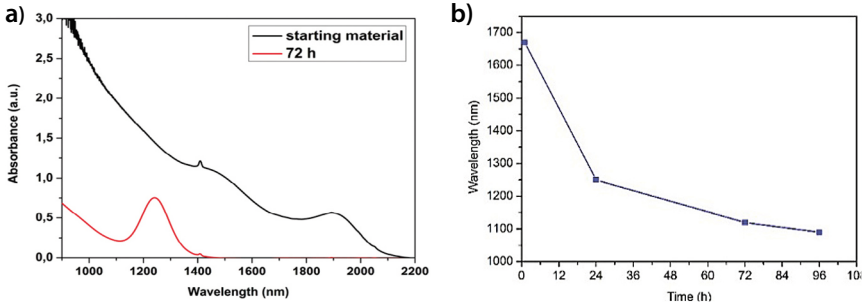

Fig. 1. *Aging of QD PbS by storage of solution CQDs in the presence of oleylamine-oleic acid mixture:* ***(a)*** *absorption spectra of samples;* ***(b)*** *Dependence of the absorption spectra from the storage time*

Mercury chalcogenides

The solution of elemental tellurium in trioctylphosphine is a commonly used reagent for the synthesis of colloidal quantum dots of mercury tellurides as well as CdTe, SnTe, PbTe, Ag_2Te. There is an absence of detailed information on this commonly used tellurium precursor. We used 125Te and 31P{1H} NMR spectroscopy along with quantum-chemical calculations to study the nature of the compounds formed by the dissolution of tellurium in trioctylphosphine [5]. Our NMR study expanded by DFT simulation results revealed the new unforeseen dimeric phosphine telluride-phosphine species dominating in the solution of this key precursor for metal telluride nanocrystals. The quantum chemical calculations also suggest that the nature of the species in the tellurium solutions in lower trialkylphosphines should be similar to the solution in trioctylphosphine and therefore should be revised. The acquired knowledge allowed us to improve the synthesis of HgTe colloidal quantum dots with absorption in mid-IR.

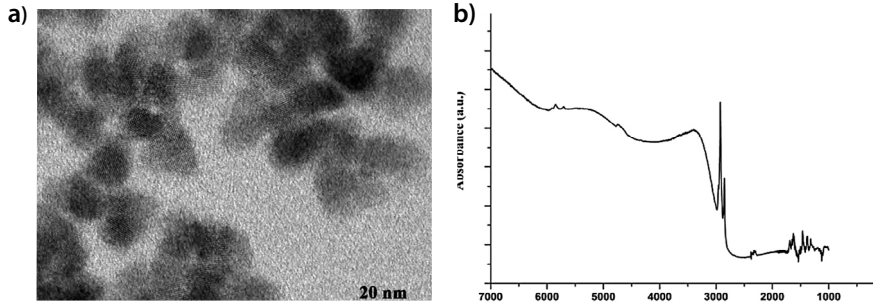

Fig. 2. (a) *TEM Image of HgTe QDs;* ***(b)*** *Absorption spectra of HgTe QDs*

References

[1] Lu, H., Carroll, G. M., Neale, N. R., & Beard, M. C. (2019). Infrared quantum dots: Progress, challenges, and opportunities. ACS Nano 13(2), 939.

[2] Shuklov, I. A., & Razumov, V. F. (2020). Lead chalcogenide quantum dots for photoelectric devices. Russ Chem. Rev. 89, 379.

[3] Hendricks, M. P., Campos, M. P., Cleveland, G. T., Jen-La Plante, I., & Owen, J. S. (2015). a tunable library of substituted thiourea precursors to metal sulfide nanocrystals. Science 348, 1226.

[4] Shuklov, I. A., Toknova, V. F., Lizunova, A. A., & Razumov, V. F. (2020). Controlled aging of PbS colloidal quantum dots under mild conditions. Materials Today Chemistry. 54, 100357.

[5] Shuklov, I. A., Mikhel, I. S., Nevidimov, A. V., Birin, K. P., Dubrovina, N. V., Lizunova, A. A., & Razumov, V. F. (2020). Mechanistic Insights into the Synthesis of Telluride Quantum Dots with Trioctylphosphine-Tellurium. Chemistry Select 5(38), 11896.

Resonance Processes During High-order Harmonics Generation in Atomic and Molecular Plasmas

Rashid A. Ganeev

Institute of Astronomy, University of Latvia, Latvia
Saitama Medical University, Japan
Rashid.Ganeev@lu.lv

High-order harmonics generation (HHG) is the efficient method for frequency conversion of laser radiation towards the extreme ultraviolet (XUV) region. We re-examine the resonance enhancement of a single high-order harmonic during the propagation of ultrafast pulses through different chromium-, tin-, and zinc-containing laser-induced plasmas (LIP). We compare the atomic (Cr, Zn, Sn) and molecular (Cr_2O_3, Cr_3C_2, ZnSe), as well as the Sn nanoparticle, plasmas to demonstrate a distinction in the enhancement factor of the single harmonic.

Part of the amplified uncompressed radiation from the Ti:sapphire laser was separated from a whole beam and used as a heating pulse (HP) for LIP formation (Fig. 1). The focused compressed (806 nm, 64 fs) driving pulses (DP) were aligned to propagate through LIP at a distance of ~200 μm above the target surface for HHG. The beta-barium borate (BBO) crystal was inserted into the vacuum chamber in the path of the 806 nm focused radiation to generate a second harmonic for the two-colour pump (TCP, 806 nm + 403 nm) of plasma.

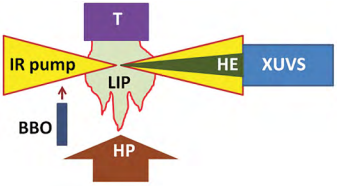

Fig. 1. *Experimental setup for HHG in LIPs. IR pump: infrared (either 806 nm or tuneable NIR) driving femtosecond pulses; BBO: nonlinear crystal for second harmonic generation; T: solid target; HE: harmonic emission; XUVS: extreme ultraviolet spectrometer*

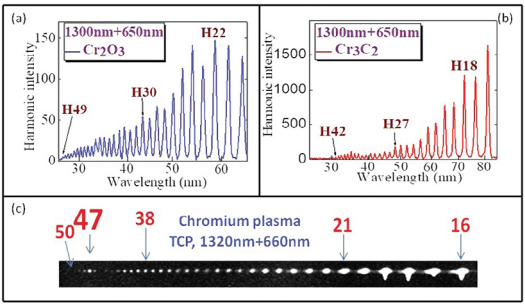

Fig. 2. *Harmonic spectra from Cr_2O_3, Cr_3C_2 and Cr plasmas using tuneable NIR driving pulses.* ***(a)*** *HHG in Cr_2O_3 LIP using 1300 nm + 650 nm driving pulses.* ***(b)*** *HHG in Cr_3C_2 plasma using 1300 nm + 650 nm driving pulses.* ***(c)*** *HHG in Cr plasma using 1320 nm + 660 nm driving pulses at best conditions of plasma formation*

We also used the optical parametric amplifier pumped by the above-described laser to apply the tuneable near infrared (NIR) radiation for HHG in LIP. Most of the experiments were carried out using the 1 mJ, 70 fs signal pulses tuneable in the range of 1280–1440 nm. The harmonic radiation was analysed using an XUV spectrometer.

We re-examine the resonance enhancement of single-harmonic emission during propagation of ultrafast pulses through the chromium-containing plasmas. We show how, in the case of the 806 nm pump, the enhancement of the 29th harmonic (λ = 27.8 nm)

in Cr-containing plasma depends on the constituency of the plasma components at different conditions of target ablation. The application of tuneable (1280–1440 nm) radiation from an optical parametric amplifier allows to demonstrate the notable variations (from the 46th to 49th order) of single-harmonic enhancement using a two-colour pump of Cr plasma. Meanwhile, no enhancement of harmonics was observed in the case of chromium carbide and chromium oxide plasmas, except for the case of overexcited Cr3C2 plasma and the 806 nm pump (Fig. 2).

We also reconsidered the mechanism of resonant amplification of a single harmonic in zinc-containing atomic and molecular plasmas when generating high-order harmonics. The selenides of this metal noticeably reduce the amplification of the single harmonic in comparison with purely atomic plasmas, probably due to the decrease of the oscillator strength of the involved ionic transitions (Fig. 3). The variations of single harmonic enhancement are demonstrated using fixed (806 nm) and tuneable (1280–1440 nm) radiation. Stronger ablation of these molecular targets did not allow the resonant amplification of the single harmonic in ZnSe plasma to be restored using different laser sources, probably due to the insufficient decay and disintegration of molecules leading to the appearance of zinc ions.

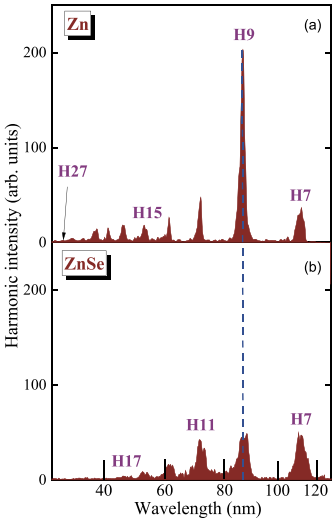

Fig. 3. *HHG from Zn-containing components of LIP using 806 nm driving pulses.* ***(a)*** *Harmonic spectrum generated in Zn plasma.* ***(b)*** *Harmonic spectrum generated in ZnSe plasma*

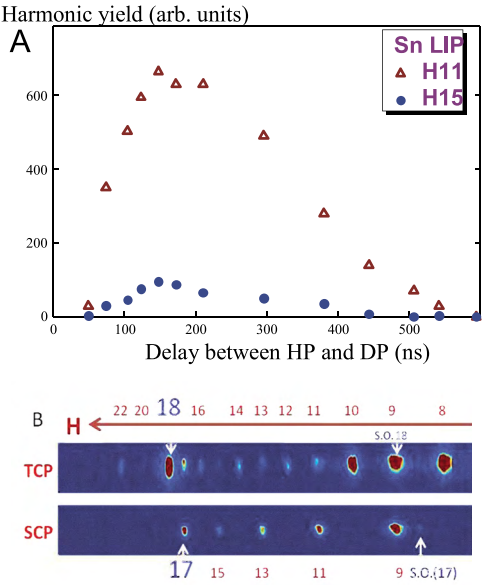

Fig. 4. ***(A)*** *Variations of the 11th (open triangles) and 15th (filled circles) harmonic yields at different delays between the heating and driving pulses.* ***(B)*** *Raw images of harmonics in the case of the 806 nm and 403 nm pump (upper panel) and the 806 nm pump (bottom panel) of tin plasma*

Finally, we compare the resonance-induced enhancement of single harmonic emissions during propagation of ultrafast pulses through different tin-containing LIPs. The enhancement of the 17th and 18th harmonics of 806 nm pulses was analysed in the case of

single-colour and TCP of atomic tin plasma, showing up to a 12-fold enhancement of even (H18) harmonic compared with the neighbouring orders in the latter case (Fig. 4). We also compare the single-atomic Sn and Sn nanoparticles-containing plasmas to demonstrate a distinction in the enhancement factor of the single harmonic in the case of tuneable near-infrared pulses. We show the enhancement of a single harmonic in the vicinity of the $4d^{10}5s^25p^2P_{3/2} \rightarrow 4d^95s^25p^2$ transitions of SnII ions and demonstrate how this process depends on the constituency of the plasma components at different conditions of the target ablation.

Our research allows us to predict modification of the mechanism of resonant amplification of single harmonics reported in other atomic plasmas (manganese, selenium, tellurium, molybdenum, indium, and arsenic) being presented in the molecular form. This process can also be reconsidered by comparing the atomic and molecular plasmas containing the above elements, as well as by tuning the wavelength of driving radiation along those resonances that are responsible for the observed amplification of harmonics.

Acknowledgements

The research was supported by JSPS KAKENHI (grant number 24760048) and ERDF (No. 1.1.1.5/19/A/003).

Coupled Oscillations in Enhancement of High-order Harmonics Generation

Pavel V. Redkin[1], Rashid A. Ganeev[2], Wei Li[1]

[1] Changchun Institute of Optics, Fine Mechanics and Physics, Chinese Academy of Sciences, China
[2] Institute of Astronomy, University of Latvia, Latvia
rdkn_pvl@mail.ru

High harmonic generation (HHG) is not only prominent for its ability to provide coherent ultrashort pulses in extreme ultraviolet using tabletop lasers, but also for an opportunity to investigate ultrafast laser-plasma interactions. During the last two decades the main drawback of HHG – low conversion efficiency – has been reduced by using resonant HHG [1–3], HHG in two-colour pulses [4], quasi-phase matching (QPM) of HHG in periodic gas [5] and plasma [6] jets. While these experimental approaches are quite simple and misleadingly intuitive, there is still no commonly accepted theoretical explanation of these phenomena. So, our goal is to highlight the current state of theoretical description of these unsolved problems.

Resonant HHG is probably the most theoretically studied problem of these three. Models of resonant HHG that support a sharp resonant line are a variation of the three-step model [7]: pumping of an excited state [8], effective radius model [9] and a four-step model using an autoionizing state [10]. It has been shown [11] that consideration of resonant inelastic scattering and multielectron effects does not change the qualitative predictions of this four-step model. While the nature of this intermediate state is currently not restricted, it is assumed to be Fano resonance [12] – a particular case for coupled oscillations. The main advantage of the coupled-oscillator model is the potential ability to explain the difference between efficiency of resonant HHG for different transitions. Despite the intuitiveness of such a classical description of resonant HHG and advantages of classical analytic description, some problems are still not addressed. First of all, the considered bound resonant state is not really an autoionizing state of an atom, because it considers the transition of one of the inner-level electrons to another level not bound into continuum. Then, exchange interactions of electrons may significantly affect the interference of two channels. Finally, the nature of resonant harmonic radiation is not distinguished between stimulated lasing without inversion [13] and stimulated super radiant emission [14]. So, the future of the quantitative description of resonant HHG is related to the fully quantum mechanical treatment of multi-electron systems.

HHG enhancement in two-colour (ω + 2ω central frequencies) fields, whose polarisations are orthogonal to each other, is still not fully understood. In experiments, a strong driving field of frequency ω is combined with a very small fraction of its second harmonic 2ω ($0.01\ I_\omega < I_{2\omega} < 0.03\ I_\omega$), but that increases non-resonant (and, in most cases, also resonant) HHG strongly for odd and even harmonics. Experiments with three-color and non-integer combinations of fields revealed that only a single high-frequency photon is taken from the weak high-frequency field. Single-active electron (SAE) approximation study [15] of 2 delayed circular fields with equal field strength (so that $I_{2\omega} = 4I_\omega$) could explain most of the experimental features, but it fails to predict the enhancement in the case when $I_{2\omega} << 4I_\omega$. Even if the second harmonic has an intensity comparable to the fundamental field, the total enhancement of HHG in fully quantum mechanical SAE approximation turns to be on the order of additional energy of the 2ω field.

While symmetry breaking is referenced as the origin of this enhancement, the actual mechanism is still unclear. Here, we propose to consider HHG enhancement in two-colour fields as a special case of coupled oscillations that is quite similar to Fano resonances for resonance HHG. It has been shown [16] that parity-time symmetry breaking changes the coupling of oscillators from strong to weak, and the splitting is similar to Rabi splitting during the resonant HHG. While this effect definitely needs a more detailed consideration, it also clarifies why SAE methods are not directly applicable to two-colour HHG unless artificial potential barriers are included to represent a strong coupling of oscillators.

QPM enhancement of HHG looks intuitive. If we separate sequential plasma jets so that the jet length is smaller or equal to the so called "length of coherence", aiming to remove negative interference of the propagated and newly generated harmonics, HHG indeed grows. But what reduces the phase mismatch between the jets so that HHG in different jets differs from the HHG in a single jet Gouy phase variation has been assumed to compensate the phase mismatch, but in typical QPM experiments its variation is not sufficient. Free electrons without ions between jets can explain the enhancement, but this assumption is quite restrictive. While in thin capillaries the influence of positive dispersion is significant to compensate this phase mismatch, this is also not the case for laser plasmas. What if the QPM in laser plasmas differs from the QPM in a gas filled capillary by principle, that is, the ablated surface playing a role in local field enhancement? Here we assume that the collective excitations in periodically modulated laser plasma can also produce an equivalent of Fano resonance in a sequence of Fabry-Perot resonators represented by jets. It has been shown [17] that consecutive Fano resonances have opposite polarity, so this effect makes them equivalent to periodically poled crystals used for quasi-phase matching for low-order harmonics.

To sum it up, we propose that the model of coupled oscillations is the universal theoretical description of seemingly very different processes of experimental HHG enhancement.

References

[1] Ganeev, R. A., Suzuki, M., Ozaki, T., Baba, M., & Kuroda, H. (2006). Strong resonance enhancement of a single harmonic generated in extreme ultraviolet range. Optics Letters 31(1699).

[2] Ganeev, R. A., Singhal, H., Naik, P. A., Arora, V., Chakravarty, U., Chakera, J. A., Khan, R. A., Kulagin, I. A., Redkin, P. V., Raghuramaiah, M., & Gupta, P. D. (2006). Harmonic generation from indium-rich plasmas. Physical Review a 74(063824).

[3] Ganeev, R. A., Suzuki, M., Redkin, P. V., Baba, M., & Kuroda, H. (2007) Variable pattern of high harmonic spectra from a laser-produced plasma by using chirped pulses of narrow-bandwidth radiation. Physical Review a 76(023832).

[4] Ganeev, R. A., Singhal, H., Naik, P. A., Kulagin, I. A., Redkin, P. V., Chakera, J. A., Tayyab, M., Khan, R. A., & Gupta, P. D. (2009). Enhancement of high-order harmonic generation using a two-color pump in plasma plumes. Physical Review a 80(033845).

[5] Pirri, A., Corsi, C., & Bellini, M. (2008). Enhancing the yield of high-order harmonics with an array of gas jets. Phys. Rev. 78(011801).

[6] Ganeev, R. A., Suzuki, M., & Kuroda, H. (2014). Quasi-phase-matching of high-order harmonics in multiple plasma jets. Physical Review a 89(033821).

[7] Lewenstein, M., Balcou, Ph., Ivanov, M. Yu., L'Huillier, A., & Corkum, P. B. (1994) Theory of high-harmonic generation by low-frequency laser fields. Physical Review a 49(2117).

[8] Milošević, D. B. (2006). Theoretical analysis of high-order harmonic generation from a coherent superposition of states. Journal of Optical Society of America B 23(308).

[9] Frolov, M., Manakov, N., & Starace, A. F. (2010). Potential barrier effects in high-order harmonic generation by transition-metal ions. Physical Review a 82(023424).

[10] Strelkov, V. V. (2010). Role of Autoionizing state in resonant high-order harmonic generation and attosecond pulse production. Physical Review Letters 104(123901).
[11] Redkin, P. V., & Ganeev, R. A. (2017). Model of resonant high harmonic generation in multi-electron systems. Journal of Physics B: Atomic, Molecular, and Optical Physics 50(185602).
[12] Strelkov, V. V., Khokhlova, M. A., & Shubin, N. Yu. (2014). High-order harmonic generation and Fano resonances. Physical Review a 89(053833).
[13] Agarwal, G. S. (1991). Origin of gain in systems without inversion in bare or dressed states. Physical Review a 44(R28).
[14] Arbel, M., Abramovich, A., Eichenbaum, A. L., Gover, A., Kleinman, H., Pinhasi, Y., & Yakover, I. M. (2001). Superradiant and Stimulated Superradiant Emission in a Prebunched Beam Free-Electron Maser. Physical Review Letters 86(2561).
[15] Frolov, M. V., Manakov, N. L., Minina, A. A., Vvedenskii, N. V., Silaev, A. A., Ivanov, M. Yu., & Starace, A. F. (2018). Control of harmonic generation by the time delay between two-color, bicircular few-cycle mid-ir laser pulses. Physical Review Letters 120(263203).
[16] Limonov, M. F., Rybin, M. V., Poddubny, A. N., & Kivshar, Yu. S. (2017). Fano resonances in photonics. Nature Photonics 11(543).
[17] Sturmberg, B. C. P., Dossou, K. B., Botten, L. C., McPhedran, R. C., & de Sterke, C. M. (2015). Fano resonances of dielectric gratings: symmetries and broadband filtering. Optics Express 23(A1672).

Investigating Laser Plasma Dynamics with High-order Harmonics Generation in Carbon-containing Nanomaterials

Vyacheslav V. Kim, Rashid A. Ganeev

Institute of Astronomy, University of Latvia, Latvia
vyacheslav.kim@lu.lv

Introduction

We study high-order harmonics generation from the plasmas produced on the surfaces of the graphite, fullerenes (C_{60}), carbon nanotubes (CNT), carbon nanofibers (CNF), diamond nanoparticles (DN), graphene (Gr) and epoxy resin composed targets. Our approach utilises a two-laser configuration with heating of targets by nanosecond laser pulses to produce plasmas that serve as the media for subsequent high-order harmonic generation (HHG) from a second femtosecond laser pulse. High-order harmonics are generated at different time delays following the plasma formation, which allows us to analyse the spreading of species with different masses. We analyse the harmonic yields from single carbon atoms, 60 atoms (fullerene), 10^6 atoms (DN), 10^9 atoms (CNTs and CNFs), and even much larger species of graphene sheets. The harmonic yields are analysed in the range of 100 ns – 1 ms delays between the heating pulses (HP) and driving pulses (DP). The harmonic yields were significantly higher within the 200 ns – 0.5 μs range of delays, but no harmonics were observed between 10 μs – 1 ms.

An analysis of the application of longer (nanosecond) pulses for target ablation during HHG in laser-induced plasma (LIP) compared to picosecond pulses, has previously been reported in [1]. Nanosecond laser ablation has been widely used to synthesize various metal and oxide nanoparticles (NPs). However, numerous factors such as duration of the laser pulse, fluence, and characteristics of irradiated targets affect the properties of synthesised NPs. The pulse duration is one of the most important parameters when considering the in-situ synthesis of NPs in LIP. The used approach has already been reported in studies to analyse harmonic's delay dependencies from different ZnO-contained targets, resonance-enhanced harmonics in mixed LIPs, and HHG during propagation of femtosecond pulses through different ablated species [2–4].

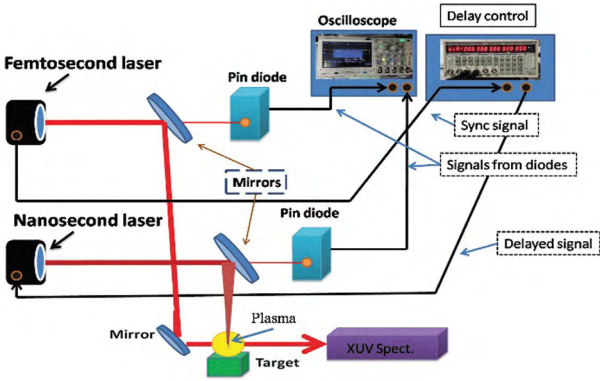

Fig. 1. *Schematic of the experimental setup for two laser HHG experiments with tuneable delay between heating nanosecond pulse and probing femtosecond pulse*

Experiment

For laser plasma formation, the 5 ns heating laser pulses (λ = 1064 nm, 5 mJ, 10 Hz) from a Nd:YAG laser were used. The HP were focused by a 300 mm focal length spherical lens on the target surface. Femtosecond pulses (50 fs, 806 nm, 2 mJ) from a Ti:sapphire laser were focused inside the plasma plume to generate harmonics (Fig. 1). The intensity of the driving pulses in the plasma area was maintained to be ~2×10^{14} W cm^{-2}. The delay between HP and DP was tuned using the delay generator. The variable electronic delay range was equal to 0–106 ns. The harmonics and plasma emission were detected using a flat field grazing-incidence XUV spectrometer.

Results

The delay dependence for the integrated harmonics signal is demonstrated on Fig. 2, panel (a). Fig. 2, panel (b) shows the saturated images of harmonics collected by a CCD camera from the phosphorous screen of the microchannel plate of the XUV spectrometer at the optimal delays of each studied sample. The purpose of such a presentation of harmonics distribution is to define the maximal order of generated harmonics, i.e., harmonic cut-off, and for better viewing of the difference in harmonic intensities from various species.

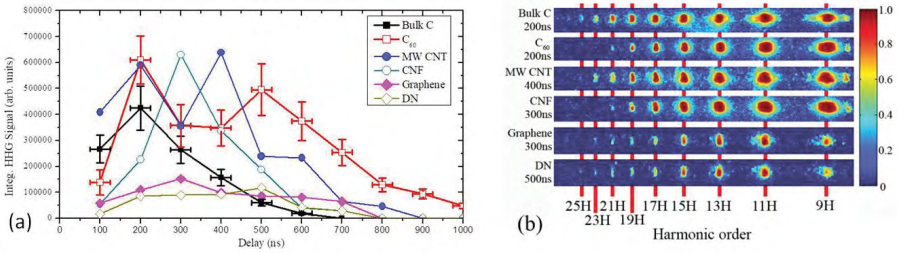

Fig. 2. *Panel **(a)**: Dependences of the integrated yield comprising 9th to 25th harmonics on the delay between nanosecond heating pulse (HP) and femtosecond driving pulse (DP). Panel **(b)**: Raw images of the harmonics at the optimal delay for each plasma sample. Images are normalised and logarithmically scaled. For bulk C, the maximal yield of harmonics is shown at a delay equal to 200 ns. The optimal delays for C60, CNT, CNF, Gr, and DN were 200, 400, 300, 300, and 500 ns, respectively*

We address the importance of considering the above delay-dependent experiments for understanding the dynamics of plasma propagation. The signature, indicating the presence of specific emitters, is the increase in the output of harmonics at certain specific delays from the beginning of ablation. An approximate similarity in the latter parameter led to similarity, to some extent, of the cut-off harmonics, while a larger number of atoms in nanostructures allowed increasing the cross section of recombination of the accelerated electron with the parent particle. The latter peculiarity distinguished the harmonic yields from the single-atomic plasma produced from ablated graphite and the multi-atomic plasma produced from other studied carbon-contained species (fullerenes, nanotubes, nanofibers, diamond nanoparticles, and graphene). Thus, by combining the analysis of delay dependences of integrated harmonic signals and of the HHG spectra in the 30–100 nm wavelength range the role of the carbon monomers, small-sized carbon molecules, and large nanoparticles in the former process has been revealed.

Acknowledgements

This work was supported by ERDF project (No. 1.1.1.5/19/A/003).

References

[1] Ganeev, R. A., Suzuki, M., Baba, M., & Kuroda, H. (2007). High harmonic generation from the laser plasma produced by the pulses of different duration. Phys. Rev. a 76(2), 023805.

[2] Venkatesh, M., Ganeev, R. A., Rao, K. S., Boltaev, G. S., Zhang, K., Srivastava, A., Bindra, J. K., Singh, S., Kim, V. V., Maurya, S. K., Strouse, G. F., Dalal, N. S., & Guo, C. (2019). Influence of gadolinium doping on low- and high-order nonlinear optical properties and transient absorption dynamics of ZnO nanomaterials. Opt. Mater. 95(10), 109241.

[3] Boltaev, G. S., Ganeev, R. A., Strelkov, V. V., Kim, V. V., Zhang, K., Venkatesh, M., & Guo, C. (2019). Resonance-enhanced harmonics in mixed laser-produced plasmas. Plasma Res. Express 1(3), 035002.

[4] Ganeev, R. A., Boltaev, G. S., Zhang, K., Maurya, S. K., Venkatesh, M., Yu, Z., Kim, V. V., Redkin, P. V., & Guo, C. (2019). Role of carbon clusters in high-order harmonic generation in graphite plasmas. OSA Continuum 2(5), 1510–1523.

Control of Quasi-Phase-Matched High Harmonic Generation in Structured Plasmas

Michael Wöstmann, Helmut Zacharias

Center for Nanotechnology and Center for Soft Nanoscience, University of Münster, Germany
H.Zacharias@uni-muenster.de

High-order harmonic generation (HHG) is an important and versatile method for the generation of ultrashort light pulses in the extreme ultraviolet (XUV) spectral range, in particular for attosecond science [1]. Unfortunately, the conversion efficiency of this process is rather low. Therefore, schemes are sought which bear the promise of a significant enhancement of the yield into a specific harmonic. One successful way is to find in various gaseous materials accidental strong resonances in the vicinity of a certain harmonic. This has been impressively shown, e.g., for In and Sn plasmas [2, 3]. Another scheme builds on the realisation of quasi-phase matching, which has been successfully applied in the near-IR spectral range in optically nonlinear solids, in particular in periodically poled $LiNbO_3$ [4]. It has also been shown previously in the field of high-order harmonic generation [5–9]. In the present contribution we want to show a system which can easily be used for plasmas to control the harmonic order which is enhanced by quasi-phase matching.

The experimental realisation is based on a physically structured plasma target [10]. Laser ablation of this target leads to a spatially structured plasma with dimensions closely resembling those of the target. Fig. 1 shows schematically the experimental set-up. The target consists of a stack of metallic disks separated by spacers with a significantly smaller diameter. Both the width and number of target disks, as well as the width of the spacers, can easily be adapted to the needs of the experiment. Rotating the target ensures fresh surfaces for each of the 1 kHz ablating pulses (12 ps, 2 mJ). The ablating laser is focused by a cylindrical lens (CL) to a line focus whose length can be adjusted by a knife edge. The fundamental (800 nm, 40 fs, 0.22 mJ, 1 kHz) if focused by a f = 500 mm lens. The generated harmonics are spectrally separated by a VLS grating and detected by a MCP/phosphore screen and measured by a CCD camera.

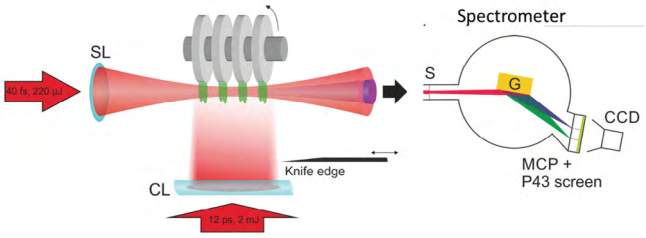

Fig. 1. *Experimental set-up showing the disk target and the XUV spectrometer with a VLS grating*

Fig. 2 shows a comparison of the intensity of the 25th harmonic (hv = 38.75 eV) for a target with four disks with that for an unstructured target (enhanced by a factor of 5). From the first intensity modulations of the unstructured target, the coherence length in the plasma for this harmonic can be derived. The intensity rises until one coherence length is reached. As expected, the coherence length decreases with an increasing order of the harmonics, from about 0.525 mm at the 13th harmonic to less than 0.35 mm for the 23rd. The optimal spacing of the disks is derived from the geometrical phase of the focused

fundamental beam. It is evident that with each new disk the harmonic intensity increases, in fact, the intensity increases quadratically with the effective length of the plasma jets.

Fig. 2b shows the easy control of the harmonic order for which QPM is achieved. By adjusting the width and spacing of the target disks this order can be shifted. For a smaller width and spacing, here 0.4 mm and 0.7 mm, respectively, higher harmonics are phase matched. In the present case that is optimal for the 21st and 23rd harmonic. Increasing both disk width and their spacing yields QPM for lower harmonics, here shown for the 17th and 19th.

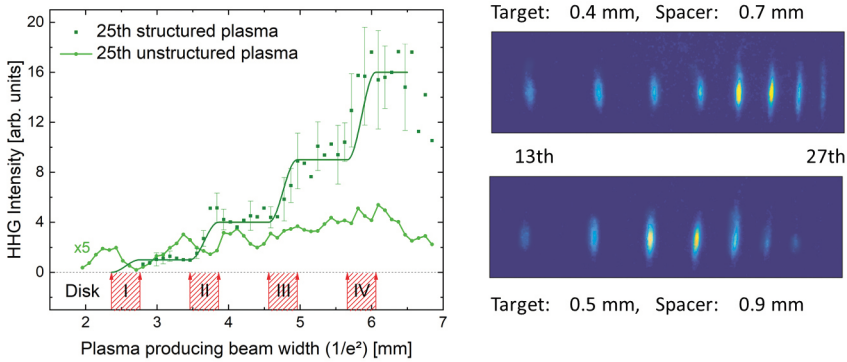

Fig. 2. (a) *Stepwise increase of the intensity of the 25th harmonic with the number of plasma jets;* ***(b)*** *control of QPM by choosing the target width and spacing*

References

[1] Krausz, F., & Ivanov, M. (2009). Attosecond Physics. Rev. Mod. Phys. 81, 163–234.

[2] Ganeev, R. A., Suzuki, M., Baba, M. Kuroda, H., & Ozaki, T. (2006). Strong resonance enhancement of a single harmonic generated in the extreme ultraviolet range. Opt. Lett. 31, 1699–1701.

[3] Suzuki, M., Baba, M. Ganeev, R. A., Kuroda, H., & Ozaki, T. (2006). Anomalous enhancement of a single high-order harmonic by using a laser-ablation tin plume at 47nm. Opt. Lett. 31, 3306–3308.

[4] Fejer, M. M., Magel, G. A., Jundt, D. H., & Byer, R. L. (1992). Quasi-phase-matched second harmonic generation: tuning and tolerances. IEEE J. Quant. Electron. 28, 2631–2654.

[5] Seres, J., Yakovlev, V. S., Seres, E., Streli, C., Wobrauschek, P., Spielmann, C., & Krausz, F. (2007). Coherent superposition of laser-driven soft-X-ray harmonics from successive sources. Nat. Phys. 3, 878–883.

[6] Pirri, A., Corsi, C., & Bellini, M. (2008). Enhancing the yield of high-order harmonics with an array of gas jets. Phys. Rev. a 78, 011801.

[7] Willner, A., Tavella, F., Yeung, M., Dzelzainis, T., Kamperidis, C., Bakarezos, M., Adams, D., Schulz, M., Riedel, R., Hoffmann, M. C., Hu, W., Rossbach, J., Drescher, M., Papadogiannis, N. A., Tatarakis, M., Dromey, B., & Zepf, M. (2011). Coherent control of high harmonic generation via dual-gas multijet arrays. Phys. Rev. Lett. 107, 175002.

[8] Ganeev, R. A., Suzuki, M., & Kuroda, H. (2014). Quasi-phase-matching of high-order harmonics in multiple plasma jets. Phys. Rev. a 89, 033821.

[9] Rosenthal, N., & Markus, G. (2015). Diskriminating between the role of phase matching and that of single-atom response in resonance plasma-plume high-order harmonic generation. Phys. Rev. Lett. 115, 133901.

[10] Sheinfux, A. H., Henis, Z., Levin, M., & Zigler, A. (2011). Plasma structures for quasiphase matched high harmonic generation. Appl. Phys. Lett. 98, 141110.

Quasi-Phase Matching of High-Order Harmonics in Mid-IR Laser Fields

Sergey Yu. Stremoukhov

Faculty of Physics, Lomonosov Moscow State University, Russia
National Research Centre "Kurchatov Institute", Russia
sustrem@gmail.com

One of the most effective methods for generating harmonics having high photon energy is to use mid-IR laser systems as a driver of the non-linear processes in gas [1]. However, along with quadratic growth of the maximal number of generated harmonics during the laser field wavelength (λ) increase, the photon flux scales as $\lambda^{-5.5}$ [2]. To overcome the harmonics efficiency, drop, the usage of a two-colour laser scheme [3], or molecular resonances located near the pump spectrum for enhancement of harmonics yield driven by mid-IR fields was presented [4]. Here, we analyse the other way to increase the harmonics photon flux using the effects of quasi-phase matching (QPM) for high harmonics generated in periodic media [5, 6].

In numerical simulations, we suppose that the perforated gas media consists of a number of gas jets having spatial sizes d divided by free spaces forming the multi gas media (MGM). It interacts with a two-colour (w + 2w) laser field consisting of two linearly polarised components with zero-degree angle between their polarisation directions. Laser field wavelength scales from near IR (800 nm) to far IR (up to 15 μm) spectral diapason. Macro-parameters of the MGM (total length of the media, pressure of the gas, d and numbers of gas jets) also scales in wide ranges.

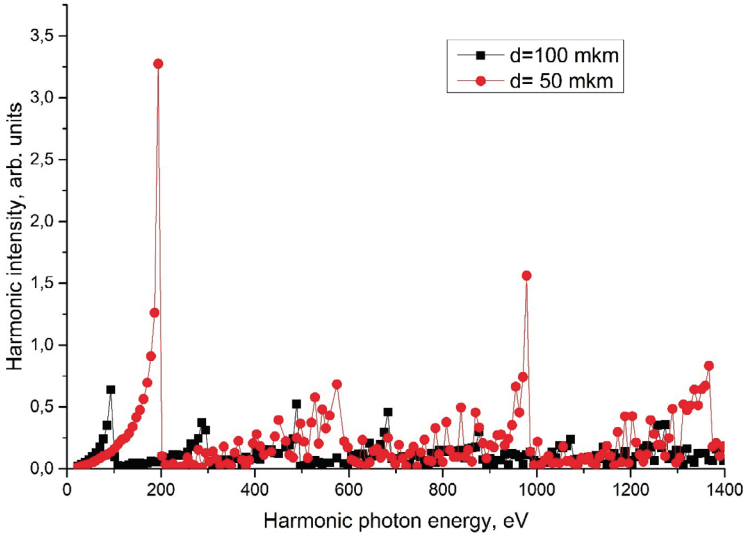

Fig. 1. *The QPM spectra generated by Argon MGM interacting with a two-colour laser field formed by the fundamental and the second harmonics of a Ti:Sa laser (λ = 800 nm). Calculations have been done for pressure 230 mbar and total MGM (25 jets for curve black curve with squares, 50 jets for red curve with circles) length L = 0.5 cm*

The numerical calculations based on the interference model of extended gas [7] and the non-perturbative theory of single atom response [8] show that, due to the QPM, the group of harmonics enhanced (please see Fig. 1). The influence of the gas media parameters and the laser wavelength on the position of enhanced harmonics and its value is analysed. Fig. 1 illustrates the influence of d on the position and efficiency of the QPM harmonics: a shorter d shifts the position of the QPM harmonics to the shorter wavelength part of the spectrum and increases its value. The simple relations between the position of the enhanced QPM harmonics, laser wavelength and MGM parameters are introduced. Boundaries of the harmonics' enhancement method are discussed.

Acknowledgements

The work was partially supported by the RFBR under Project No. 18-02-40014.

References

[1] Popmintchev, T., Chen, M.-C., Popmintchev, D., Arpin, P., Brown, S., Ališauskas, S., Andriukaitis, G., Balčiunas, T., Mücke, O. D., Pugzlys, A., Baltuška, A., Shim, B., Schrauth, S. E., Gaeta, A., Hernández-García, C., Plaja, L., Becker, A., Jaron-Becker, A., Murnane, M. M., & Kapteyn, H. C. (2012). Bright Coherent Ultrahigh Harmonicsin the keV X-ray Regime from Mid-Infrared Femtosecond Lasers. Science 336(1287).

[2] Tate, J., Auguste, T., Muller, H. G., Salières, P., Agostini, P., & DiMauro, L. F. (2007). Scaling of Wave-Packet Dynamics in an Intense Midinfrared Field. Physical Review Letters 98(013901).

[3] Lan, P., Takahashi, E. J., & Midorikawa, K. (2010). Wavelength scaling of efficient high-order harmonic generation by two-color infrared laser fields. Physical Review a 81(061802).

[4] Migal, E. A., Stremoukhov, S. Yu., & Potemkin, F. V. (2020). Ionization-free resonantly enhanced low-order harmonic generation in a dense gas mixture by a mid-IR laser field. Physical Review a 101(021401(R).

[5] Ganeev, R. A., Stremoukhov, S. Y., Andreev, A. V., & Alnaser, A. S. (2019). Application of Quasi-Phase Matching Concept for Enhancement of High-Order Harmonics of Ultrashort Laser Pulses in Plasmas. Applied Science 9(1701).

[6] Hareli, L., Shoulga, G., & Bahabad, A. (2020). Phase matching and quasi-phase matching of high-order harmonics generation – a tutorial. Journal of Physics B: Atomic, Molecular and Optical Physics 53(233001).

[7] Stremoukhov, S., & Andreev, A. (2018). Quantum-mechanical elaboration for the description of low- and high-order harmonics generated by extended gas media: prospects to the efficiency enhancement in spatially modulated media. Laser Physics 28(035403).

[8] Andreev, A. V., Stremoukhov, S. Yu., & Shoutova, O. A. (2012). Light-induced anisotropy of atomic response: prospects for emission spectrum control. European Physical Journal D 66(16).

Nonlinear Optical and Laser Effects in Micro Resonators Based on Silica and Non-silica Tellurite and Chalcogenide Glasses

Elena A. Anashkina, Alexey V. Andrianov

Institute of Applied Physics, Russian Academy of Sciences, Russia
elena.anashkina@ipfran.ru

One of the trends in modern photonics is the development of miniature devices based on micro resonators with whispering gallery modes (WGMs) [1, 2]. Such micro resonators have huge Q-factors and large nonlinear coefficients, which allows exploiting nonlinear and laser effects at very low pump powers. Promising applications of micro resonators are optical filtering and switching, remote sensing, spectroscopy and telecommunication [1–6]. Micro resonators can be used to generate non-classical states of light [2], e.g., squeezed light [7] and quantum correlated photon pairs [8]. Active micro resonators are used to obtain laser radiation [9]. In nonlinear micro resonators, Kerr optical frequency combs (OFCs) can be generated which significantly expands application areas of micro resonators [1]. Existing technologies make it possible to produce high-Q micro resonators based on various materials including silica and non-silica glasses [3]. Non-silica tellurite and chalcogenide glasses have huge values of cubic Kerr and Raman nonlinearities and mid-IR transparency (up to ~5–5.5 μm for tellurite and up to 8–20 μm for chalcogenide glasses), so their use expands the capabilities of silica micro resonators.

Here we present some of the recent achievements of our team concerning theoretical and experimental investigation of silica, tellurite, and chalcogenide glass spherical micro resonators.

We studied the OFC generation in a silica microsphere for a pump wavelength in a normal dispersion region, in a low anomalous dispersion region, and very close to a zero-dispersion wavelength [10]. Kerr-assisted and Raman-assisted (Stokes) combs as well as anti-Stokes combs emerging due to the four-wave mixing between the Kerr and Raman combs were demonstrated [10]. The mechanisms underlying the observed processes were studied [10].

We studied Raman-assisted nested OFCs in two different mode (TE and TM) families with soliton-like spectral envelopes for each mode family in a silica microsphere [11]. We studied the regime in which the pump wavelength (without an OFC nearby) was in the normal dispersion region and Raman-assisted OFCs were generated in the anomalous dispersion region [11].

We demonstrated Raman lasing in an As_2S_3 chalcogenide glass microsphere pumped by a C-band narrow line laser [12]. Single-mode Raman lasing tuneable between 1.610–1.663 μm was attained when tuning a pump laser wavelength in the 1.522–1.574 μm range (Fig. 1) [12]. When the pump power significantly exceeded the threshold, multimode cascade Raman lasing was achieved with the maximum Raman order of four at a wavelength of 2.01 μm (Fig. 1) [12].

We developed theoretical approaches and created a numerical code to investigate lasing in tellurite microspheres, including simultaneously on different radiative transitions of the same rare-earth ion [13]. The models were developed taking into account the mode competition, and the found solutions were checked for stability [13]. For the first time, a detailed theoretical analysis of CW multicolour lasing at different radiative transitions was conducted for Tm-doped tellurite micro resonators [13]. It was found that, depending on the Q-factor and pump power, single-colour lasing, two-colour lasing, and three-

colour lasing is possible. We also developed a simple yet efficient analytical model to describe lasing in Er-doped tellurite microspheres [14]. It was theoretically demonstrated that for low Q-factors, generation occurs in the C-band, and for relatively high Q-factors, generation occurs in the L-band, and switching between these regimes occurs with a jump, which agrees with experimental observations [14].

A theoretical model was developed to describe thermo-optical effects in silica and tellurite micro resonators [15]. First, in the frame of finite element simulation, temperature distributions were calculated. Then, taking into account the found temperature distributions, shifts of the WGM eigenfrequencies were calculated. Within the frame of the developed model, detailed theoretical studies of steady-state and transient thermal effects were carried out in tellurite and silica microspheres. Results for the tellurite microspheres agree with the experimental results [15].

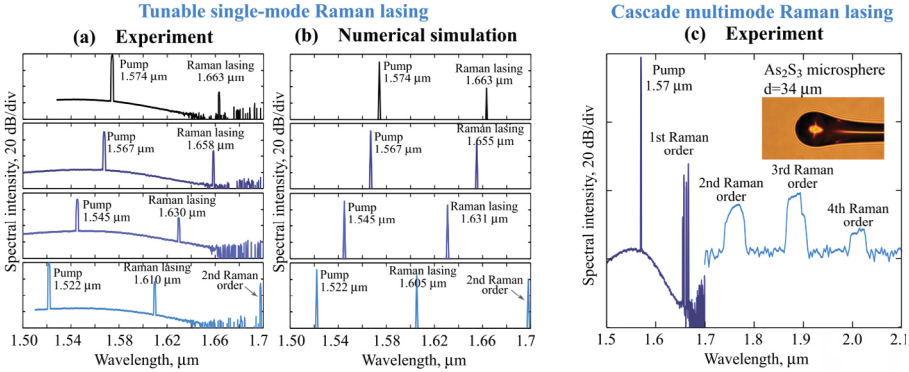

Fig. 1. *Experimental spectra of tuneable single-mode Raman lasing* ***(a)*** *and the corresponding numerically simulated spectra* ***(b)*** *in 34-μm As_2S_3 glass microsphere [12].* ***(c)*** *Experimental spectrum of four-cascade Raman lasing recorded by OSA (dark blue curve) and by PbSe detector plus monochromator (light blue curve) [12]. The inset shows the micro photo of the used home-made As_2S_3 glass microsphere*

Acknowledgements

This work is supported by the Russian Science Foundation, Grant No. 20-72-10188 (study of micro resonators based on silica and tellurite glasses) and by the Mega-grant of the Ministry of Science and Higher Education of the Russian Federation, Contract No. 14. W03.31.0032 (study of micro resonators based on chalcogenide glasses).

References

[1] Pasquazi, A., Peccianti, M., Razzari, L., Moss, D. J., Coen, S., Erkintalo, M., Chembo, Y. K., Hansson, T., Wabnitz, S., Del'Haye, P., Xue, X., Weiner, A. M., & Morandotti, R. (2018). Micro-combs: a novel generation of optical sources. Physics Reports, 729, 1–81.

[2] Strekalov, D. V., Marquardt, C., Matsko, A. B., Schwefel, H. G., & Leuchs, G. (2016). Nonlinear and quantum optics with whispering gallery resonators. Journal of Optics 18(12), 123002.

[3] Kovach, A., Chen, D., He, J., Choi, H., ..., & Armani, A. M. (2020). Emerging material systems for integrated optical Kerr frequency combs. Advances in Optics and Photonics 12(1), 135–222.

[4] Foreman, M. R., Swaim, J. D., & Vollmer, F. (2015). Whispering gallery mode sensors. Advances in optics and photonics 7(2), 168–240.

[5] Pfeifle, J., Brasch, V., Lauermann, M., Yu, Y., Wegner, D., Herr, T., ..., & Koos, C. (2014). Coherent terabit communications with micro resonator Kerr frequency combs. Nature photonics 8(5), 375–380.

[6] Salgals, T., Alnis, J., Murnieks, R., Brice, I., Porins, J., Andrianov, A. V., Anashkina, E. A., Spolitis, S., & Bobrovs, V. (2021). Demonstration of a fiber optical communication system employing a silica microsphere-based OFC source. Optics Express 29(7), 10903–10913.
[7] Otterpohl, A., Sedlmeir, F., Vogl, U., Dirmeier, T., Shafiee, G., Schunk, G., ..., & Marquardt, C. (2019). Squeezed vacuum states from a whispering gallery mode resonator. Optica 6(11), 1375–1380.
[8] Caspani, L., Reimer, C., Kues, M., Roztocki, P., Clerici, M., Wetzel, B., ..., & Morandotti, R. (2016). Multifrequency sources of quantum correlated photon pairs on-chip: a path toward integrated Quantum Frequency Combs. Nanophotonics 5(2), 351–362.
[9] He, L., Özdemir, Ş. K., & Yang, L. (2013). Whispering gallery microcavity lasers. Laser & Photonics Reviews 7(1), 60–82.
[10] Anashkina, E. A., & Andrianov, A. V. (2021). Kerr-Raman Optical Frequency Combs in Silica Microsphere Pumped Near Zero Dispersion Wavelength. IEEE Access, 9, 6729–6734.
[11] Andrianov, A. V., & Anashkina, E. A. (2021). Raman-assisted optical frequency combs generated in a silica microsphere in two whispering gallery mode families. Laser Physics Letters 18(2), 025403.
[12] Andrianov, A. V., & Anashkina, E. A. (2021). Tunable Raman lasing in an As2S3 chalcogenide glass microsphere. Optics Express 29(4), 5580–5587.
[13] Anashkina, E. A., Leuchs, G., & Andrianov, A. V. (2020). Numerical simulation of multi-color laser generation in Tm-doped tellurite microsphere at 1.9, 1.5 and 2.3 microns. Results Phys. 16, 102811.
[14] Anashkina, E. A., & Andrianov, A. (2021). Erbium-Doped Tellurite Glass Microlaser in C-Band and L-Band. Journal of Lightwave Technology. https://doi.org/10.1109/JLT.2021.3064999
[15] Andrianov, A. V., Marisova, M. P., Dorofeev, V. V., & Anashkina, E. A. (2020). Thermal shift of whispering gallery modes in tellurite glass microspheres. Results in Physics 17, 103128.

From Ultra-stable Laser Resonators for Atomic Spectroscopy and Fiber-based Femtosecond Optical Frequency Combs to Whispering-gallery-mode Micro Resonator Sensors and Microsphere Optical Frequency Combs for Telecommunication Data Transfer

Jānis Alnis, Aigars Atvars, Roberts Berķis, Dina Bērziņa, Uldis Bērziņš, Inga Brice, Artūrs Ciniņš, Kristians Draguns, Kārlis Grundšteins, Viesturs Ignatāns, Lāse Mīlgrāve, Pauls Kristaps Reinis, Arvīds Sedulis, Alma Ūbele

Institute of Atomic Physics and Spectroscopy, University of Latvia, Latvia
janis.alnis@lu.lv

Improving the precision of optical spectroscopy of atomic hydrogen over several decades at the Max Planck Institute of Quantum optics [1] has led to the development of an optical frequency comb method that allows one to count the frequency of light and has activated a field of optical atomic clocks. The stability of the laser spectral line has reached the thermal noise limit of sub-Hz linewidth [2]. The thermal noise limit was also reached in the optical whispering gallery mode (WGM) micro resonators [3]. Ultra-stable laser radiation can be transferred using an interferometrically stabilised optical fiber link across the continent between the metrology labs [4].

The Fotonika-LV Project [5] in Latvia has allowed the establishment of a Quantum optics lab in 2013, acquiring a fiber-based optical frequency comb (Menlo Systems 250 MHz) and building a stable laser resonator [6]. In order to learn how to use the comb, we re-measured the rubidium saturated absorption line frequencies [7]. We have built a two-mirror ring-down resonator for acetone measurements in breath [8]. Afterwards we switched from classical two-mirror resonators to so-called whispering gallery mode (WGM) micro resonators that circulate the light by total internal reflection and can be used in biosensors [9]. a resonance condition occurs when in a roundtrip fits an integer number of light waves. We make SiO_2 microsphere WGM resonators by melting a tip of high purity telecom fiber and reach optical Q factors in the 10^6–10^8 range. The most straightforward application is a WGM temperature sensor [10] as both the index of refraction and physical dimensions change with temperature. The next application is to coat the micro resonator surface with a thin coating, for example, ZnO using atomic layer deposition method [11], and a glucose oxidase enzyme for glucose sensing [12]. Sensitivity can be further enhanced by adding gold nanoparticles to the coating to excite surface plasmon resonances [13]. Drifts of microsphere resonances can be referenced to atomic rubidium lines [14]. WGM resonances can also be excited in a liquid droplet, and we demonstrated glycerol droplet WGM with very high sensitivity to relative humidity [15].

Another application is to induce nonlinear optical phenomena such as four-wave mixing, Kerr and Raman effects by pumping microspheres with several hundreds of milliwatts of CW laser power. Thanks to the high optical Q factor, the circulating power in an approximately 10 mm^2 mode area can reach GW/cm^2. At such high intensities new optical frequencies are generated. The resonator allows generating frequencies that satisfy constructive interference after a roundtrip. This leads to the generation of a Kerr frequency comb in the micro resonator manifesting as equally spaced lines in the optical spectrum [16]. We have demonstrated the use of the Kerr frequency comb in a silica microsphere for telecommunications by using comb lines as a carrier for telecom data [17]. Comb use for telecommunications requires only a single comb generator laser instead of separate lasers for each colour.

Acknowledgements

The research was supported by the ERDF project No. 1.1.1.1/18/A/155 "The Development of optical frequency comb generator based on a WGMR and its applications in telecommunications" and the Latvian Council of Science project No. lzp-2018/1-0510 "Optical whispering gallery mode micro resonator sensors".

References

[1] Parthey, C. G., Matveev, A., Alnis, J., Bernhardt, B., Beyer, A., Holzwarth, R., Maistrou, A., Pohl, R., Predehl, K., Udem, T., Wilken, T., Kolachevsky, N., Abgrall, M., Rovera, D., Salomon, C., Laurent, P., & Hänsch, T. W. (2011). Improved measurement of the hydrogen 1S–2S transition frequency. Phys. Rev. Lett. 107, 203001.

[2] Alnis, J., Matveev, A., Kolachevsky, N., Udem, T., Hänsch, T. W. (2008). Subhertz linewidth diode lasers by stabilization to vibrationally and thermally compensated ultralow-expansion glass Fabry-Pérot cavities. Physical Review a 77(5), 053809.

[3] Alnis, J., Schliesser, A., Wang, C. Y., Hofer, J., Kippenberg, T. J., & Hänsch, T. W. (2011). Thermal-noise-limited crystalline whispering-gallery-mode resonator for laser stabilization. Phys. Rev a 84, 011804(R).

[4] Predehl, K., Grosche, G., Raupach, S. M. F., Droste, S., Terra, O., Alnis, J., Legero, Th., Hänsch, T. W., Udem, Th., Holzwarth, R., & Schnatz, H. (2012). a 920-Kilometer Optical Fiber Link for Frequency Metrology at the 19th Decimal Place. Science 336, 441–444.

[5] Fotonika-LV, Unlocking and Boosting Research Potential for Photonics in Latvia – Towards Effective Integration in the European Research Area. FP7-REGPOT-2011-1 project (2012–2015).

[6] Bluss, K., Atvars, A., Brice, I., & Alnis, J. (2015). Broadband Fabry-Pérot resonator from Zerodur for laser stabilization below 1 kHz linewidth with <100 Hz/s drift and reduced sensitivity to vibrations. Latvian Journal of Physics and Technical Sciences N3, 11–20.

[7] Brice, I., Rutkis, J., Fescenko, I., Andreeva, Ch., & Alnis, J. (2015). Optical frequency measurement of Rb 5S-5P transition with a frequency comb. European Group of Atomic Systems EGAS47, Riga, July 14–17.

[8] Revalde, G., Alnis, J., Nitiss, E., Bluss, K., & Grundsteins, K. (2017). Cavity Ring-Down Spectroscopy measurements of Acetone concentration. Journal of Physics Conference Series 810(1), 012036.

[9] Brice, I., Pirktina, A., Ubele, A., Grundsteins, K., Atvars, A., Viter, R., & Alnis, J. (2017). Development of optical WGM resonators for biosensors. SPIE proceedings, 105920B.

[10] Berķis, R., Alnis, J., Brice, I., Atvars, A., Draguns, K., Grundšteins, K., & Reinis, P. K. (2021). Mode family analysis for PMMA WGM micro resonators using spot intensity changes. Laser Resonators, Microresonators, and Beam Control XXIII 11672, 1167217.

[11] Brice, I., Viter, R., Draguns, K., Grundsteins, K., Atvars, A., Alnis, J., Coy, E., & Igorlatsunskyi, I. (2020). Whispering gallery mode resonators covered by a ZnO nanolayer. Optik 219, 165296.

[12] Brice, I., Grundsteins, K., Atvars, A., Alnis, J., Viter, R., & Ramanavicius, A. (2020). Whispering gallery mode resonator and glucose oxidase based glucose biosensor. Sensors and Actuators B: Chemical 318, 128004.

[13] Brice, I., Grundsteins, K., Atvars, A., Alnis, J., & Viter, R. (2019). Whispering gallery mode resonators coated with Au nanoparticles. Nanoengineering: Fabrication, Properties, Optics, Thin Films, and Devices, SPIE 110891T.

[14] Brice, I., Atvars, A., Viter, R., & Alnis, J. (2019). Whispering gallery mode resonator sensors referenced to saturated absorption lines in rubidium atoms and a fs frequency comb. CLEO-Europe, ch_p_30.

[15] Reinis, P. K., Milgrave, L., Draguns, K., Brice, I., Alnis, J., & Atvars, A. (2021). High-Sensitivity Whispering Gallery Mode Humidity Sensor Based on Glycerol Microdroplet Volumetric Expansion. Sensors 21, 1746.

[16] Braunfelds, J., Murnieks, R., Salgals, T., Brice, I., Sharashidze, T., Lyashuk, I., Ostrovskis, A., Spolitis, S., Alnis, J., Porins, J., & Bobrovs, V. (2020). Frequency comb generation in WGM microsphere based generators for telecommunication applications. Quantum Electronics 50(11), 1043.

[17] Salgals, T., Alnis, J., Murnieks, R., Brice, I., Porins, J., Andrianov, A. V., Anashkina, E. A., Spolitis, S., & Bobrovs, V. (2021). Demonstration of fiber optical communication system employing silica microsphere-based OFC source. Optics Express, in press.

Theoretical Analysis of the Limiting Factors for Quantum Noise Squeezing of Ultrashort Pulses in Optical Fibers

Arseny A. Sorokin[1], Alexey V. Andrianov[1], Gerd Leuchs[1,2], Elena A. Anashkina[1]

[1] *Institute of Applied Physics, Russian Academy of Sciences, Russia*
[2] *Max Planck Institute for the Science of Light, Germany*
arsorok1997@yandex.ru, elena.anashkina@ipfran.ru

Quantum noise suppression of CW and pulsed light is required for many applications including quantum sensing, quantum communication, and detection of gravitational waves [1]. There are several ways to obtain squeezed light which is a quantum state with a variance of one field quadrature being below the value of a coherent or a vacuum state (whereas the conjugated quadrature variance is above the variance of the vacuum in order to satisfy Heisenberg's uncertainty relation) (see [1] and references therein). One way is Kerr squeezing in optical fibers demonstrated for the first time in [2] and is still actively investigated [3]. For quantum noise suppression of CW radiation, fiber lengths of about a hundred meters are required, and limiting factors are optical loss and guided acoustic wave Brillouin scattering (GAWBS) [4]. For solitons with duration ~100–200 fs and a high peak power, significantly shorter fibers are required (of about ten meters), and instead of loss or GAWBS, Raman effects limit squeezing [5].

Here we analyse the possibility of quantum noise squeezing of solitons with duration of 200 fs, 500 fs, and 1 ps in an optical fiber with realistic parameters using home-made software. The simulation of pulse propagation with allowance for quantum noise entails modelling multimode many-body quantum system dynamics. We achieve this here with a truncated Wigner technique, which provides accurate results for relatively short propagation distances and a large number of photons. We model the Raman-modified stochastic nonlinear Schrödinger equation [6] with allowance for losses. The initial condition is a fundamental soliton with adding normally distributed stochastic quantum noise. In modelling, we switch on/off Raman effects and loss to find their contributions to the squeezing of solitons with different durations. The simulated polarisation squeezing [7] as a function of a fibre length is plotted in Fig. 1 (a, b, c) for soliton durations of 200 fs, 500 fs, and 1 ps, respectively.

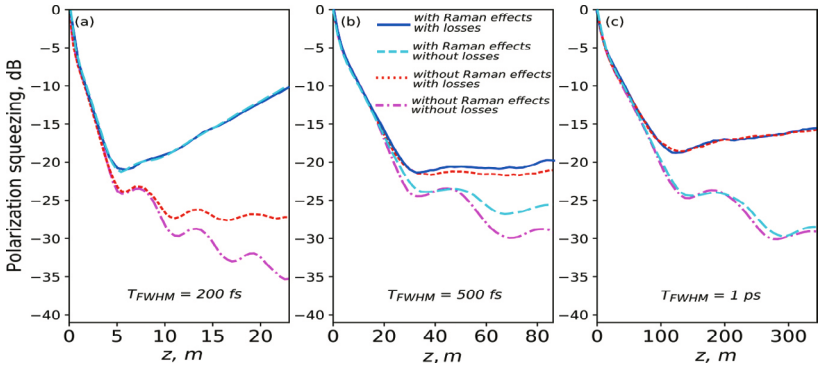

Fig. 1. *Polarisation squeezing simulated for pulse durations of 200 fs* ***(a)****, 500 fs* ***(b)****, and 1 ps* ***(c)*** *using sets of 1000 independent realisations. Here the nonlinear Kerr coefficient is 0.093 (W km)1, dispersion is 28.0 ps2/km, fibre loss is 1 dB/km, central wavelength is 1.5 μm, temperature is 300 K*

For fundamental solitons, the peak power is inversely proportional to the square of the pulse duration, so for longer pulses the required distances are longer, and the loss impact is stronger. For shorter pulses, their spectra are wider, so the overlap with spectrum of the Raman function is larger. When Raman effects are switched on, squeezing of the shortest 200-ps pulses is dramatically decreased, while squeezing of 500-fs and 1-ps pulses is slightly affected. Simulations demonstrate that optimal fiber lengths are the following: <10 m for 200-fs pulses, several tens of meters for 500-fs pulses, and >100 m for 1-ps solitons. Solitons with a duration of 500 fs are preferable to attain the strongest quantum noise squeezing (21 dB), since for them the balance between limiting factors (losses for 1-ps pulses and Raman effects for 200-fs pulses) is satisfied.

Acknowledgements

This work was funded by the Mega-grant of the Ministry of Science and Higher Education of the Russian Federation, Contract No. 14.W03.31.0032 and by the Russian Foundation for Basic Research, Grant No. 19-29-11032.

References

[1] Andersen, U. L., Gehring, T., Marquardt, C., & Leuchs, G. (2016). 30 years of squeezed light generation. Physica Scripta 91(5), 053001.

[2] Shelby, R. M., Levenson, M. D., Perlmutter, S. H., DeVoe, R. G., & Walls, D. F. (1986). Broad-band parametric deamplification of quantum noise in an optical fiber. Physical review letters 57(6), 691.

[3] Anashkina, E. A., Andrianov, A. V., Corney, J. F., & Leuchs, G. (2020). Chalcogenide fibers for Kerr squeezing. Optics Letters 45(19), 5299–5302.

[4] Shelby, R. M., Levenson, M. D., & Bayer, P. W. (1985). Guided acoustic-wave Brillouin scattering. Physical Review B 31(8), 5244.

[5] Dong, R., Heersink, J., Corney, J. F., Drummond, P. D., Andersen, U. L., & Leuchs, G. (2008). Experimental evidence for Raman-induced limits to efficient squeezing in optical fibers. Optics Letters 33(2), 116–118.

[6] Drummond, P. D., & Corney, J. F. (2001). Quantum noise in optical fibers. I. Stochastic equations. JOSA B 18(2), 139–152.

[7] Corney, J., Heersink, J., Dong, R., Josse, V., Drummond, P., Leuchs, G., & Andersen, U. L. (2008). Simulations and experiments on polarization squeezing in optical fiber. Phys. Rev. a 78(2), 023831.

TRIZ Forecast of the Development of Research on Optical Micro Resonators

Aigars Atvars[1], Alexander Narbut[2,3]

[1] *Institute of Astronomy, University of Latvia, Latvia*
[2] *Institute of Atomic Physics and Spectroscopy, University of Latvia, Latvia*
[3] *COMCON*TRIZ & FRT corporation, Ukraine*
aigars.atvars@lu.lv, alexander.narbut@gmail.com

The research on optical micro resonators has attracted significant attention in the last decades [1–3]. The micro resonators are optical structures that confine light due to total internal reflection and form an array of optical resonances that can be explored. These objects are used as sensors (temperature, humidity, wavelength, bio-sensing [4], and others) and as tools to study the nonlinear effects of optical materials (for example, the generation of a micro resonator frequency comb [3]). Various aspects of micro resonators have already been reported that reveal the novelty of the thought; yet forecasts of the further development of this research may be of high value. The theory of inventive problem solving (TRIZ) provides various guidelines for such achievements.

TRIZ has been developed by G. Altshuller and his colleagues since 1956 to advance the technology [5–6]. It contains tools that help to create solutions for technical problems and has underlying concepts that form the theory of this approach. According to TRIZ, technical systems, contrary to natural systems, are created to realise some function. These systems develop according to some laws that can be revealed by analysing the former development of various technical systems. G. Altshuller revealed and described these laws that are applicable for further development of technical systems. The most significant novelty of TRIZ is the use of the concept of contradiction, which inhibits the development of the technical system, but is also the basis for such development. The main instrument of TRIZ is the Algorithm for Inventive Problem Solving (recommended version ARIZ-85V), which includes many additional tools, such as the System of Standards-77. Nowadays, TRIZ is used in many areas of technology and science, including the patenting process [7–9].

Within TRIZ tools, there are various guidelines that can be used to forecast the development of systems. The description of some of them and application examples within the optical micro resonator field are given in Tab. 1.

Tab. 1. *The list of guidelines for system development and their applications seen in micro resonator research*

Guideline	Description of the guideline	Example from optical micro resonator research
Use of resources	System can be developed by better use of resources within the system or outside. The use of easily available or cheap resources is recommended. Geometry or space is also a resource	Readily available optical fibres can be used as materials for ball micro resonators. Fibre cleaver can be used to melt ball resonators from optical fibres

Guideline	Description of the guideline	Example from optical micro resonator research
Trimming	System can be developed by eliminating one of its parts and by redistribution of its functions to other parts	The prism is eliminated and substituted by tapered fibre which fills the functions of the prism and the laser ray that travelled to the prism
Synchronisation of parameters	System can be developed by synchronisation of its parameters among themselves or with significant external objects	Synchronisation of the refraction index of the prism and resonator Synchronisation of a wavelength of the system with the requirements of the industry (1.5 μm for telecommunication)
The use of internal effects (microsystems)	System can be developed by using internal resources of elements of the system, for example, their physical properties	The resonator is made of dielectric material (for example, SiO2) that has electrostriction properties and can be explored as such
Development in super-system	System can be developed by combining it with similar or other systems. Together they form a super-system.	An array of resonators are explored. Micro resonators are used for applications in various fields, for example, sensing (temperature, humidity, bio-sensing, and others)
Dynamization	System can be developed by changing its properties in time. For example, system adapts to the external environment	Typically, micro resonators have static positions of resonance frequencies. Resonators can be heated to change their resonance positions
Expansion over morphological matrix	System can be developed and explored (especially in research) by varying its elements	Various materials of resonators (SiO_2, MgF_2, CaF_2) Various geometries of resonators (ball, ring, toroid, bubble, spiral) Various additional effects (acoustic waves, machine learning) Various wavelengths (visible, IR, UV) Various intensities of laser (average, strong)
The development according to 77 standards	System can be developed by the use of the System of 76 Standard Solutions of TRIZ. This system can be used multiple times to apply for various parts of the system	Standard 1.1.3. – the use of additives to increase the performance of the system. Example: covering the resonator with some layer that is sensitive to biomolecules to improve the performance of the micro resonator

The guidelines given in Tab. 1 can be used to advance the research field of optical micro resonators. The preliminary analyses show that the perspective directions for development are – dynamization, trimming, and joining in super-systems.

Acknowledgements

The research was supported by the Latvian Council of Science project No. lzp-2018/1-0510 and ERDF project No. 1.1.1.5/19/A/003.

References

[1] Vahala, K. J. (2003). Optical microcavities. Nature 424(6950), 839–846.

[2] Yang, S., Wang, Y., & Sun, H. D. (2015). Advances and prospects for whispering gallery mode microcavities. Advanced Optical Materials 3(9), 1136–1162.

[3] Shen, B., Chang, L., Liu, J., et al. (2020). Integrated turnkey soliton microcombs. Nature 582(7812), 365–369.

[4] Brice, I., Grundsteins, K., Atvars, A., Alnis, J., Viter, R., & Ramanavicius, A. (2020). Whispering gallery mode resonator and glucose oxidase based glucose biosensor. Sensors and Actuators, B: Chemical 318.

[5] Altshuller, G. S. (1984). Creativity as an Exact Science (The Theory of the Solution of Inventive Problems). New York, London, Paris, Montreux, Tokyo: Gordon and breach science publishers, p. 176.

[6] Narbut, A. Th. (2015). Classical TRIZ, Project's Manual. University of Latvia. https://www.trizinfor.org/store/TRIZclassEn.pdf

[7] Nazidizaji, S., Tome, A., & Regateiro, F. (2015). Modelling design problems by Su-Field method – toward a problem-solving approach in architectural design studio. Procedia – Social and Behavioral Sciences 197, 2022–2031.

[8] Carvalhoa, M. A. de, Buzinar, C. G., Brandalizec, G. G., & Medeiros Chagasa, L. G. de (2012). Creativity in design and process problems with triz (theory of inventive problem solving) / systematic innovation. Product management & Development 10(2), 87–94.

[9] Verhaegen, P. A., D'hondt, J., Vertommen, J., Dewulf, S., & Duflou, J. R. (2009). Interrelating Products through Properties via Patent Analysis. Proceedings of the 19th CIRP Design Conference – Competitive Design, 252.

The Optimal (Tom and Jerry) Pairs of Cold Rydberg Atoms in the Penning Ionization Processes

Artūrs Ciniņš[1], Kaspars Mičulis[1], Nikolai Bezuglov[2]

[1] *Institute of Atomic Physics and Spectroscopy, University of Latvia, Latvia*
[2] *Saint Petersburg State University, Russia*
kaspars.miculis@lu.lv

We studied Penning ionization (PI) processes involving Rydberg states of alkali atoms in cold gas media. PI analysis has been performed in terms of the autoionization widths $\Gamma_N(R)$ of a quasi-molecule formed by a pair of collision partners with the fix internuclear distance R. Due to a long-range dipole-dipole interaction, one d- atom undergoes a transition from state $N_d = n_d l_d$ to a deeper bound state, while the other i-atom gains the released energy and jumps from state $N_i = n_i l_i$ to the continuum. An important feature of PI is the nontrivial dependence of its efficiency on the effective (n^*) and orbital (l) quantum numbers of the Rydberg states $N = N_i N_d$ of the atoms pair, in particular, on the size ~ n^{*2} of the particles. We have found optimal $N^{(opt)} = N^i N^{d(opt)}$, highly asymmetric ($n^{*2}_{d,opt} << n^{*2}_d$) configurations of Rydberg pairs (we call atoms 'Tom' and 'Jerry' for 'big' and 'small' ones[1]), which lead to explosive intensification (by several orders of magnitude, see Fig. 1) of the PI processes. This property makes PI an important source of primary (seed) charged particles when a cold Rydberg medium evolves into cold plasma [1]. We performed systematic calculations and have derived analytical expressions for both the optimal {*nili*, *nd_opt ld*} pairs and the corresponding reduced Penning autoionization widths $\tilde{\Gamma}_N(R) \equiv R^6 \Gamma_N(R)$ for different orbital l_i – l_d configurations of alkali atoms. As an example, the case of s-s states ($l_i = l_d = 0$) of Cs atoms pairs is exhibited in Fig. 1.

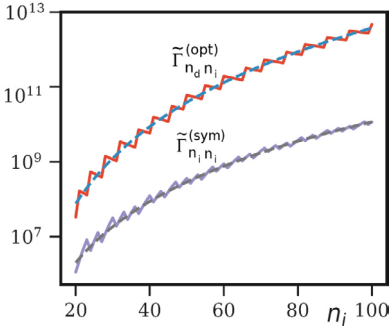

Fig. 1. *Reduced autoionization widths $\tilde{\Gamma}^{(opt)}_N$ (optimal pairs) and $\tilde{\Gamma}^{(sym)}_N$ (symmetric pairs) as functions of the principal quantum number n_i of ionizing i-atoms. Numerical (solid lines) and analytical results (dashed lines)*

Acknowledgements

This work was supported by the Latvian Council of Science Grant No. lzp-2019/1-0280.

References

[1] Efimov, D. K., Miculis, K., Bezuglov, N. N., & Ekers, A. (2016). Strong enhancement of Penning ionization for asymmetric atom pairs in cold Rydberg gases: The Tom and Jerry effect. J. Phys. B: At. Mol. Opt. Phys. 49, 125302.

Spectroscopy of the Atomic Boron

Arnolds Ūbelis

National Science Platform FOTONIKA-LV, University of Latvia, Latvia
arnolds.ubelis@lu.lv

Research on atomic spectroscopy of hardly volatile chemical elements like Boron (melting point 2076 °C, boiling point 3927 °C) is an experimental challenge caused by difficulties of atomisation. Therefore, the knowledge base of basic properties of B I and B II is not rich at all and need to be improved due to the increasing demand from various technology disciplines, atomic physics and astrophysics especially.

On the other hand, the implantation of boron ions in high purity germanium crystals [1], remaining the key material used for high energy radiation sensors, currently demands development of a handier and more cost-effective apparatus. The efforts of our team to respond to such a demand resulted in the development of a hybrid plasma source coupling together a hollow cathode and RF inductively coupled plasma discharge sources ensuring the atomisation of elemental Boron. The light spectrum coming from such device is dominated by the group of intensive resonance line duplets of B I and several resonance lines of B II. Therefore, we have a unique source for more comprehensive investigation of spectroscopy of B I and B II, particularly to measure branching ratios and to obtain transition probabilities of B I in the spectral region 1600–2500 Å. The latest data on Boron spectroscopy were published in 2009 [2], in 2010 [3] and are collected in a worldwide known database [4, 5].

We are going to use a mirror/quartz-prism high dispersion monochromator SPM-2 (*Carl Zeiss Jena*) upgraded with advanced hardware and software. The optical pass between the Boron atomic spectra source and the monochromator will be washed by a directed flow of nitrogen to ensure branching ratios measurements for the following duplets of B I: 1666.850, 1667.272; 1817.843, 1818.348; 1825.894, 1826.400; 2088.889, 2089.570; 2496.769, 2497.722 and B II resonance lines.

References

[1] Fair, R. B. (1998). History of Some Early Developments in Ion-Implantation Technology Leading to Silicon Transistor Manufacturing. Proc. of the IEEE 86(1).
[2] Zhang, T.-Y., & Zheng, N.-W. (2009). Theoretical Study of Energy Levels and Transition probabilities of Boron Atom. Acta Physica Polonica a 116(2).
[3] Fuhr, J. R., & Wiese, W. L. (2010). Tables of Atomic Transition Probabilities for Beryllium and Boron. J. Phys. Chem. Ref. Data 39(1).
[4] NIST Atomic Energy Levels and Spectra Bibliographic Database. http://physics.nist.gov/elevbib
[5] NIST Atomic Spectroscopic Database. http://physics.nist.gov

Oscillator Strengths of Arsenic Resonance Lines

Uldis Bērziņš, Arnolds Ūbelis, Armans Bžiškjans, Andris Vanags

Institute of Atomic Physics and Spectroscopy, University of Latvia, Latvia
uldis.berzins@lu.lv

Introduction

The observation of the absorption lines of neutral arsenic (As I) were first reported in the case of the studies of the binary star *Chi Lupi* during the first mission of the Hubble Space Telescope launched into low Earth orbit in 1990 [1]. Later, arsenic lines were detected in a couple of metal poor stars [2–4], and in interstellar space [5]. The determination of the oscillator strengths of those transitions would allow the discrimination between different evolution models of those objects. We experimentally determined the oscillator strengths (f) for the As I ($4P^2 5s\text{-}4p^3$) transitions (197.3 nm, f = 0.127, and 193.8 nm, f = 0.059) evaluated from the branching fraction measurements of the radio frequency inductively coupled plasma by combining them with the selected lifetime values reported in literature [6].

The uncertainty in the determination of oscillator strengths depends on the precision in lifetime measurements and from the error bars in branching fraction determination. Since we use the lifetime data from literature, we cannot improve them. The accuracy of branching fractions depends on the scattering of measurement data, the calibration error of the spectral response of the experimental system, and the influence of the self-absorption of resonance lines.

Experiment

The As I emission lines were obtained from laboratory-made radio frequency (RF) inductively coupled plasma sources. Two sealed off lamp bulbs were made of high quality Spectrosil type silica of 18 mm diameter spheres filled with As + Xe and As + Xe + KBr. They were placed in the coil of the radiofrequency generator (Fig. 1). The spectral lines of arsenic were analysed by a monochromator SPM-2 (Carl Zeiss Jena) allowing high spectral resolution in the 200–300 nm range. The application of this monochromator allowed us to work using a reasonably opened slit in the case of very weak signals from the light source. Intensities of individual spectral lines were detected using a photomultiplier tube PMT 39A attached at the exit slit of a monochromator. Photocurrent was amplified and measured using a voltmeter. The calibration of spectral response of this system was performed using a hydrogen lamp DBC-25 and a deuterium lamp made and calibrated in the Vavilov State Optical Institute. The calibration error is estimated not to exceed 15% in the area 190–300 nm.

The branching fractions were determined for all lines starting from two excited levels $^4P_{1/2}$, and $^4P_{3/2}$ levels of $4p^2 5s$ electron configuration corresponding to measured resonance lines 197.262 nm and 193.759 nm, and transition to the ground state $^4S^o_{3/2}$. Other measured lines are related to the allowed transitions onto metastable states $^2P^o_{1/2}$, $^2P^o_{3/2}$, $^2D^o_{3/2}$ and $^2D^o_{5/2}$ of ground configuration $4p^3$. In order to control the influence of self-absorption we measured the intensity ratios for two spectral lines at different RF generator powers We could observe the influence of self-absorption online pairs with resonance lines at larger powers.

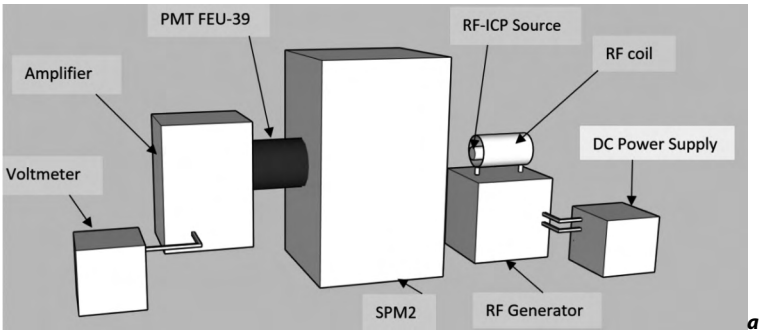

Fig. 1. *Schematic of the experimental set-up for branching fraction measurements*

Results

The branching fractions were determined from intensity ratio measurements at conditions where self- absorption was absent, and they are presented in Tab. 1. The relative uncertainties for the branching fractions were obtained from the errors in the intensity ratio measurements, and they are distributed inversely proportional to the branching fraction values. Thus, for larger fractions the relative error is smaller. Since in our measurements the ratio between the fraction of resonance transition and the fraction of sum for other lines is 0.94/0.06 that means that the relative error for the branching fraction for resonance line is about 1%. From branching fractions and experimental lifetimes, the absorption oscillator strengths were calculated. Together with data from literature they are presented in Tab. 2.

Tab. 1. *The branching fractions from $4p^25s\ ^4P_{1/2}$ and $4p^25s\ ^4P_{3/2}$ states*

Transition $4p^25s\ ^4P_{1/2}$	λ, nm	Branching fraction	Transition $4p^25s\ ^4P_{3/2}$	λ, nm	Branching fraction
$-^4S^o_{3/2}$	197.262	0.939	$-^4S^o_{3/2}$	193.759	0.943
$-^2D^o_{3/2}$	249.294	0.0569	$-^2D^o_{3/2}$	243.723	0.00998
$-^2P^o_{1/2}$	307.531	0.0016	$-^2D^o_{5/2}$	245.653	0.0426
$-^2P^o_{3/2}$	311.959	0.0024	$-^2P^o_{1/2}$	299.098	0.00093
			$-^2P^o_{3/2}$	303.285	0.0039

From branching fractions and experimental lifetimes, the absorption oscillator strengths were calculated. Together with data from literature they are presented in Tab. 2.

Tab. 2. *The oscillator strengths for arsenic resonance lines*

Transition $4p^25s$-$4p^3$	λ, nm	Our data	***Bengtsson et al 1992*** *[6]*	***Holmgreen 1975, DV*** *[7]*	***Holmgreen 1975, DL*** *[7]*
$^4P_{1/2}$-$^4S^o_{3/2}$	197.262	0.127(15)	0.123(17)	0.06	0.11
$^4P_{3/2}$-$^4S^o_{3/2}$	193.759	0.059(7)	0.059(8)	0.03	0.06

We see good agreement between our data and other experimental data [6]. Theoretical data calculated with dipole lengths approximation DL [7]. We use the experimental set up differently from that [8] used for determination of oscillator strengths in [6]. Our approach allows demonstrating better confidence in the determination of the oscillator strengths of arsenic resonance lines resulting in a more accurate definition of the arsenic concentration in astrophysical objects.

Acknowledgements

This work was supported by ERDF project No. 1.1.1.5/19/A/003. We also thank Andris Lezdiņš for his contribution and to Prof. Rashid A. Ganeev for discussions.

References

[1] Leckrone, D. S., Johansson, S. G., & Wahlgren, G. M. (1991). High resolution UV spectroscopy of the chemically peculiar B-star, chi Lupi. In: The First Year of HST Observations. HST Workshop: the year of first light. A. Kinney and C. Blades (eds.). Baltimore: STSCI.

[2] Roederer, I. U. (2012). Germanium, Arsenic and Selenium Abundances in Metal-Poor Stars. Ap J. 756, 36–47.

[3] Roederer, I. U., & Lawler, J. E. (2012). Detection of Elements in all Three r- Process Peaks in the Metal-Poor Star HD 160617. Ap J. 750, 76–97.

[4] Roederer, I. U., Schatz, H., Lawler, J. E., Beers, T. C., Cowan, J. J., Frebel, A., Ivans, I. I., Sneden, Ch., & Sobeck, J. S. (2014). New Detections of Arsenic, Selenium and Other Heavy Elements in Two Metal-Poor Stars. Ap J. 791, 32–44.

[5] Cardelli, J. A. (1994) The Abundance of Heavy elements in Interstellar Gas. Science 265, 209–213.

[6] Bengtsson, G. J., Berzinsh, U., Larsson, J., & Svanberg, S. (1992). Determination of Radiative Lifetimes in Neutral Arsenic Using Time Resolved Spectroscopy in the VUV Region. A&A 263, 440–442.

[7] Holmgreen, L. (1974). Theoreticlly Calculated Transition Probabilities and Lifetimes for the First Excited Configuration np2(n+1)s in the Neutral As, Ab and Bi Atoms, Phys Scr 11, 15–22.

[8] Lotrian, J., Guern, Y., & Cariou J. (1980). Experimentally determined transition probabilities of the system 4p3 + 4p25s of neutral arsenic. J. Phys. B. Atom. Molec. Phys. 13, 685–688.

Laser Induced Breakdown Spectroscopy as an Emerging Technique for Mineral and Space Exploration

Javed Iqbal[1,2,4], François Vidal[1], Rashid Ganeev[2,3]

[1] *Institut National de la Recherche Scientifique, Centre énergie matériaux télécommunications, Canada*
[2] *Institute of Astronomy, University of Latvia, Latvia*
[3] *Voronezh State University, Russia*
[4] *Department of Physics, University of Azad Jammu and Kashmir Muzaffarabad, Pakistan*
javed.iqbal@lu.lv

The mineral exploration industry requires new methods and tools to address the challenges of declining mineral reserves and increasing discovery costs. Laser-induced breakdown spectroscopy (LIBS) represents an emerging geochemical tool for mineral exploration that can provide rapid, in situ, compositional analysis and high-resolution imaging in both laboratory and field settings. The LIBS technique is used for stand-off detection of geological samples for use on landers and rovers to Mars, and for other space applications. LIBS can detect elements with a low atomic number (i.e., light elements), some of which are important path finder elements for mineral exploration or are classified as critical commodities for emerging green technologies. LIBS data can be acquired in situ, facilitating the interpretation of geochemical data in a mineralogical context, which is important for unravelling the complex geological history of most ore systems. LIBS technology is available as a handheld analyser, thus providing a field capability to acquire low-cost geochemical analyses in real time. Here, using a calibration model built from powdered reference materials doped with gold in solution, the gold concentration of ore samples coming from different gold mines, were determined by LIBS and then compared to those obtained from conventional laboratory techniques. The accuracy of these results are based on the in-homogeneity of gold distribution at the sampling scale. The influence of the chemical composition of the calibration samples on the plasma properties was investigated by measuring the plasma electron density and temperature. LIBS has wide potential to be utilised in mineral exploration, prospect evaluation, and deposit exploitation quality control. LIBS is ideally suited for field exploration programs that would benefit from rapid chemical analysis under ambient environmental conditions.

Acknowledgements

We are thankful to Professor François Vidal from INRS, QC, Canada for his support and the European Regional Development Fund Project No. 1.1.1.5/19/A/003 "Development of Quantum Optics and Photonics at the University of Latvia".

Moon-Earth: A Concept for Building a Space-resources Based Economy

Vidvuds Beldavs

Riga Photonics Centre
vid.beldavs@fotonika-lv.eu

A breakthrough is on the horizon for launch costs to decrease from more than $ 5,000 / kg to Low Earth Orbit to potentially $ 200 / kg or less by 2040 [1]. SpaceX has driven the push to lower costs with reusable rockets. Elon Musk, the founder of SpaceX even sees costs reaching $ 10 / kg. Launch costs in this range enable the construction of very large structures in Earth orbit as well as industrial and commercial facilities on the Moon. The recently announced Voyager space hotel by the Orbital Assembly Corporation (OAC) with rooms for over 400 guests targets a launch date of 2027 [2]. While 2027 appears fantastical to many, the OAC approach is grounded on deep experience with manufacturing with plausible steps for meeting increasingly challenging objectives. The technical feasibility of each step is well grounded. Given the progress in reducing launch costs towards $ 200 / kg, then the driver will become reasons for increasing launch rates. Hotels, space manufacturing and large-scale research facilities in orbit can create targets for launching more and more rockets with costs declining with increased launch reliability and frequency. Much lower launch costs create the potential for dramatically lower costs not only to orbit Earth but to reach the Moon and to develop industrial infrastructure on the Moon. Lunar exploration has barely scratched the surface of revealing the resource base of the Moon, but available data indicates that the Moon has many of the materials required by an industrial civilisation. Potentially vast concentrations of valuable metals could exist under the Aitken Basin in the South polar region and elsewhere, but such exploration remains to be done [3]. As the use of lunar materials expands the cost of building industrial, scientific and commercial facilities in outer space from lunar resources will drop below the cost of sourcing most types of materials from the Earth. This opens the prospect for a lunar-centric space economy identified as Moon-Earth.

Key assumptions of a lunar centric model for space industrialisation are:

- Large structures in space need to be assembled from components manufactured in space. Construction of the ISS is not a good model for the future when much larger structures will be built.
- The Moon is the low-cost site for materials for space manufacturing. Many important materials are on or near the surface, and the vacuum and fractional gravity of the Moon promises launch costs from the Moon that are a fraction of launch from Earth.
- Lunar industrial development can make important contributions to developments in Mars orbit. The Δv of shipment to Mars orbit from the lunar surface is less than launch from the surface of Mars [4]. Industrial development in Mars orbit using lunar materials can lower costs and improve the effectiveness of operations on Mars.
- It will become increasingly urgent to limit launch of spacecraft to LEO from Earth as congestion from satellite mega constellations increases and suborbital intercontinental transportation takes off following the model proposed by Elon Musk.
- Climate change is a threat to all countries and urgent action is called for to limit or eliminate large scale resource extraction on Earth, as well as to limit launches through the atmosphere.

- Billionaires can speed up development, but international cooperation is critically needed to demonstrate the feasibility of self-sustaining lunar industrial development.
- The ILD as a framework continues to be relevant to foster vitally important strategically directed international cooperation in outer space development [5].
- These assumptions could drive the creation of a financial model that would permit the calculation of the size of the space economy by 2040 given these assumptions, and an alternative scenario where the assumptions are not accepted, and the tragedy of the time horizon continues to limit investment in space development. Given that a $ 10 trillion space economy could be created by 2040, then the difference in total wealth between the two scenarios could be a compelling argument for international cooperation in the creation of mechanisms to finance accelerated space development.

References

[1] Dinkins, S. (2019). How low can launch costs go? The Space Review. https://thespacereview.com/article/3740/1

[3] Crawford, I. A. (2015). Lunar resources: a Review. Progress in Physical Geography 39(2), 137–167. DOI 10.1177/0309133314567585. [See Section 5, Metals. "…they are caused by surviving fragments of an originally ~110 km-sized metallic core of a differentiated asteroid, could potentially indicate the presence of considerable quantities of ear-surface metallic Fe (and associated Ni and PGMs)]

[4] Mars/Moon/Earth Delta-Vs. https://upload.wikimedia.org/wikipedia/commons/7/74/Delta-Vs_for_inner_Solar_System.svg

[5] Beldavs, V. (2021). The promise of return on investment does not disappear in cislunar space and beyond. The Space Review. https://www.thespacereview.com/article/4127/1

Some Results of Three Projects of the Institute of Astronomy of UL

Ilgmārs Eglītis, Ilgonis Vilks, Anna Bule, Adelaida Sokolova

Institute of Astronomy, University of Latvia, Latvia
ilgmars.eglitis@lu.lv

1. Carbon star survey in the selected zones at the Baldone Observatory

Infrared 2MASS (J–K) colour distribution for C and M-stars differs. Late carbon stars are redder than late M stars. It gives the possibility to complete the checking of potential late carbon star candidates by infrared photometric colours (J–K) > 1.3 mag. The potential list of carbon stars contains more than 20,000 objects; therefore, the program of observation was planned to cover five-degree delta slices, in each season of observation, beginning from the pole gradually descending to the celestial equator.

Observations were made with the 1.2 m Schmidt system telescope of the Baldone Astrophysical observatory with a four degree objective prism and CCD ST – 10XME from 2006 until early 2017, and CCD STX-16803 from late 2017 until 2019.

49 new carbon stars have been discovered in the constellations Cassiopeia, Perseus, Auriga, Cygnus, Cepheus and Pegasus. Without spectral images of potential C-stars, the positions of 347 spectral CCD images of bright standard C-star fields were exposed to study their spectral characteristics.

The distance in kpc can be calculated from the equation Mk – mk + 5lgr + Ak + 10 = 0, where Ak is interstellar absorption, Mk absolute magnitude in K passband, mk observed K magnitude. Mauron (2008) showed that the absolute K magnitude of late carbon stars varies in a small range of magnitude from –8.1 to –7.4 depending on $(J–K)_0$ colour indices in LMC. The interstellar absorption Ak and $(J–K)_0$ can be calculated from interstellar reddening. Ak = 0.302E(B–V) and $(J–K)_0$ = (J–K) – 0.405E(B–V), where E(B–V) is taken from infrared full-sky dust maps obtained by Schlafly and Finkbeiner, 2011 [2].

Comparisons of the Gaia satellite and Baldone Observatory obtained distances were made. The distances of the Gaia satellite and the distances obtained at the Baldone Observatory correlate within ±0.9 kpc; r(B) = 1.07r(G) – 0.41.

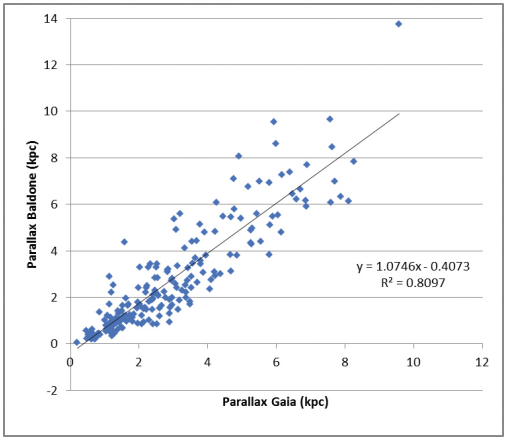

Fig. 1. *Comparison of the Gaia satellite and Baldone Observatory obtained distances*

Carbon star concentrations at distances 2, 4, 6–7 kpc from the Sun were observed. According to the distances they are located near Orion, Perseus, and Outer arms, however, in general, carbon stars poorly tied to the galaxy's branches.

2. Observations of asteroids using the Baldone Schmidt telescope

The research was carried out within the project "Complex investigations of small objects of the Solar system". In 221 observation nights 5,544 CCD images were obtained, which covered 648 square degrees of sky. More than 6,000 astrometric positions for 1,122 asteroids were published and 49 new asteroids were discovered. Of them were 3,412 CCD images devoted to studying photometric characteristics of 25 NEO-type asteroids. For asteroids Nr.11508 (Stolte), 6178 (1986 DA), 2014 LJ21, 850 (Altona), 2583 (Fatyanov), 345705 (2006 VB14) and 26724 (2001 HU8) rotation periods were obtained. Photometric data reductions for the images of five Near-Earth Objects were done using the MPO Canopus and MaxIM DL programs. Through experimentation with different rotation periods the Fourier fitting was used to determine the best size of periods.

Tab. 1. *H20 results (March 2019)*

Nr, Name	Nights, Observation Nr	P(sun, years)	P(rotation, h)
11508, Stolte	9, 167	4.64	3.049
6178, 1986 DA	5, 150	5.10	3.12
2014 LJ21	5, 123	4.91	16.41
850, Altona	7, 264	5.20	11.19
2583, Fatyanov	4, 465	3.38	5.66
345705, 2006 VB14	7, 39	0.67	3.25
26724, 2001 HU8	1, 52	5.50	1.43

The G(RP) photometric magnitudes for reference stars were taken from the Gaia DR2 release [3]. For the other 18 asteroids, photometric data reductions are continuing.

3. The results of the "Online Observatory" project

ERASMUS+ project "Online Observatory" (KA201-2018-008, 2018–2020) started in the autumn of 2018. The Online Observatory was founded by five European observatories (Baldone Observatory; Brorfelde Observatory, Denmark; Harestua Solar Observatory, Norway; Helsinki Observatory, Finland; Faulkes telescope project, UK) in 2018, all of which have a special interest in communicating astronomy and where visitors get hands-on experience about how to be an astronomer. Their combined efforts resulted in the Online Observatory, where activities developed at each observatory are made accessible for schools and others for educational purposes (https://onlineobservatory.eu/).

The outcomes contain 71 resources for educational purposes in astronomy beginning with Virtual tours at the five observatories, about the sky's observation, Moon, Planets and exoplanets, the Sun and stars, and concluding with the Universe. Thirteen of them have been prepared by the staff of the Institute of Astronomy (Baldone Astrophysics Observatory).

Acknowledgements

This publication makes use of data products from the Two Micron All Sky Survey, which is a joint project of the University of Massachusetts and the Infrared Processing and Analysis Center/California Institute of Technology, funded by the National Aeronautics and Space Administration and the National Science Foundation.

This work uses results from the European Space Agency (ESA) space mission Gaia. Gaia data are being processed by the Gaia Data Processing and Analysis Consortium (DPAC). Funding for the DPAC is provided by national institutions, in particular the institutions participating in the Gaia Multi-Lateral Agreement (MLA). The Gaia mission website is https://www.cosmos.esa.int/gaia. The Gaia Archive website is http://archives.esac.esa.int/gaia.

This research is funded by the Latvian Council of Science, project 'Complex investigations of Solar System small bodies', No. lzp-2018/1-0401.

References

[1] Cutri, R. M. et al. 2MASS All Sky Catalog of point sources. http://cdsbib.u-strasbg.fr/cgi-bin/cdsbib?2003yCat.2246....0C

[2] Schlafly, E. F., & Finkbeiner, D. P. (2011). Measuring Reddening with Sloan Digital Sky Survey Stellar Spectra and Recalibrating SFD. ApJ. 737(103), 13. https://iopscience.iop.org/article/10.1088/0004-637X/737/2/103/pdf

[3] Brown A. G. A. et al. (2018). Gaia Data Release 2. A&A 616, 1–22. DOI 10.1051/0004-6361/201833955.

Radiation Detection Materials and Detector Technologies for Radiation Detectors

Vladimirs Gostilo, Anna Bulycheva, Rais Nurgalejevs, Igors Krainjukovs

Baltic Scientific Instruments, Ltd., Latvia
office@bsi.lv

Nuclear radiation detectors are widely used in radiation monitoring equipment for the nuclear industry and environmental monitoring, mining industry and medicine, nuclear science and space applications and in many other applications. Radiation detectors based on semiconductor materials surpass all other types of detectors in terms of energy resolution and have a high radiation detection efficiency. Scintillation detectors are superior to other types in terms of radiation detection efficiency, but they are inferior to semiconductor detectors in terms of energy resolution.

Specialising in the development and manufacturing of precise spectrometric equipment, which allows not only registering nuclear radiation, but also analysing its composition, distribution and activity of emitting radionuclides, Baltic Scientific Instruments carries out research and development in the field of detector materials and technologies that allow creating precise spectrometric detectors for various applications. The main research, development and production are conducted with semiconductor materials HPGe, Si, CdZnTe/CdTe, TlBr, as well as the highest precision scintillation crystals LaBr3, CeBr3, SrI2, whose spectrometric performance has been significantly improved in recent years.

The company has clean boxes, zones and rooms for working in clean conditions and glove boxes to work in special atmospheres, as well as the necessary equipment used in technological operations for cutting, slicing, dicing, polishing, lapping, chemical etching, impurities diffusion and drift, vacuum annealing, materials vacuum evaporation, photolithography, wire bonding, micro assembling.

In addition to the release of serial detectors for industrial applications (nuclear industry, environmental monitoring, mining and the metallurgical industry), the company provides the development and manufacture of unique ultra low-background detectors for international scientific experiments in the search for dark matter, neutrino-antineutrino research, double beta decay registration, underground investigations.

The company has significant experience in the development and manufacture of specialised detectors for imaging systems used in medicine, space and industrial applications. We are continually dedicated to researching, developing and mastering advanced detector technology. All research and development are carried out in close cooperation with international research organisations and foreign universities. The company's specialists constantly participate in international conferences and publish the results obtained at the highest scientific level. Some of the company's scientific products are shown in Fig. 1.

Fig. 1. *Semiconductor Detectors:*

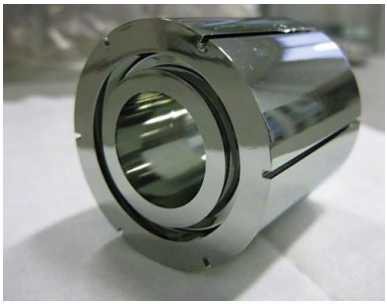

a)

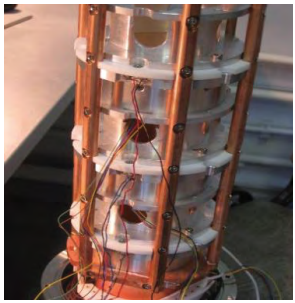

b)

(a) *segmented HPGe detector for nuclear reactions search;* ***(b)*** *ultra low background HPGe 4-crystals assembly for neutrino registration*

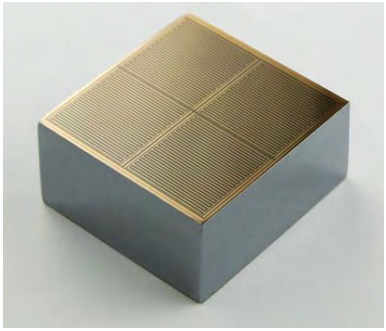

c)

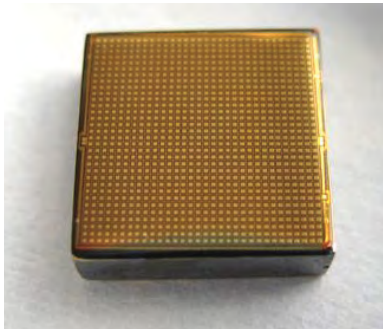

d)

(c) *4-segmented CZT Coplanar Grid detector for HEP;* ***(d)*** *32x32 pixel CZT detector for medical imaging applications*

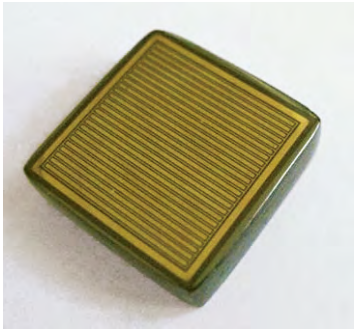

e)

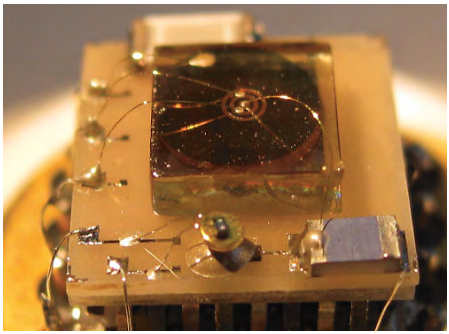

f)

(e) *CdTe strip detector for position sensitive experiments;* ***(f)*** *prototype of TlBr Ring detector for medical application*

Towards Energy-Efficient Technologies with Smart Optical Sensing and Shape-Assistant Trapping of Infrared Emission

Oleg Dimitriev[1], Petro Smertenko[1], Olexander Gridin[1], Eduard Manoilov[1], Vadym Naumov[1], Arnolds Übelis[2]

[1] *Institute of Semiconductor Physics, National Academy of Sciences of Ukraine, Ukraine*
[2] *National Science Platform FOTONIKA-LV, University of Latvia, Latvia*
petro.smertenko@gmail.com

Energy efficiency (EE) is a mainstream for sustainable development and progress in Europe [1]. According to EU statistics, buildings are responsible for almost one third of final energy consumption and up to half of carbon dioxide emissions into the atmosphere. At the same time, 64% of energy consumed in the residential sector is used for heating homes, with renewables accounting for 27% of household space heat consumption. In the last decades, great progress has been made in improving the energy efficiency of households through the development of smart houses, for example, by designing buildings with walls filled with phase-change materials, smart windows that control incoming and outgoing light radiation, programmable sensors that tune the heating, etc. However, little has been done with the design of the shape of the buildings, both exteriors and interiors. Most houses still use traditional shapes with rectangular wall joints and box-like structure. Obviously, advanced energy-efficient solutions to improve EE housing require innovative science-based approaches [2, 3]. a properly designed house shape can help reflect or trap infrared radiation, redistribute thermal fluxes and thus optimise heat emissions. Moreover, such optimisation can be carried out during the initial design of a building, as well as during its retrofitting and renovation.

In this work, we have conducted comparative studies of heat distribution in buildings of two shapes: rectangular and circular dome-like. One of the advantages of the dome shape is the following. The minimum surface area with the same usable area as a rectangular one means that less heat is absorbed. Accordingly, the cost of cooling and air conditioning can be reduced. The buildings are of the same height, land area, and inter-building distance (Fig. 1). The angle of the incident light (red arrows) corresponds to the midday sun in summertime. In the case of a rectangular shape, the reflected light (black arrows) is lost between the walls, thus contributing to their heating, while in the case of a circular shape the light is reflected into the environment.

Fig. *1. Pathways of light propagation in space of rectangular (left) and circular (right) shapes: red arrows – incident radiation, black arrows – reflected radiation*

Fig. 2 shows an example of the test survey of two smart houses of rectangular and circular geometry with approximately the same living area (~50 m2), which are located in a suburban village in the Kiev region (50°10′42″N, 30°18′57″E). The presented data demonstrates the temperature distribution in the interior space, scanned by IR optical sensing throughout the house, beginning from the oven (as shown by red arrows on

the plan) as a function of the daytime. The ovens in both houses were turned 'on' in the midday (3 PM local time). One can see that the differences in the temperature gradient in the houses are significant. It is almost 2 times higher for the rectangular-shaped house with a temperature sweep from 12 to 75 °C versus 17 to 38 °C for the dome-shape house, which means that a rectangular shape consumes more heat and possesses higher heat losses (according to Fourier's law of thermal conductivity), and it has less efficient heating of the house's area compared to the dome-shaped building. Research is in progress.

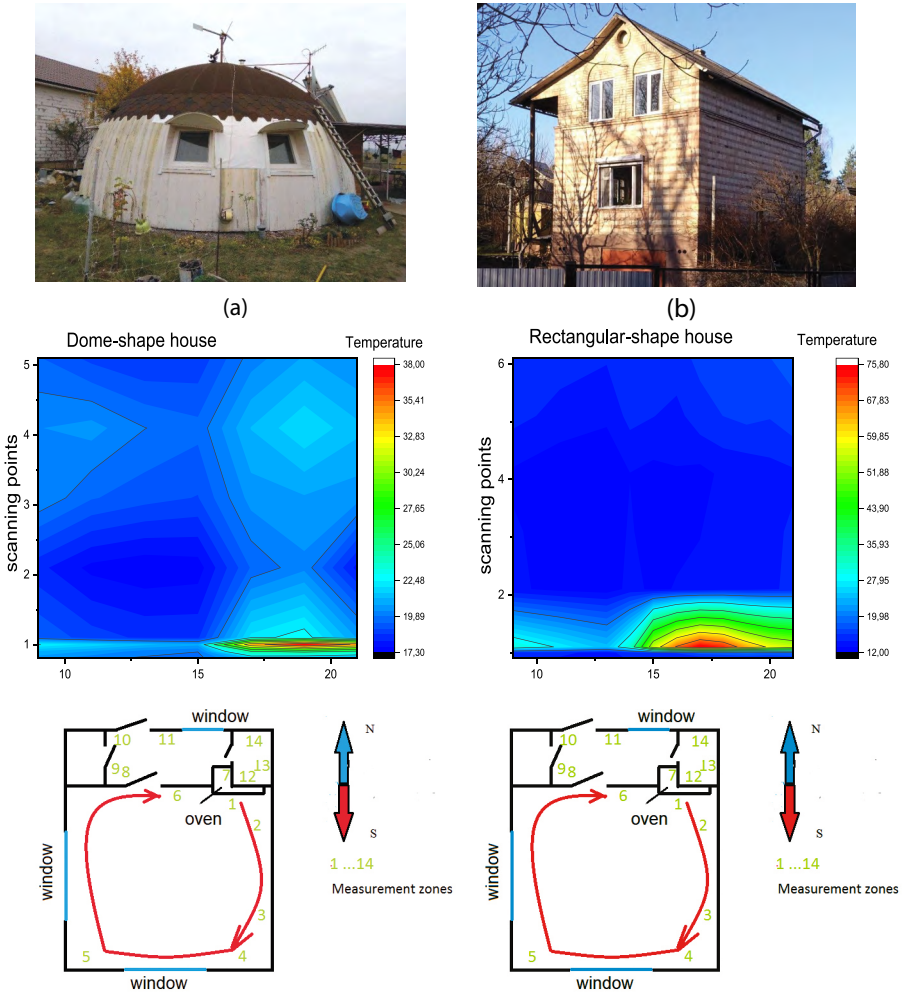

Fig. 2. *Test buildings (photo on the top), temperature distributions (maps in the middle) for houses of different shapes, and a plan of IR sensing (at the bottom, red arrows correspond to the measurement steps), as measured on the same day:* ***(a)*** *dome-shaped house,* ***(b)*** *rectangular-shaped house*

References

[1] UNECE (2020). Promoting Energy Efficiency Standards and Technologies to Enhance Energy Efficiency in Buildings. United Nations ECE Energy Series No. 60. Geneva. https://www.unece.org/publications/

[2] Dimitriev, O. P. (2019). Harvesting of the infrared energy: Direct collection, up-conversion, and storage. Semiconductor Physics, Quantum Electronics & Optoelectronics 20(4), 418–423.

[3] Jin, J.-T., & Jeong, J.-W. (2014). Optimization of a free-form building shape to minimize external thermal load using a genetic algorithm. Energy and Buildings 85, 473–482.

Monitoring of Radioactive Waste in the Nuclear Industry

Serhii Pohuliai, Aleksandrs Sokolovs, Aleksandrs Kipluks

Baltic Scientific Instruments, Ltd., Latvia
office@bsi.lv

All nuclear facilities (Nuclear Power Plants, reprocessing plants, nuclear laboratories...) in the process of activity generate wastes along with their main product. Due to the specifics of those activities the wastes could be radioactive and dangerous for human beings. Decommissioning and disassembly of nuclear facilities themselves will add to the quantity of radioactive wastes (RAW) which should be recycled in accordance with the existing Standard[4]. RAW should be characterised according to its physical, chemical, and radiation properties so that the safest and most economically effective variant for the waste treatment can be chosen.

Having its own production of radiation detectors, Baltic Scientific Instruments designs and produces Free Release and Waste Assay Monitors for small, medium, and large volumes of RAW for the Nuclear Industry. Some such Monitors are presented in Fig. 1. Due to the specific conditions at all nuclear facilities, all the fabricated Monitors are mostly customised. The main part of fabricated Monitors is based on semiconductor HPGe detectors (10–50% efficiency depending on RAW activity); the most precise types of advanced scintillation detectors ($LaBr_3$, $CeBr_3$, SrI_2 with dimensions 2×2″ and 3×3″) are used as well.

All the monitors that we develop are fully automated and equipped with a software suite that includes the WAM-soft software package for system control and automation, the SpectraLineHandy software package and the EffMaker software package. The WAM-soft package allows the operator to configure the measurement configuration of RAW radiation (place the objects to be measured into the desired position, adjust the shutter opening of the collimators, start the rotation, etc.). The SpectraLineHandy software package executes control of the spectrometer, displays the measured spectra, identifies the radionuclides and determines the RAW activity by applying calculated efficiencies for gamma quanta registration obtained by any calibration method. The EffMaker software package is used for the calibration of the monitors with the Monte Carlo simulation method and for simulation of nonstandard measurement tasks.

All the developed WAMs have metrological assurance. On the basis of the existing metrological standards, applicable regulations, and measurement methods accepted in the nuclear industry, we have selected as metrological assurance certain calibration and monitor validation methods, manufactured a set of the volumetric activity reference sources for direct verification of calibration results, and provided a package of application programs to support the measurements and ensure reliable results. The calibration of the monitors' efficiency is made with standard sources in point geometry, as well as with a complex calculation of the effectiveness curves using the Monte Carlo simulation method. The comparison of the calculated dependencies of the registration efficiency on energy and those ones obtained from real measured barrels with sources of calibrated activities demonstrate that the differences in the values do not exceed 20%. To allow direct verification of the monitors' calibration we have manufactured and certified volumetric activity sources in the form of real 200, 400 and 700 L barrels that contain matrix-fillers.

[4] International Atomic Energy Agency, Classification of Radioactive Waste: General Safety Guide, IAEA Safety Standards Series No. GSG-1, IAEA, Vienna (2009).

a)

b)

c)

Fig. 1. (a) *Free Release Monitor;* ***(b)*** *HERCULES Stationary Waste Assay Monitor;* ***(c)*** *Mobile Waste Assay Monitor*

Small Form-factor Super-multiview 3D Display Using the Gabor Superlens

Boriss Janins, Jurijs Antonovs

SLICKER Ltd, Latvia
boriss.janins@slicker3d.com

Stereoscopic two view solutions are not able to provide natural 3D perception. Future-oriented research focuses on a glasses-free super-multiview display (SMV), with the viewing angles from 36 and above to overcome vergence-accommodation conflict (VAC).

Slicker Ltd's multi-national team of experienced in the field researchers and entrepreneurs is bringing to the market breakthrough game-changing technology, based on optical nano thickness layers covering square meters of any transparent surface.

The prototype (TLR ≥ 6) of the 3D light panel with changeable images as well as a working SLICKER 3D SMV (Super multi-view) display has been tested. a fundamentally new way to get a 3D image based on very economical film optics containing Gabor super lens array is secured by patent: US9778471B2, published 2017-10-03 [1].

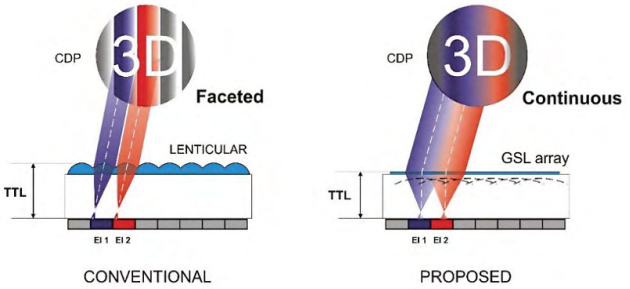

Fig. 1. *Slicker SMV 3D display concept*

European Commission has awarded its *Seal of Excellence* to SLICKER for the Horizon 2020 phase 2 proposal "game-Changing 3D".

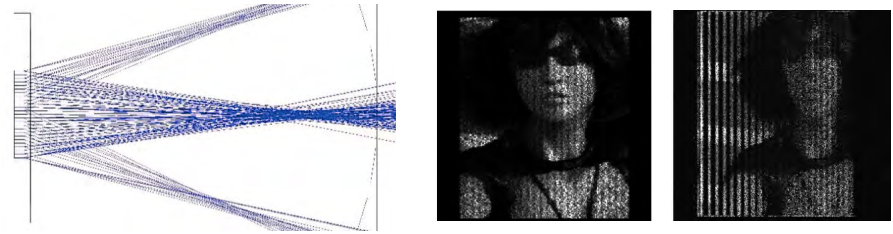

Fig. 2. *Image simulation for 0° and 25° (1/2 of image, black lines are space multiplexion phase)*

The project proposal "968828, Game-Changing3D" of the company to the call H2020-EIC-SMEinst-2018-2020-3 (deadline October 7, 2020) was awarded the European Commission's Seal of Excellence.

Ref. Ares(2020)7091180 - 25/11/2020

European Commission

SEAL OF EXCELLENCE

Certificate delivered by the European Commission,
as the institution managing Horizon 2020,
the EU Framework Programme for Research and Innovation 2014-2020

The project proposal
968828, Game-Changing3D
NEXT STEP 3D IMAGING

submitted under the Horizon 2020's **SME Instrument (grant only and blended finance)**
call **H2020-EIC-SMEInst-2018-2020 (H2020-EIC-SMEInst-2018-2020-3)** of **7 October 2020**
in the area of **EIC-SMEInst-2018-2020**

SME instrument

by
Slicker
Krūzes Street 2B
LV-1046 Riga
Latvia

following evaluation by an international panel of independent experts

WAS SCORED AS A HIGH-QUALITY PROJECT PROPOSAL
IN A HIGHLY COMPETITIVE EVALUATION PROCESS*

This proposal is recommended for funding by other sources, since Horizon 2020 resources available for this specific Call were already allocated following a competitive ranking.

* This means passing all stringent Horizon 2020 assessment thresholds for the 3 award criteria (excellence, impact, quality and efficiency of implementation) required to receive funding from the EU budget Horizon 2020.

Elisa Ferreira,
Commissioner for
Cohesion and Reforms

Mariya Gabriel,
Commissioner for Innovation, Research,
Culture, Education and Youth

Brussels, 25/11/2020

References

[1] Method and device for producing multi-view images and optical film used in said method and device. https://patents.google.com/patent/US9778471B2/en

Poster Sessions

Technological Challenges for the Next Generation Boron Ion Implantation Device

Jānis Blahins[1], Uldis Bērziņš[1], Valdis Avotiņš[2], Arnolds Ūbelis[1]

[1] *Institute of Atomic Physics and Spectroscopy, University of Latvia, Latvia*
[2] *Department of Science, University of Latvia, Latvia*
janis.blahins@lu.lv

The recently started project is aimed to perform proof of concept and to validate frontier technology for a small-sized next generation 100 keV Boron ion implantation device in the laboratory environment. The project is in response to the current demand for user friendly, small-sized and cost-effective ion implantation technology from the research driven SMEs in Latvia and Germany to sustain their global competitiveness. The innovation is based on the use of a hollow cathode plasma combined within an RF inductively coupled plasma producing Boron ions from pure metallic Boron directed in an ion optics track to form a high energy ion beam close to 100 kV.

The Project will elaborate and test the following technologies and approaches:

1) boron ion production: use of a hollow cathode RF ICP ion with magnetic plasma rope guiding the plasma to an ion optics track;
2) beam acceleration using a linear electrostatic accelerator adjustable depth up to 100 keV;
3) QMS filter for ion beam formation;
4) classical Einzell-lens adapted for ion focusing and guidance systems;
6) quartz/glass technologies advantageous for high vacuum needs and miniaturisation of a laboratory device.

The following key characteristics for Boron ion implantation need to be reached: 10–100 keV ion beam energy with a density of 1 × E13 to 1 × E16 atoms/cm^2 over ~100 cm^2 target, by exposure time less than 100 sec.

Boron is a metalloid complicated substance, characterised by high chemical inertness, hardness and thermal resistance and showing both metallic and non-metallic properties. It condenses at 3,927 °C. Current commercial ion implant devices use highly toxic boron fluoride gas to avoid condensation. Use of low toxicity boron rich powder as a target will be the key innovation.

The main reason why the classic industrial scale ion implant equipment is multi-ton in weight and with a high price is mostly due to the size and weight of the magnetic mass-selector (magnet) for purifying the ion beam.

In the last decades, a magnet-free device with an outstanding filter efficiency came into the analytical chemical industry under the name of quadrupole mass-selector (QMS). It had never been implemented before because the transmissivity of QMS is harshly dependent on the geometry accuracy of QMS rods and positioning. a pencil sized filter has the transmissivity of 10% at 10micron accuracy and near 90% at 2-micron accuracy. Therefore, the application of QMS technology is essential for winning in size, weight, price, and purity.

Two-photon Selection Rules of HF Structure for Rydberg Atomic States

Artūrs Ciniņš[1], Kaspars Mičulis[1], Nikolai Bezuglov[2]

[1] *Institute of Atomic Physics and Spectroscopy, University of Latvia, Latvia*
[2] *Saint Petersburg State University, Russia*
arturs.cinins@lu.lv

We described the creation of optical dressed states in a multilevel two-state quantum system with essential in experimental situation HF splitting. As an example we study sodium systems of levels $3s_{1/2} - 3p - 5s_{1/2}(-4d)$ due to its reach structure that allows us to consider a great number of excitation schemes. When the system interacts with a very strong laser field the coupling operator forms the structure of both bright and dark states. Autler-Townes spectra we observe with a weak probe laser (a weak probe field in the first excitation step and a strong coupling field in the second step). We treat the lack of some bright peaks in Autler-Townes spectra as a consequence of a specific architecture of dressed states in HF components, incorporated into independent (orthogonal) ladder excitation schemes. In several cases we reveal the modified 2photon selection rule as well that in terms of the total angular momentum F is reduced to $\Delta F = 0$. The last is the result of constructive/destructive interferences of atomic states upon their coupling by a strong laser field at the ladder's middle steps. That fact opens practically important perspectives to realise selective addressing of unresolvable HF F-components of atoms and molecules.

Acknowledgements

This work was supported by the Latvian Science Council Grant No. lzp-2019/1-0280.

Whispering Gallery Mode Silica Microsphere Resonator Applications for Biosensing and Communications

Inga Brice[1], Toms Salgals[2,3], Vjačeslavs Bobrovs[2], Roman Viter[1], Jānis Alnis[1]

[1] *Institute of Atomic Physics and Spectroscopy, University of Latvia, Latvia*
[2] *Institute of Telecommunications, Riga Technical University, Latvia*
[3] *AFFOC Solutions Ltd., Latvia*
inga.brice@lu.lv

Inside whispering gallery mode (WGM) resonators, the light beam can be confined in a circular symmetry structure and sustained with small reflection losses. By choosing an appropriate material with a very low absorption, and fabricating a very smooth surface, WGM resonators can reach ultra-high quality (Q) factors. High Q factors allow light to circulate inside longer and have very narrow resonances. This makes them suited as laser cavities, resonant filters, sensitive sensors, generation of nonlinear effects at relatively low powers. The simplest 3D WGM resonator is a sphere. These microsphere resonators are easy to fabricate. The principle is based on melting the tip of an optical waveguide fiber and allowing the surface tension of liquid glass do all the work to reform the material into a sphere. The sphere has low surface roughness, helping the resonator achieve ultra high Q-factors in the range of 10^6–10^9.

WGM microsphere resonators for biosensing

WGMR sensor operation principles are based on a shift of WGM resonance due to external influence (temperature, pressure, humidity etc.). WGM resonances in the WGMRs are a function of their geometry and refractive index. To enhance optical properties or detect molecules or biomolecules the surface of a WGMR has to be functionalised with a nanomaterial layer. Sensing molecule adhesion to the surface is a good step towards biosensor development but not enough to call it a biosensor. One of the requirements for WGMR biosensors, which is often forgotten, is selectivity – the ability to distinguish the desired biomolecules from other molecules. Many enzymes, for example, glucose oxidase (GOx) which oxidizes glucose, or genes/antigens have selective properties and have to be tailored for each biomolecule.

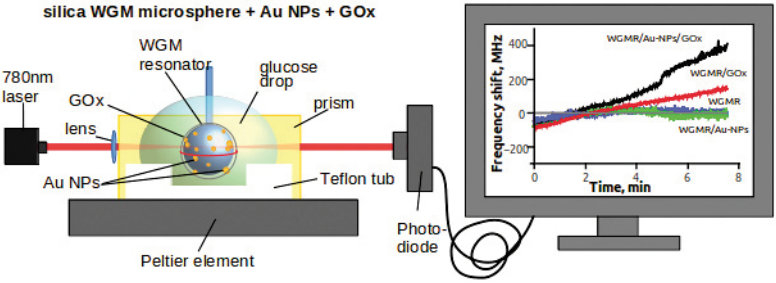

Fig. 1. *Responses of a glucose sensor based on differently modified silica microsphere WGM resonators: bare resonators – WGMR (blue curve), resonators coated with gold nanoparticles – WGMR/Au-NPs- (green curve), resonators coated with glucose oxidase layer – WGMR/GOx (red curve) and both layers to enhance sensitivity and provide selectivity – WGMR/Au-NPs/GOx (black curve)*

The fabricated silica microsphere WGM resonator's surface was coated with multiple different functionalising layers. Gold nanoparticles (Au NPs) were used to enhance the sensitivity together with GOx to ensure selectivity (Fig. 1). The research demonstrated that WGM resonators can be coated with materials, which increase the sensitivity towards the selected analyte – glucose – and to enhance the sensitivity of the WGR microsphere based sensor.

Several ZnO structures were tested to increase the surface area for protein binding which were selective for analyte/antibody reactions. Three types of ZnO coating on the WGM resonator's surface (WGMR/ZnO) structures were tried. ZnO nanorods had too rough a surface for potential application in the WGM resonator's sensors. ZnO nanolayer coated using atomic layer deposition and 10–15 nm layer thickness showed the best results and highest Q factors [2]. The ZnO nanocrystal structure obtained by drop coating zinc acetate solution on WGM microspheres was the easiest and fastest method, but only 50% of the samples were usable for further modifications. Bovine leukaemia virus (BLV) cattle virus and Bovine serum albumin (BSA) was added to the WGMR/ZnO structure to test BLV-positive test samples (Fig. 2.).

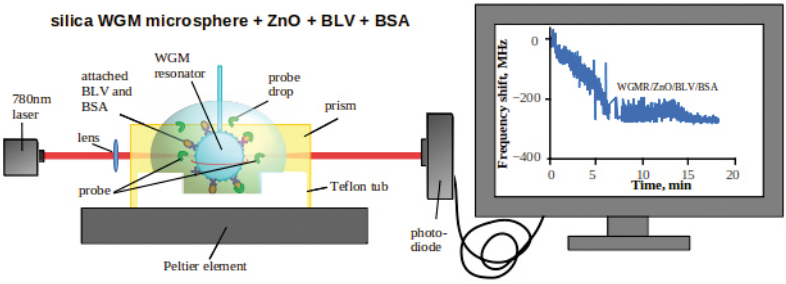

Fig. 2. *Responses of the cattle virus sensor based on antigen/antibody reaction modified silica microsphere WGM resonator*

WGM microsphere resonators for communications

An Optical frequency comb (OFC) can be generated using third-order Kerr-nonlinearity induced four wave mixing (FWM), generating the equidistant optical side-bands in the WGM micro resonators. The generated equidistant frequencies may allow the substitution of an expensive laser array solution for a wavelength-division multiplexing (WDM) data transmission system.

Silica microsphere WGM resonators with 170 μm diameter were used to generate OFCs with ~400 GHz repetition rate. Two more intense generated optical carriers (+1) and (–1) were filtered and used to demonstrate data transmission [3]. Stability is an important parameter for telecom data transmission and long-term stability was explored. The temperature influence on the system was deemed crucial as it could affect multiple points, like the coupling position, impacting WGM resonator OFC resonances and polarisation of the input, which were determined to be integral for OFC generation [4].

Acknowledgments

This research was funded by ERDF project No. 1.1.1.1/16/A/259 "Development of novel WGM micro resonators for optical frequency standards and biosensors, and their characterization with a femtosecond optical frequency comb" and ERDF project No. 1.1.1.1/18/A/155 "Development of an optical frequency comb generator based on a whispering gallery mode micro resonator and its applications in telecommunications".

References

[1] Brice, I., Grundsteins, K., Atvars, A., Alnis, J., Viter, R., & Ramanavicius, A. (2020). Whispering gallery mode resonator and glucose oxidase based glucose biosensor. Sensors Actuators B Chem. 318, 128004.

[2] Brice, I., Viter, R., Draguns, K., Grundsteins, K., Atvars, A., Alnis, J., Coy, E., & Iatsunskyi, I. (2020). Whispering gallery mode resonators covered by a ZnO nanolayer. Optik. 219, 165296.

[3] Salgals, T., Alnis, J., Murnieks, R., Brice, I., Porins, J., Andrianov, A. V., Anashkina, E. A., Spolitis, S., & Bobrovs, V. (2021). Demonstration of a fiber optical communication system employing a silica microsphere-based OFC source, Opt. Express. 29, 10903.

[4] Brice, I., Grundsteins, K., Sedulis, A., Salgals, T., Spolitis, S., Bobrovs, V., & Alnis J. (2021). Frequency comb generation in whispering gallery mode silica microsphere resonators. SPIE Laser Reson. Microresonators, Beam Control XXIII 1167213.

The Small Size Boron Ion Implanter Concept

Jānis Blahins, Arnolds Ūbelis

National Science Platform FOTONIKA-LV, University of Latvia
Institute of Atomic Physics and Spectroscopy, University of Latvia
janis.blahins@lu.lv, arnolds.ubelis@lu.lv

Currently, besides semiconductor manufacturing, ion implantation is used for many purposes: e.g., sensor manufacturing, hardening of metal surfaces, friction modification, altering of chemical resistance, painting, etc. Particularly, boron ion implantation in high purity germanium (HPG) crystals is the key material used for high energy radiation sensors produced in Riga. Therefore, we analysed the available technologies and implantation devices in the context of the possibility to reach the technology breakthrough of boron implantation into HPG crystals. The key for implantation apparatus is the ion source of the selected element followed by a beam forming ion optics unit and a mass filter separating for impurities, ion beam accelerator and raster scanning system combined with a moving targeted crystal. The ion sources may differ substantially by approach and used techniques and are adapted and optimised to the selected dopant ion (e.g., boron for germanium crystals). Historically gas-type ion sources were exploited to produce the boron ions, like Penning source, Bernas, Sidenius and Freeman sources or Duoplasmotron. Due to the extremely low volatility with a melting point at 2,076 °C and a boiling point at 3,927 °C [1] obtaining a solid-state Boron ion source is a technological challenge. Historically boron trifluoride gas BF3 was chosen as the best raw material. Still two aspects cause serious problems: the incandescent cathode of the source corrodes in the atmosphere of aggressive gases; and BF_3 is extremely toxic. All able substitute gases have roughly the same problem, thus the use of solid-state boron may miniaturise the source, as well as make it less poisonous and better serviceable.

The development of hardly volatile ion sources was raised after reviewing an article describing the possibility of a hollow cathode (HC) discharge for various needs [2, 3]**.** Further research exposed that the effectiveness could increase if HC discharge is combined with radio-frequency (RF) glow discharge or RF inductively coupled plasma (ICP) sources. Soon the coupling of an ICP or CCP (capacitive coupled plasma) actuator with the HC was reported by [4, 5]. It is known that HC are in strong demand in analytical spectroscopy, as well for the space micro propulsion thruster industry [6, 7]. Detailed studies of published research allowed us to offer a new approach in boron ion implantation technologies. The key to emerging disruptive innovation is in the development of sophisticated hybrid geometry of ICP–HC–ICP plasma coupling. As a result, we elaborated the following prospective geometry of a unique device (Fig. 1), substantially different from existing commercial devices for Boron Ion implantation and new for implantation apparatus markets [8, 9]. The deposit is targeted by 10^{13}–10^{16} atoms/cm^2 thus the beam current should stand over 20 microamperes.

First, the design begins with the carrier gas – argon is laid in the vacuum tract by a tiny adjusted flux. Pressure is kept ~1 Torr and excited by an ICP coil, thus the flame tail is slightly inside the boron insert. The effect of the tail may be increased if the proper ramp-voltage is applied between the ICP ground and the HC cathode. The Boron insert forms an inner surface of hollow cathode cylinder with a wide output aperture, where the body of the insert may be heated toward 600 °C. Between the cathode and the anode works a voltage multiplier circuit, giving semi-constant current of a self-adjusted high voltage. Ions crowd the space next to the anode, where a second ICP exciter increases

the electron temperature of the plasma. Via the narrow aperture (~1 mm), the cone-shaped electrode extracts plasma to the focusing electrodes and QMS mass selector. The vacuum in the QMS is ca of micro-Torr or deeper. Then, the DC accelerator Viderøe tubulus provides positive kinetic energy to the beam, adjustable between 10 and 100 kV, where the system's zero voltage point is the entrance of the accelerator; the voltage is created by means of an RF Cockroft-Walton circuit. The vacuum here is on the order of a nano-Torr. Then, stay declining system providing an x and y scan of the target surface by slightly defocusing the beam. To make the implantation surface ideally uniform, the target is slowly rotated in a narrow angle to the axis. To avoid the target charge-up, preventing further implantation, the anticharge e-gun under the certain angle radiates the defocused e-beam from filament, scanning x and y to form a uniform negative surface charge.

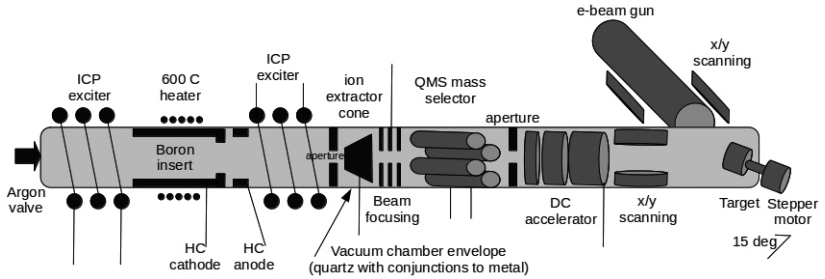

***Fig** 1. The boosted combined ICP-HC-ICP ion source in the full proposed implanter concept*

The next alteration in the diagram is traditional magnetic mass filter purifying ions. We studied several possibilities, including different sector magnet geometries [10], Wien filter and QMS filter [11]. Among the prospects the Quadrupole Mass Selector (QMS) seems like a realistic and preferable alternative. It seems cheaper and mechanically simpler than a sector magnet, high selective with ultra-purity, less weight, less power demand. The QMS consists of four cylindrical rods of QMS set ideally parallel to each other and fed by a DC and RF voltage superposition. The system separates ions by (m/z) ratio. The ion-transparency of the QMS filter sharply depends on mechanical accuracy [12] having a critical jump between good and bad between 1–10 microns of position and shape geometry deviations. Currently the best in the market advertises accuracy of 0.25 microns [13]. The QMS filter demands sophisticated electronics to produce extra stable frequency and voltage, where a fresh and simple solution is DDS – Direct Digital Synthesis [14]. Ion beam technologies demand ensuring the vacuum in this device also. The offered approach allows to use glass silica technologies and glass to metal seals based on kovar (iron-nickel-cobalt alloy), having thermal expansion similar to high-borosilicate glass. Graded quartz seals to high-borosilicate glass will be applied.

After optimisation of the developed hybrid plasma source, the next innovations are foreseen. *Firstly*, to apply a laser ablation technique to intensify the atomisation of boron in HC by a laser ablation technique developed by [15]. *Secondly*, [16] reported about of boron cathodic arc ion source. [17] described generation of boron ions for a beam using the approach of Wiliams. *Thirdly*, another principle of ion source giving excellent ion beam current ca 75 mA is reported in detail by [18], where the LaB6 tablet was used (which is a conductor) and specific two-power-supplies pulse-excitation circuit. *Fourthly*, boron heated to over 600 °C has a sharp decrease of electric resistance about 6 orders in

comparison to room temperature [19]. The effect was used by several authors [20–21] in efforts to develop a high current boron ion beam source. Success with an HC ion source with preheating optimised for production of double-charged ions (yet non-boron) is reported [23] – some applications may benefit from a twin-charge.

Discussion/Conclusions

We suggest the use of (and further research on it) at least four possible innovations:

1) For the ion source, to use the metallic boron filled HC with ICP pre-activated carrier gas, with or without pulsed power or accelerating ramp-voltage and/or pre-heating of boron.
2) If larger beam currents are mandatory, the vacuum-arc with pulsed power supply are more effective however, more tricky to build.
3) For mass separation, the use of the QMS-MS instead of a magnetic-MS may provide a win of size, weight, price, and purity.
4) For vacuum chambers and pipes, where proper and practical, it is good to consider the use of quartz as a material providing support of extraordinary purity.

Acknowledgments

Special thanks to ERDF Project No. 1.1.1.1/19/A/144 for funding this job.

References

[1] Brotherton, R. J., & Steinberg, H. (2016). Progress in Boron Chemistry: Volume 2. Kent: Elsevier Science & Technology (at 6-ch., p. 251, tab. 5).

[2] Gundersen, M. A., Schaefer, G., & Schoenbach, K. H. (1990). Basic Mechanisms Contributing to the Hollow Cathode Effect in Physics and Applications of Pseudosparks. NATO Ser. B: Phys 219. Springer.

[3] Greenfield, S., Durrani, T. M., Tyson, J., & Watson, C. A. (1990). a Comparison of Boosted-Discharge Hollow Cathode Lamps and Inductively Coupled Plasma as Excitation Sources in ICP Atomic Fluorescence Spectrometry. Chem. Dept. Fac. Pub. scholarworks.umass.edu/chem_faculty_pubs

[4] Christensen, S. M. (2012). Modelling and measuring the characteristics of an inductivly coupled plasma antenna for micro-propulsion system. a master thesis, Boise State University. https://scholarworks.boisestate.edu/cgi/viewcontent.cgi?article=1345&context=td

[5] Plasek, M. L., Jorns, B., Choueiri, E. Y., & Polk, J. E. (2012). Exploration of RF-Controlled High Current Density Hollow Cathode Concepts. Princeton Univ. alfven.princeton.edu/publications/plasek-jpc-2012-4083

[6] Plasek, M. L., Wordingham, C. J., Choueiri, E. Y., & Polk, J. E. (2013). Modeling and Development of the RF-Controlled Hollow Cathode Concept. Conf. July, p. 20. DOI 10.2514/6.2013-4036.

[7] Gott, R. P. (2017). The development and analysis of a heaterless, insertless, microplasma-based hollow cathode. The Dept. of Mech and Aerospace Engineering of the University of Alabama, p. 73.

[8] Current, M. I., Rubin, L., & Sinclair, F. (2018). Chapter 3: Commercial Ion Implantation Systems. In: Ion Implantation Science and Technology. Ion Implant Technology Co, p. 44.

[9] Hanley, P. R. (1983). Physical Limitations of Ion Implantation Equipment. In: Ion Implantation: Equipment and Technique. H. Ryssel et al. (eds.). Berlin, Heidelberg: Springer-Verlag.

[10] Prohaska, T., Irrgeher, J., Zitek, A., & Jakubowski, N. (2005). Sector Field Mass Spectrometry for Elemental and Isotopic Analysis. Royal Society of Chemistry. ISBN 978-1-84973-392-2.

[11] Blahins, J., Bziskjan, A., & Apsitis, A. (2021). Technical solutions how to create miniature boron ion implantation apparatus. Solid State Physics institute of Latvia Univ. spring conference, pp. 45, 65.

[12] Taylor, S., & Gibson, J. (2008). Prediction of the effects of imperfect construction of a QMS filter. Journal of mass spectrometry 43, 609–616. DOI 10.1002/jms.1356.

[13] Reliance Precision ltd. Clean Assembly and Manufacturing Solutions for the Scientific. Medical and Analytical Industries 11, p. 16. www.reliance.co.uk/wp-content/uploads/2017/03/SPSI3-Scientific-Issue-B-web.pdf
[14] Gentile, K., & Cushing, R. (1999). Technical Tutorial on Digital Signal Synthesis. Analog Devices publ. B21, pp. 83–89. analog.com/en/education/education-library/technical-tutorial-dds.html
[15] Karatodorov, S. I. (2017). Combined plasma source for emission spectroscopy: laser-induced plasma in hollow cathode discharge. Inst. of Solid State Phys, Bulgarian Ac. of Sci., p. 132.
[16] Williams, J. M., Klepper, C. C., Chivers, D. J., Hazelton, R. C., & Freeman, J. H. (2008). Operation and Applications of the Boron Cathodic rc Ion Source. AIP Conf Proc 1066, 469–472. doi.org/10.1063/1.3033664
[17] Bugaev, A. S., Vizir, A. V., Gushenets, V. I., Nikolaev, A. G., Oks, E. M., Savkin, K. P., Yushkov, Y. G., & Tyunkov, A. V. (2019). Generation of boron ions for beam and plasma technologies. Russian Phys J. 62(7), Nov.
[18] Gushenets, V., Bugaev, A., & Oks, E. (2019). Boron vacuum-arc ion source with LaB6cathode. Rev. Sci. Instrum. 90, 113309. DOI 10.1063/1.5127096
[19] Greiner, E. S., & Gutowski, J. A. (1957). Electrical Resistivity of Boron. Journal of Applied Physics 28, 1364. DOI 10.1109/TPS.2011.2167634
[20] Frolova, V. P., Gushenets, V. I., et al. (2017). Generation of boron ions for beam and plasma technologies. IEEE Trans. Plasma Sci. 45, 2070–2074.
[21] Gushenets, V. I., Oks, E. M., & Bugaev, A. S. (2018). Generation of boron ions for beam and plasma technologies. Proc. 28 Int. Symp. Discharges & Electrical Insul. in Vac, Greifswald, 411–414.
[22] Ishikawa, D., & Hasegawa, S. (2019). Development of Removable Hollow Cathode Discharge Apparatus for Sputtering Solid Metals. Journal of Spectroscopy 19, April, 1–6. DOI 10.1155/2019/7491671.
[23] Turek, M., Drozdziel, A., Pyszniak, K., Maczka, D., & Slowinski, B. (2012). Production of Doubly Charged Ions Using a Hollow Cathode Ion Source with an Evaporator. Vol.123(2013). Acta Physica Polonica-A No. 5. Proc. of IX Int. Conf. ION. Poland: Kazimierz Dolny.

The Dispersion Engineering of Whispering Gallery Mode Resonators

Kristians Draguns[1,2], Inga Brice[1], Aigars Atvars[1], Jānis Alnis[1]

[1] *Institute of Atomic Physics and Spectroscopy, University of Latvia, Latvia*
[2] *AFFOC Solutions Ltd., Latvia*
kristians.draguns@lu.lv

Whispering gallery mode resonators (WGMRs) are axisymmetric optically transparent structures with a size of a few hundred micrometres. The light can be confined inside the resonator by total internal reflection. The mode density of the WGMRs is very high, so we can observe strong light-matter interactions. One of the interesting applications is the generation of optical frequency combs using for-wave mixing [1].

Every wavelength of light inside a medium, experience a different refractive index n due to material dispersion. But also, the geometry of the resonator contributes to the total dispersion [2]. We can use geometric dispersion to engineer the geometry of the resonator such that the dispersion is desirable. Kerr combs can be generated in anomalous dispersion, so it is important where the zero-dispersion wavelength (ZDW) lays. For optimal comb generation, it is good that the dispersion line is not steep. For telecommunication's applications, the pump wavelength is 1550 nm.

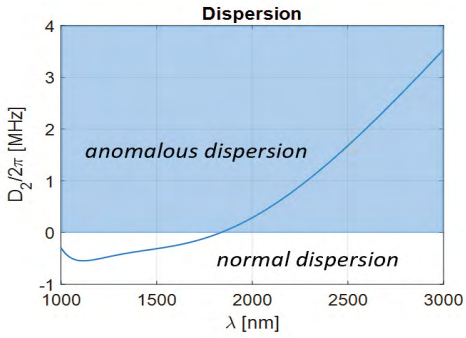

Fig. 1. *Dispersion for R = 332 μm belt type WGMR*

Various WGMR geometries are being explored to achieve optimal dispersion for comb generation.

Acknowledgment

This research was funded by the European Regional Development Fund Project No. 1.1.1.1/18/A/155.

References

[1] Chembo, Y. K. (2016). Kerr optical frequency combs: Theory, applications and perspectives. Nanophotonics 5, 214–230.

[2] Fujii, S., & Tanabe, T. (2020). Dispersion engineering and measurement of whispering gallery mode microresonator for Kerr frequency comb generation. https://doi.org/10.1515/nanoph-2019-0497

Optical Fibre Taper Simulation and Manufacture: from Standard to Micro Size

Jaime R. Ek-Ek[1,2], Fernando Martinez-Piñon[1], Frans Segerink[2], Jeroen P. Korterik[2], Raúl Castillo Perez[3], Carlos Enrique Jacome-Peñaherrera[3], Herman L. Offerhaus[2], Jose A. Alvarez Chavez[3]

[1] Instituto Politecnico Nacional, Centro de Investigacion e Innovacion Tecnologica, México
[2] Optical Sciences Group, University of Twente, The Netherlands
[3] Escuela Superior de Ingenieria Mecanica y Electrica, México
ekrafa@gmail.com, r.ek-ek@utwente.nl

The mode field intensity and adiabaticity are calculated for different points along the transition of an optical fibre taper from the standard 125 μm down to 1 μm diameter for low loss operation at 1300 nm wavelength. The first section of the taper is evaluated using a weak guidance approximation. The second section is treated as a three-index layer structure (double-clad) and evaluated with eigenvalue equations for three refractive indices. The third and thinnest section of the taper is studied using an exact mode eigenvalue equation. Tapers ranging from 38 to 40 mm length were fabricated. With this simplified set-up, tapers with a relatively good beam quality, low losses and variable length can be fabricated for applications in sensing and bio-medical applications.

The taper has been assumed to be a symmetrically biconical shape with 19 equidistant points (marked by the letters A-S, 2 mm apart) along the taper from the initial standard size a (125 μm diameter) to the smallest waist diameter of S (440 nm). For obtaining the results, weakly guiding approximation [1], Monerie [2] and exact mode equations [3] were used to evaluate and obtain the shapes of the position o of the fundamental mode field in different points along the taper as shown of Fig. 1. It is important to find out if the optical fibre taper is adiabatic, that is, the taper has very low loss [4], our first optical fibre taper is shown in Fig. 2 and Fig. 3, shows the taper shape obtained.

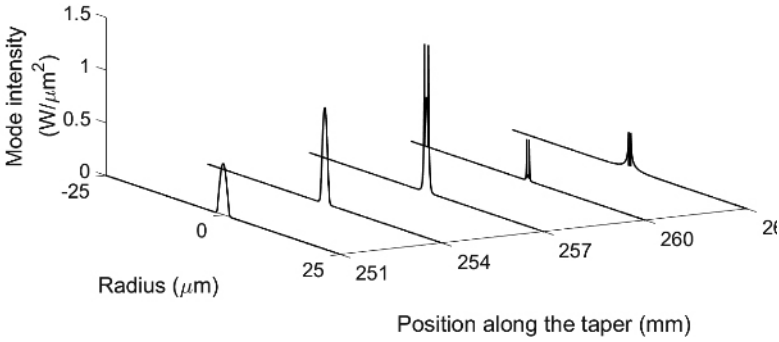

Fig. 1. *Normalised Mode intensity profile along the tapered fibre*

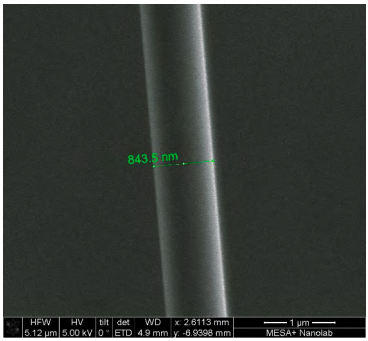

Fig. 2. *Optical Fibre Taper Diameter in SEM*

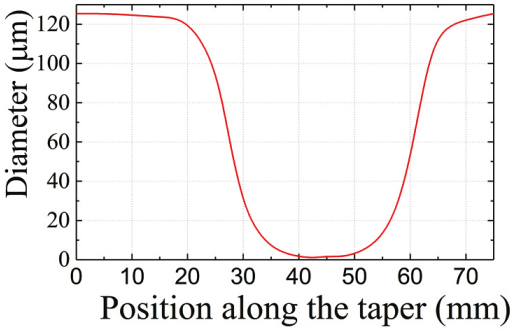

Fig. 3. *Optical Fibre Taper shape*

References

[1] Love, J. D., Henry, W. M., Stewart, W. J., Black, R. J., Lacroix, S., & Gonthier, F. (1991). Tapered single-mode fibres and devices. I. Adiabaticity criteria. IEE Proceedings J. Optoelectronics 138(10), 343–354. DOI 1049/ip-j.1991.0060.

[2] Monerie, M. (1982). Propagation in doubly clad single-mode fibers. Ieee Journal of Quantum Electronics 18(4), 535–542.

[3] Tong, L., Lou, J., & Mazur, M. (2004). Single-mode guiding properties of subwavelength-diameter silica and silicon wire waveguides. Optical Society of America. Optics Express 12(6), 1025–1035.

[4] Snyder, A. W., & Love, J. D. (1984). Waveguide with exact solutions. In: Optical Waveguide Theory. London: Chapman and Hall, pp. 250–251.

Liquid Whispering Gallery Mode Humidity Sensor and Its Applications

Lāse Mīlgrāve, Pauls Kristaps Reinis, Kristians Draguns, Inga Brice, Jānis Alnis, Aigars Atvars

Institute of Atomic Physics and Spectroscopy, University of Latvia, Latvia
pauls_kristaps.reinis@lu.lv, lase.milgrave@lu.lv

Precise air humidity measurements and control are necessary in many fields: agriculture, industrial manufacturing, scientific research, medicine, and others [1]. To achieve high sensitivity and precision, optical whispering gallery mode (WGM) sensors are widely researched. WGM resonators have high quality (*Q*) factors as they trap light inside them for long periods of time. Other positive qualities include their ability to operate in extreme environments and their electromagnetic immunity [2]. Resonant wavelength λ depends on the refractive index n and the radius R of the resonator: $\lambda m = 2\pi Rn$, where m is an integer number of optical waves fitting into the parameter [3]integrated optical circuits, semiconductor lasers, and photonic crystals. Optical dielectric resonators supporting Whispering Gallery Modes (WGMs. As air humidity changes, the R and n of the resonator change and cause the resonant wavelength to shift. This shift is detected, and the resonator can be used as a humidity sensor.

In this experiment, glycerol microdroplet (R = 370 µm at 50% RH (relative humidity)) was used as a spherical WGM resonator. Glycerol is highly hygroscopic, transparent, non-toxic, and viscous [4], making it a good choice for the liquid resonator material. a droplet is created at the tip of an optical fibre, which is attached to an XYZ table to change the position of the droplet when necessary. The droplet and other optical components are inside a climate chamber. To excite WGM in the droplet, a 760 nm tenable VCSEL laser was used. Due to the nature of liquids, it was possible to use free space coupling [5], which resulted in a simple set-up (Fig. 1). Photodiode collects the transmission spectrum and data is transferred to an oscilloscope.

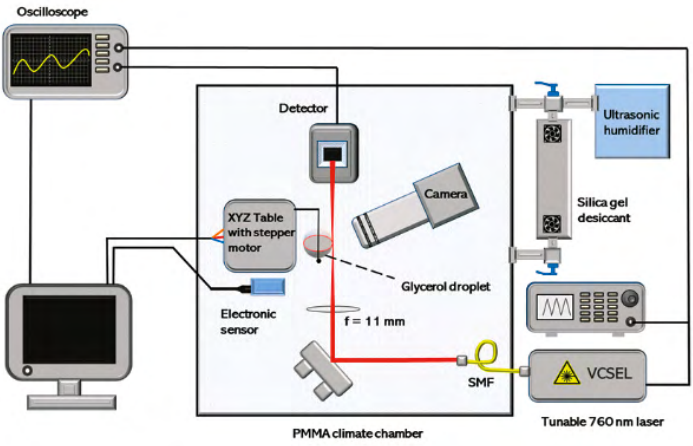

Fig. 1. *Experimental set-up for humidity measurements*

We used *LabView* and *Python* for data analysis. An original method for data analysis was created – we use a Lissajous figure to detect the wavelength shift (change in the radius vector angle) and to tell if the RH is increasing or decreasing (the direction of the Lissajous figure). Data was analysed in real time.

The glycerol droplet as a humidity sensor was tested in the 50–70% RH region. We tested such parameters as hysteresis, repeatability, lifetime, and temperature independence. From the acquired data, sensitivity and resolution were calculated.

Results of this experiment showed that glycerol has great potential as a WGM humidity sensor. We achieved the highest reported sensitivity in this type of sensor: 2.85 nm/% RH with the resolution $1 \cdot 10^{-4}$ & RH. It showed high repeatability and stability. One of the benefits, when compared to other WGM sensors, is its temperature independence – small temperature fluctuations in the environment did not cause wavelength shift [6].

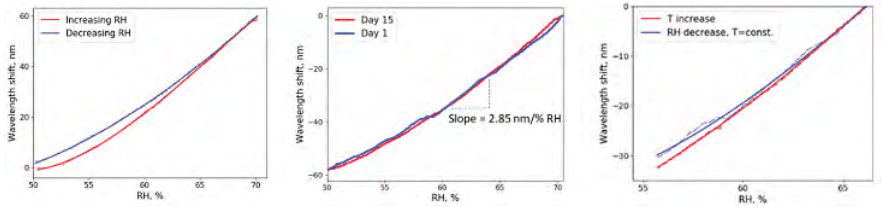

(a) (b) (c)

Fig. 2. *Experimental results:* ***(a)*** *hysteresis;* ***(b)*** *repeatability, stability, sensitivity;* ***(c)*** *temperature dependence*

Based on these results, we demonstrate possible applications for our novel humidity sensor and indicate ways for further research. The demonstrated WGM glycerol droplet humidity sensor has qualities to measure and detect very small RH changes. Due to this, one should be able to successfully integrate it into systems where very precise environment control is needed. Chemistry and especially the pharmaceutical industries require such a precise environment control [7, 8]. Many chemicals need distinct RH conditions for optimal and safe storage. Pharmaceutical compounds often require RH to be in a very narrow region between 50–60% RH, which coincides with the optimal work range for the demonstrated WGM glycerol droplet humidity sensor. The measured sensitivity, selectivity, and resolution of our sensor could be used in monitoring pharmaceutical and chemical compounds and processes. Further research into creating a portative set-up, calibrating the sensor, and researching the selectivity and response time of the sensor is needed.

Acknowledgements

This research was funded by LZP project No. lzp-2018/1-0510 "Optical whispering gallery mode micro resonator sensors".

References

[1] Chen, Z., & Lu, C. (2005). Humidity sensors: a review of materials and mechanisms. Sens. Lett. 3(4).

[2] Petermann, A. B., Hildebrandt, T., Morgner, U., Roth, B. W., & Meinhardt-Wollweber, M. (2018). Polymer based whispering gallery mode humidity sensor. Sensors (Switzerland) 18(7).

[3] Righini, G. C. et al. (2011). Whispering Gallery Mode microresonators: Fundamentals and applications. La Riv. del Nuovo Cim. 34(7).

[4] Labrador-Páez, L., Soler-Carracedo, K., Hernández-Rodríguez, M., Martín, I. R., Carmon, T., & Martin, L. L. (2017). Liquid whispering-gallery-mode resonator as a humidity sensor. Opt. Express 25(2).

[5] Wang, Y. et al. (2016). a review of droplet resonators: Operation method and application. Opt. Laser Technol. 86.
[6] Reinis, P. K., Milgrave, L., Draguns, K., Brice, I., Alnis, J., & Atvars, A. (2021). High-sensitivity whispering gallery mode humidity sensor based on glycerol microdroplet volumetric expansion. Sensors 21(5).
[7] Trask, A. V., Motherwell, W. D. S., & Jones, W. (2006). Physical stability enhancement of theophylline via cocrystallization. Int. J. Pharm. 320.
[8] Barona, D. et al. (2021). Modulated Uniaxial Compression Analysis of Respirable Pharmaceutical Powders. *KONA Powder Part. J.* 38.

Microsphere-based OFC-WGMR Multi-wavelength Source and Its Applications in Telecommunications

Toms Salgals[1,2], Jānis Alnis[3], Rihards Mūrnieks[1,4], Inga Brice[3], Jurģis Poriņš[1], Alexey V. Andrianov[5], Elena A. Anashkina[5], Sandis Spolītis[1,2], Vjačeslavs Bobrovs[1]

[1] Institute of Telecommunications, Riga Technical University, Latvia
[2] AFFOC Solutions Ltd., Latvia
[3] Institute of Atomic Physics and Spectroscopy, University of Latvia, Latvia
[4] Communication Technologies Research Center, Riga Technical University, Latvia
[5] Institute of Applied Physics, Russian Academy of Sciences, Russia
toms.salgals@rtu.lv

The "Development of optical frequency comb generator based on a whispering gallery mode micro resonator and its applications in telecommunications" project aims to obtain new knowledge on whispering gallery mode resonator-based optical frequency combs (WCOMBs) and to develop, construct and test a comb generator prototype for telecommunication's applications. The planned result of the project is a portable WCOMB prototype for a commercial fiber optical communication system.

Optical frequency combs (OFCs) using different kinds of whispering-gallery-mode (WGMRs) micro resonators have a high potential to replace tens of tuneable continuous-wave (CW) lasers with a single laser source in telecom (WDM) optical communication systems. For the first time, the use of silica microspheres (SiO_2) for OFC represents a cheap alternative over the other microcombs. By using arc discharge of a commercially available fusion splicer, it is possible to quickly fabricate microspheres with repeatable parameters such as diameter, and it is easy to control the free spectral range (FSR) which is proportional to the sphere diameter. Our designed microspheres have a high Q-factor (10^7–10^8), where the carrier wavelengths of WGMR-OFC are relatively stable over time and FSR matches the ITU-T spectral grid [1].

One way to enter the light into the resonator is by prism coupling [2]. This scheme is an alternative to the tapered fiber coupling scheme and has some advantages and disadvantages. Advantage – that the setup can be made with standard optical components and the setup does not have the fragileness that is present in a tapered fiber coupling setup. Disadvantage – coupling efficiency is only about 5–40%. Considering the aspect, that the tapered fiber method of microsphere excitation allows to fine-tune the coupling conditions, which is not possible for chip-based resonators, we have chosen them for OFC generation in optical communication systems.

To the best of our knowledge, we experimentally for the first time present a designed silica microsphere whispering-gallery-mode micro resonator (WGMR) OFC as a C-band light source where 400 GHz spaced carriers provide data transmission of up to 10 Gbps NRZ-OOK modulated signals over the standard ITU-T G.652 telecom fiber span of 20 km in length.

We search for stable combs on an optical spectrum analyser (OSA) by tuning external cavity CW semiconductor laser in wavelength and found that the most appropriate wavelength (λ = 1552 nm), where a CW laser with a linewidth of about 100 kHz and +6 dBm optical output power can be used as an OFC comb pump source. After OFC generation the carriers (-1) and (+1) are similar but one can be a few dBm more intense than the other if multiple solitons are circling inside the resonator. The optical carriers λ = 1549 nm

depicted as (-1) and λ = 1555 nm depicted as (+1) are used further to demonstrate NRZ-OOK modulated 2.5 Gbps and 10 Gbps data transmission, please see Fig. 1 (a). The OFC performance over a 10-hour period, power stability and power distribution stability over the wavelength of the OFC carriers, please see Fig. 1 (a) and Fig. 1(b).

The experimental setup of a silica microsphere-based WGMR-OFC light source optical communication system, please see Fig. 1 (c). The light coming from the pump source is further amplified up to +23 dBm by the erbium-doped fiber amplifier (EDFA). The polarisation state of the amplified signal is adjusted using the polarisation controller (PC1) before coupling the signal into the microsphere. The isolator on the EDFA output is used to prevent back-scattered light from entering the output port of the CW laser. The silica microsphere and tapered fiber are enclosed in a separate box for dust and airflow prevention, providing even further stability to the resulting OFC. The X, Y, and Z micro-translation stage is used to position the microsphere to touch the tapered fiber at a place slightly thicker than the taper waist, which changes such coupling conditions as coupled power and the Q factor of the resonances [3].

We have chosen B2B transmission and a distance of 20 km corresponding to the NGPON2 requirements. The error-free transmission is established during the experiment in both cases of 2.5 and 10 Gbps data rates for an OFC comb pump source operating at 1552 nm wavelength. It allows using WGMR-OFC as a light source where 400 GHz spaced carriers provide 2.5 and 10 Gbps NRZ modulated data transmission over 20 km SMF fiber [1].

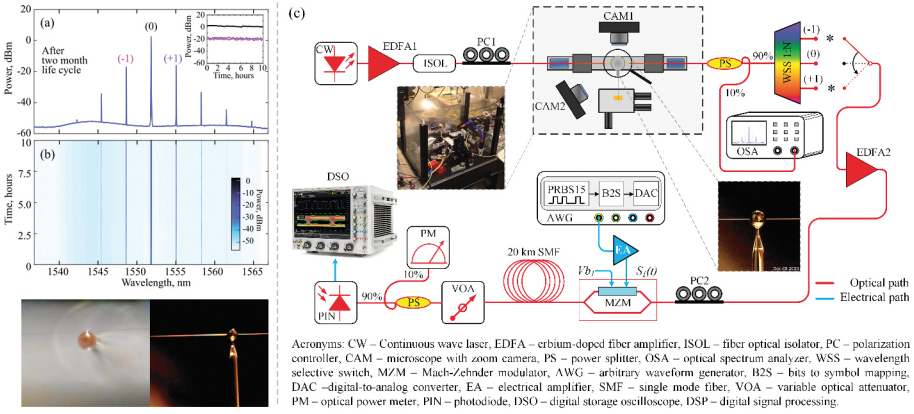

Fig. 1. *Measured OFC performance over a 10-hour period:* ***(a)*** *optical spectrum with inset representing captured power stability, and* ***(b)*** *power distribution stability over the wavelength.* ***(c)*** *The experimental setup of the designed silica microsphere WGMR-OFC as a light source where 400 GHz spaced carriers provide NRZ-OOK modulated 2.5 and 10 Gbps data transmission over 20 km SMF fiber. Insets show tapered fiber and silica microsphere resonator positions of coupling conditions and WGMR-OFC reduced humidity and dust-prevention cover box*

Acknowledgments

This research was funded by the European Regional Development Fund project No. 1.1.1.1/18/A/155 "Development of optical frequency comb generator based on a whispering gallery mode micro resonator and its applications in telecommunications" and supported by the Riga Technical University's Doctoral Grant programme.

References

[1] Salgals, T., Alnis, J., Murnieks, R., Brice, I., Porins, J., Andrianov, A., Anashkina, E., Spolitis, S., & Bobrovs, V. (2021). Demonstration of fiber optical communication system employing silica microsphere-based OFC source. Optics Express 29, 10903–10913.

[2] Brice, I., Grundsteins, K., Sedulis, A., Salgals, T., Spolitis, S., Bobrovs, V., & Alnis, J. (2021). Frequency Comb Generation in Whispering Gallery Mode Silica Microsphere Resonators. Online: SPIE Proceedings, Article No. 1167213. ISSN 0277-786X. e-ISSN 1996-756X.: DOI 10.1117/12.2577148.

[3] Braunfelds, J., Murnieks, R., Salgals, T., Brice, I., Sharashidze, T., Lyashuk, I., Ostrovskis, A., Spolitis, S., Alnis, J., Porins, J., & Bobrovs, V. (2020). Frequency Comb Generation in WGM Microsphere Based Generators for Telecommunication Applications. Quantum Electron. 50(11), 1043–1049.

The Development of Next Generation Technology for Ultra Purity Crystal Growth Based on MHD Semi Levitation

Viesturs Silamiķelis, Aigars Apsītis, Valdis Avotiņš, Arnolds Ūbelis

Institute of Atomic Physics and Spectroscopy, University of Latvia
arnolds.ubelis@lu.lv

The recent papers on unique computer-simulations and experimental results on aluminium magneto-hydrodynamic (MHD) levitation co-authored by scientists from the University of Latvia and Hanover University and followed by pilot research highlighted the potential for technological innovation leading to remarkable progress in crystal growth technology.

The new 32-month long project supported by the Central Financial Contracting Authority is the timeliness response and is going to develop further and to challenge the application of MHD levitation crystal growth technology in semi levitation mode for the Germanium. The project will be implemented by a multi-disciplinary team of physicists, electronic engineers, chemists, and material scientists of the University of Latvia together with two industrial partners – research driven SMEs AGL Technologies, Ltd. and Cryogenic and Vacuum Systems, Ltd.

The research efforts during the implementation of the project will result in the proof of concept and custom-made cost-efficient laboratory devices (TLR eventually 3–4) combining in not interrupted sequence: multiple zone purification, Czochralski and melted zone (pedestal) techniques to grow high-purity crystals avoiding their contacts with mechanical parts in the crystal growth zone by the application of MHD semi levitation.

Coverless melting techniques in a vacuum or in the environment of high-purity gases is going to be performed in a synthetic silica glass-metal assembled device. The core of studies:

1) model simulation of the melted zone hydrodynamic stability under MHD semi levitation;
2) research to find the optimum interrelations between the power of MHD inductors, frequency, temperatures profiles and geometry of the melted zone;
3) assembling of low temperature (Sn ~300 °C) and high temperature (Ge ~1000 °C) experimental set-ups for the initial and the final test of the semi levitation concept accordingly;
4) experimental studies evaluating the potential of the MHD semi levitation concept in HP Ge crystal growth technologies in high vacuum and clean gas environment, surrounded by a synthetic silica glass envelop.

The timeliness of our project particularly is evidenced:

1) by a short survey performed by a research team from South Dakota University, US [1]. The article highlights the astrophysical interest in next generation Germanium based detectors demanding ultra-high purity Ge crystals;
2) the report about the start of a project developing a levitation method lead by Dr. Arie van Houselt [2];
3) the article [3] on contactless processing of SiGe-melts in EML under reduced gravity;
4) by the review article of Dieter M. Herlach, Daniel Simons published in 2018 [4].

Presently large germanium single crystals of high purity (reaching 99,99999999999%) are grown by Czochralski techniques, the ingots being subject to repeated cycles (more than 50) of zonal purification in a separate appliance.

References

[1] Wang, G., Mei, H., Mei, D., Guan, Y., & Yang, G. (2015). High purity germanium crystal at the University of South Dakota. J. Phys. Conference Series 606, 012012.

[2] Houselt, A. van. (2016). Superior crystals grown from levitating droplets. Phys.Org. December 6. https://phys.org/news/2016-12-superior-crystals-grown-levitating-droplets.html

[3] Luo, Y., Damaschke, B., Schneider, S., Lohöfer, G., Abrosimov, N., Czupalla, M., & Samwer, K. (2016). Contactless processing of SiGe-melts in EML under reduced gravity. Microgravity 2(1).

[4] Herlach, D. M., & Simons, D. (2018). Crystal growth kinetics in undercooled melts of pure Ge, Si and Ge–Si alloys. Philosophical Transactions of the Royal Society A: Mathematical, Physical and Engineering Sciences 376(2113).

Modelling of the Cladding-Pumped Erbium/Ytterbium Co-Doped Fibre Amplifier for C-Band Operation

Kaspars Zaķis[1], Andis Supe[1], Sandis Spolītis[1,3], Sergejs Olonkins[1,2], Aleksejs Udaļcovs[2], Jurģis Grūbe[4], Edgars Elsts[4], Oskars Ozoliņš[1], Vjačeslavs Bobrovs[1]

[1] *Institute of Telecommunications, Riga Technical University, Latvia*
[2] *AFFOC Solutions Ltd., Latvia*
[3] *Communication Technologies Research Center, Riga Technical University, Latvia*
[4] *Institute of Solid State Physics, University of Latvia, Latvia*
kaspars.zakis@rtu.lv

With space-division multiplexing receiving increased attention as a method to exceed bandwidth limitations, compatible schemes for efficient amplification become necessary [1]. Erbium (Er^{3+}) and Ytterbium (Yb^{3+}) co-doping is considered an effective approach for increasing pump power conversion efficiency of cladding-pumped optical amplifiers. The Yb^{3+} ions absorb pump radiation and then resonantly transfer a portion of their energy to Er^{3+} for signal amplification. With the investigation into the effect of various design specifications (e.g., fibre length, pump power, and propagation direction) on amplifier characteristics and their wavelength dependence, our research is dedicated to identifying such a cladding-pumped Er^{3+}/Yb^{3+} co-doped fibre amplifier configuration based on experimentally extracted fibre parameters that provide high, uniform gain with a low noise figure in the optical Cband [2].

As is common practice, the manufacturer of our erbium/ytterbium-doped fibre (EYDF) sample only provides information on its basic geometry and Er^{3+}/Yb^{3+} concentration ratio. The accuracy of the simulation model is primarily dependent on the ion absorption and emission cross-sections and the overlap factor value; thus, it is crucial to determine these values as accurately as possible. The initial overlap factor estimate is calculated as the cross-sectional ratio between the core and inner cladding (as shown in Fig. 1.), which must then be refined by matching the simulation model results to experimental measurements due to the model assuming that the cladding is circular, whereas the physical fibre has a flower-shaped inner cladding.

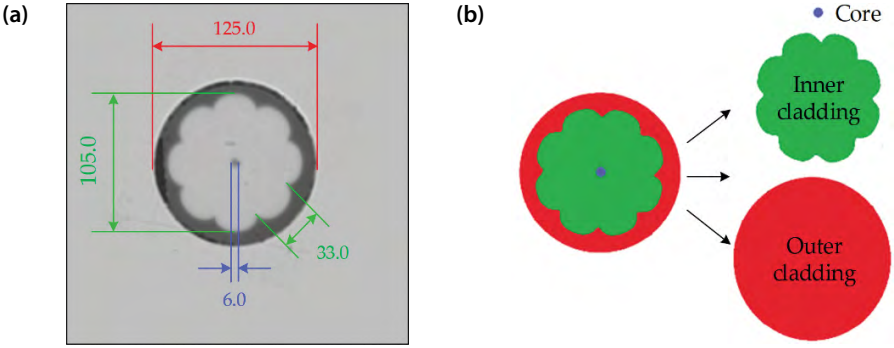

Fig. 1. (a) *Microscope image of the EYDF cross-section with its geometrical measures, and* ***(b)*** *RGB representation of its outer cladding (red), inner cladding (green), and core (blue) used for the overlap factor estimation*

It can be noted that the overlap factor may change as a function of pump power, which should be validated for any particular fibre at the expected operational pump power level [3].

Throughout our analysis, we used an optical pump source operating at $^{\lambda}P = 975$ nm and $P_P = 3$ W that is based on the specifications of the multimode light diode in our laboratory setup. Higher pump power levels were not considered at this time as a change from 3 W up to 4 W resulted in an insignificant increase in the output signal power of just 0.3 dB. It is determined that the optimal configuration at a per-channel input power of −20 dBm for 40 channels requires a 7 m long EYDF with a co-propagating pump. This results in an output power of 22 dBm, a gain of 19.7–28.3 dB, a noise figure of 3.7–4.2 dB, and a power penalty of 0.1 dB at a bit error rate of 10^{-9} using a 40×10 Gbps NRZOOK signal.

While the highest gain is achieved at a doped fibre length of 8 m, it is only marginally higher than at 7 m, while both the noise figure and gain uniformity are worse, which is a consequence of pump depletion and high signal attenuation within the fibre. It is also seen that both smaller and larger fibre lengths result in worse gain uniformity. At the same optimal length, a counter-propagating pump achieves 1 dB higher gain at the cost of 1 dB higher noise figure, which is not a worthwhile trade-off, thus motivating the choice of a co-propagating pump. Specific to the per-channel input power level, a sufficient but limited number of channels must be present to ensure efficient consumption of the generated population inversion and a minimal noise figure, otherwise, the unused portion of the population inversion eventually gives rise to amplified spontaneous emission noise. As a whole, the established dependence of these amplifier characteristics on the input parameters enables the assembly and further development of a cladding-pumped EYDFA in a laboratory setting.

Acknowledgments

This work has been supported by the European Regional Development Fund project No. 1.1.1.1/18/A/068. Institute of Solid State Physics, the University of Latvia as the Centre of Excellence has received funding from the European Union's Horizon 2020 Framework Programme H2020-WIDESPREAD-01-2016-2017-TeamingPhase2 under grant agreement No. 739508, project CAMART^2.

References

[1] Mizuno, T., & Miyamoto, Y. (2017). High-capacity dense space division multiplexing transmission. Optical Fiber Technology 35, 108–117.

[2] Supe, A., Olonkins, S., Udalcovs, A., et al. (2021). Cladding-Pumped Erbium/Ytterbium Co-Doped Fiber Amplifier for C-Band Operation in Optical Networks. Applied Sciences 11, 1702.

[3] Várallyay, Z., Szabó, Á., Rosales, A., et al. (2015). Accurate modeling of cladding pumped, star-shaped, Yb-doped fiber amplifiers. Optical Fiber Technology 21, 180–186.

Wavelength Measuring for Optical Telecommunications, Using Tapered Fibre, Image Analysis and PMMA WGM Micro Resonators

Roberts Berķis, Kristians Draguns, Jānis Alnis, Inga Brice, Aigars Atvars

Institute of Atomics Physics and Spectroscopy, University of Latvia, Latvia
roberts.berkis@lu.lv, aigars.atvars@lu.lv, kristians.draguns@lu.lv, inga.brice@lu.lv, janis.alnis@lu.lv

Whispering gallery mode

The whispering gallery modes (WGM) micro resonators are based on elliptical objects, which can be made from optically transparent materials, that can enable an optical wave circulating inside the ellipse using total internal reflection. If there is a monochromatic light source with constant intensity to the ellipse, constructive interference may be observed which in the case of a sphere could be written as [1]:

$$2\pi Rn = M\lambda, \quad (1)$$

where λ is the resonance wavelength, M is azimuthal mode number and R is the radius of the sphere.

The most important parameter of WGM micro resonators is the Q (quality) factor. It describes the lifetime of a photon that is circulating inside the optical micro resonator. In real life applications there are multiple losses and impurities that limit the lifetime of a photon [2].

PMMA WGM micro resonator characterisation

Poly methyl methacrylate acrylic (PMMA) WGM micro resonators are available with a quality factor of 10^3–10^4 [3], while the Q factor is lower than WGM made from SiO_2 or ZnO [4], they are available commercially, solving the main problem for successful WGM micro resonator integration into a working sensor system, that is the manufacturing cost.

Using high resolution cameras such as the "Xenics Xs-5049" it is possible to monitor individual sectors of the micro resonator (Fig.1) and watch each sector intensity change, based on the wavelength, that is fed to the tapered fiber.

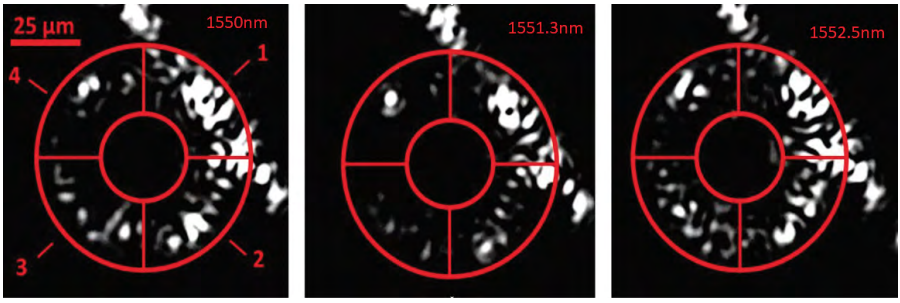

Fig. 1. *45 µm PMMA WGM micro resonator attached to tapered fibber waist region, intensity using a "Xenics Xs-5049" camera, for different wavelengths (1550 nm, 1551.3 nm and 1552.5 nm)*

From each specific region of the micro resonator, a normalised intensity map can be obtained (Fig. 2), which can be used to navigate a specific wavelength. Each region intensity corresponds to a different mode interaction with impurities on the WGM PMMA micro resonator surface.

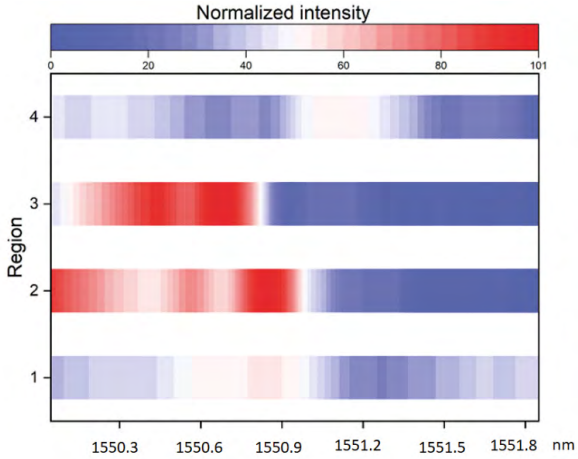

Fig. 1. *Normalised intensity map based on wavelength changes for a 50 µm PMMA WGM micro resonator*

Conclusions

The following work presents a new type of measuring system, where two main regular problems, that tie with WGM micro resonators – surface impurities and multiple modes, that lead to system improvements where few PMMA WGM micro resonators can be used as a measuring tool for telecommunication purposes [5]. These developed methods are valid not only for wavelength measuring but could be used for different bio measurements as well.

Acknowledgments

This research was funded by the Latvian Council of Science project No. lzp-2018/1-0510 "Optical whispering gallery mode micro resonator sensors" and ERDF 1.1.1.5/19/A/003 project No. 1.1.1.5/19/A/003 "The Development of Quantum Optics and Photonics in University of Latvia".

References

[1] Foreman, M. R., Swaim, J. D., & Vollmer F. (2015). Whispering gallery mode sensors: erratum. Adv. Opt. Photonics 7, 632.

[2] Zheng, Y., Wu, Z., Ping Shum, P., Xu, Z., Keiser, G., Humbert, G., Zhang, H., Zeng, S., & Quyen Dinh, X. (2018). Sensing and lasing applications of whispering gallery mode micro resonators. Opto-Electronic Adv. 1, 18001501–18001510.

[3] Berkis, R., Alnis, J., Atvars, A., Brice, I., Draguns, K., & Grundsteins, K. (2019). Quality Factor Measurements for PMMA WGM Microsphere Resonators Using Fixed Wavelength Laser and Temperature Changes. Proc. 2019 IEEE 9th Int. Conf. Nanomater. Appl. Prop. N., 9–12.

[4] Shitikov, A. E., Bilenko, I. A., Kondratiev, N. M., Lobanov, V. E., Markosyan, A., & Gorodetsky, M. L. (2018). Billion Q-factor in silicon WGM resonators. Optica 5, 1525.
[5] Petermann, A. B., Rezem, M., Roth, B., Morgner, U., & Meinhardt-Wollweber, M. (2016). Surface-immobilized whispering gallery mode resonator spheres for optical sensing. Sensors Actuators, a Phys. 252, 82–88.

Additional Contributions

Perspectives about Long-range Interatomic Interactions in Transition Metal Homonuclear Diatomics: Sc_2 and Y_2

Ulises Miranda Ordóñez

Institute of Atomic Physics and Spectroscopy, University of Latvia
ulises.ordonez@lu.lv

Scandium and yttrium have an n*d* n+1s^2-type valence shell. While both elements have as a ground state a ^{2}D, their 3 lowest excited states correspond to different atomic terms, despite the similarities in electronic structure [1]. These excited states of the atom play an important role in the determination of the ground state of the homonuclear diatomic (or dimer) [2, 3]. In both Sc_2 and Y_2 the ground state is a $^5\Sigma_u^-$ [2–5], which in the long range of the potential energy curve, have non-zero first- and second-order electrostatic interactions [6]. The second order electrostatic interactions must be considered and there are several approaches to calculate them. However, first-order electrostatic interactions are rarely found in homonuclear dimers and, if it is the case, one usually deals with both atoms in the ground state. Accurate calculation of these interactions using the operator of electrostatic interactions [7, 8] requires the square of the mean radius of the open shell. In the ground states of Sc_2 and Y_2 one may have to consider 3 open shells: (a) n*d* for the ground state, corresponding to the ^{2}D atomic term; (b) n*d* and n+1*s* or n*d*, n+1*s* and n*p*, for the excited state, corresponding to an ^{4}F atomic term. The latter is a rather complex point that has to do with the dissociation limit which is related to the ground state of the dimer. In Sc_2 one must use the excited state with 3 open shells, because the electron configuration of this Sc atom in this excited state is Sc (4*s*3*d*4*p*; $^4F^o$) [3]. a similar situation seems to be found in Y_2 [9]. Relativistic [10] and non-relativistic [11] data of the ground state of the elements are available, but, to the best of our knowledge, there is a lack of data of the excited states of transition metals atoms. This poses a problem for the accurate determination of first-order interatomic interactions but gives us a great chance to work on an almost forgotten field of atomic physics. Certainly, the continuation of the research on these aspects of atomic physics will allow progress in the investigation on the smallest atomic clusters.

References

[1] NIST Atomic Spectra Database Levels Form. https://physics.nist.gov/PhysRefData/ASD/levels_form.html
[2] Kalemos, A., Kaplan, I. G., & Mavridis, A. (2010). The Sc2 revisited. J. Chem. Phys. 132, 024309.
[3] Miranda, U. (2019). Long-range interactions and role of static and dynamic correlation energy in scandium dimer. Molecular Physics 117, 404–415.
[4] Verhaegen, G., Smoes, S., & Drowart, J. (1964). Mass-spectrometric determination of the dissociation energy of the molecules Sc2, Y2, La2, and YLa. J. Chem. Phys. 40, 239–241.
[5] Tamukong, P. K., Hoffmann, M. R., Li, Z., & Liu, W. (2014). Relativistic GVVPT2 Multireference perturbation theory Description of the electronic states of Y2 and Tc2. Journal of Physical Chemistry a 118, 1489–1501.
[6] Le Roy, R. J. (1973). Molecular Spectroscopy, Specialist Periodical Reports. R. F. Barrow, D. A. Loong, and D. J. Millen (eds). Vol. 1, Chapter 3. London: Royal Society of Chemistry, pp. 113–176.
[7] Kaplan, I. G. (2006). Intermolecular Interactions: Physical Picture, Computational Methods and Model Potentials. Chichester: Wiley.
[8] Nikitin, E. E., & Umanskii, S. Y. (1984). Theory of Slow Atomic Collisions. Berlin: Springer.
[9] Miranda, U. Unpublished results on the electronic structure of Y2. To be submitted this year.
[10] Desclaux, J. P. (1973). Relativistic Dirac-Fock expectation values for atoms with Z=1 to Z=120. Atomic Data and Nuclear Data Tables 12, 311–406.
[11] Bunge, C. F., & Barrientos, J. A. (1993). Roothaan-Hartree-Fock ground state atomic wave functions: Slater-type orbital expansions and expectation values for Z=2-54. Atomic Data and Nuclear Data Tables 53, 113–162.

FBG Sensors for Structural Health Monitoring of Road Infrastructure

Jānis Braunfelds[1,2], Jurģis Poriņš[1], Sandis Spolītis[1,2], Vjačeslavs Bobrovs[1]

[1] *Institute of Telecommunications, Riga Technical University, Latvia*
[2] *Communication Technologies Research Center, Riga Technical University, Latvia*
janis.braunfelds@rtu.lv, jurgis.porins@rtu.lv, sandis.spolitis@rtu.lv, vjaceslavs.bobrovs@rtu.lv

With every day, more and more new roads are being built all around the world. Due to different aspects like climate, season, weather changes, and high usage of transportation, as well as natural depreciation over time, lead to the need for reconstruction of older roads that are used on a daily basis. Knowing that the total population of humankind increases, and communication technological aspects develop rapidly, it is safe to say, that infrastructure for a physical connection between places will be needed further on, more than ever. From the previously said – to save resources, ensure public safety, and provide longer-lasting infrastructure, a structural health monitoring (SHM) application for roads should be researched and developed. Asphalt is one of the most used surface materials for the road building industry. This material also provides a relatively easy fiber optical sensor technology instalment, which can be effectively used for SHM applications – road infrastructure monitoring as well as for resource optimisation when road building or their repairs are planned [1–4]. FBG sensor technology, is one of the most promising and is widely used, mainly due to their significant advantages like passiveness, size, multiplexing ability, high sensitivity, remote sensing capabilities and resistance to electromagnetic interference, etc. [1, 3, 5, 6].

This paper focuses on the research of the optical (based on fiber Bragg grating (FBG) technology) strain and temperature sensor applications in road SHM. The integration of FBG strain and temperature sensors was realised into the road pavement in one of the largest Latvian road sites A2 (Riga–Sigulda) and A8 (Riga–Jelgava). We found the pavement structure in Latvia that is going to be built in the construction seasons of 2019–2020 and 2020–2021 for embedding (Fig. 1) of FBG sensors and measurements (Fig. 2). The research was realised in cooperation with SJSC "Latvian State Roads" and contracting companies "Binders" Ltd., JSC "ACB" which are performing the pavement reconstruction projects of the main roads A2 and A8.

Fig. 1. *FBG strain and temperature sensor integration into road pavement*

Fig. 2. *Real-time strain measurements by embedded FBG sensors*

Experiments and the measured results are very topical for local and international road pavement designers and road management service to forecast the collapsing of the road, permanent deformation, vehicular weight and the number of axles, traffic monitoring, and road pavement temperature monitoring.

Acknowledgments

This research was funded by the European Regional Development Fund (ERDF) industrial PhD research project No. 1.1.1.3/18/A/001 (PVS 3912.6.2), and the Doctoral Grant programme of Riga Technical University in Latvia.

We thank SJSC "Latvian State Roads", "Binders" Ltd., and JSC "ACB" for providing us access to the road infrastructure, support during experimental measurements, and valuable advice.

References

[1] Braunfelds, J., Senkans, U., Skels, P., Janeliukstis, R., Salgals, T., Redka, D., Lyashuk, I., Porins, J., Spolitis, S., Haritonovs, V., & Bobrovs, V. (2021). FBG-Based Sensing for Structural Health Monitoring of Road Infrastructure. Journal of Sensors, Article ID 8850368, pp. 1–11.

[2] Kara De Maeijer, P., Van den Bergh, W., & Vuye, C. (2018). Fiber Bragg Grating Sensors in Three Asphalt Pavement Layers. Infrastructures 3, 16.

[3] Li, K., & Xie, J. (2011). Experiment and Research of Using Fiber Bragg Grating to Monitor the Dynamic Response of Asphalt Concrete. Applied Mechanics and Materials 97–98, 301–304.

[4] Meng, L., Wang, L., Hou, Y., & Yan, G. (2017). a Research on Low Modulus Distributed Fiber Optical Sensor for Pavement Material Strain Monitoring. Sensors 17, 2386.

[5] Senkans, U., Braunfelds, J., Lyashuk, I., Porins, J., Spolitis, S., & Bobrovs, V. (2019). Research on FBG-Based Sensor Networks and Their Coexistence with Fiber Optical Transmission Systems. Journal of Sensors 2019, Article ID 6459387, pp. 1–13.

[6] Wang, H., Liu, W., He, J., Xing, X., Cao, D., Gao, X., Hao, X., Cheng, H., & Zhou, Z. (2014). Functionality Enhancement of Industrialized Optical Fiber Sensors and System Developed for Full-Scale Pavement Monitoring. Sensors 14, 8829-8850.

Universities and Sustainable Development

Dina Bērziņa

Institute of Atomic Physics and Spectroscopy, University of Latvia, Latvia
dina.berzina@lu.lv

The novel Framework Programme for Research and Innovation "Horizon Europe" calls for new objectives – contribution to tackling global challenges including the Sustainable Development Goals [1].

Tertiary education is recognising the value of prioritising sustainable development across all their activities. Currently there is a global consensus on the importance of the 17 domains identified by the United Nations Sustainable Development Goals (SDGs) [2] and the challenges mankind is facing in ensuring the well-being of the people and our planet. Solving of the urgent challenges the world is facing is provided by research-driven universities within the bounds of research and educational activities: university researchers are the ones coming up with expert advice to governmental officials by offering potential solutions, helping the media in explaining the complexity of the events happening, and engaging the general public around these issues, as well.

There are a great variety of university ranking lists: global [3–7], subject targeted [8–10], regional (derived from global rankings, e.g. [6, 7]) and national ones. THE Times Higher Education Impact Ranking [11] is the only one that assesses universities against the UN SDGs [2] and demonstrates a university's contribution to them.

The THE Impact ranking was first launched in 2019 and provides comparison across four areas: teaching (ensuring enough skilled practitioners to deliver on the SDGs), research (performing research on SDG relevant topics), outreach (collaboration with local, regional, national, and international communities), and stewardship (supervising of the physical resources) [11]. Any university that provides data on the SDG 17 (***partnerships for the goals*** – a university's contribution to the SDGs through collaboration with other countries, promotion of the best practices and publications) and at least three other SDGs, is included in the overall ranking. a university's final overall score is calculated by combining the SDG 17 score with the top three other scores. If the university does not submit data for the mandatory SDG17 or less than four SDGs in total, it is only assessed within the submitted criteria, but is not included in the overall ranking.

Universities' interest in the THE Impact ranking has more than doubled over the three years: the inaugural list in 2019 covered 467 universities which were assessed for only 11 of the 17 SDGs; the 2020 ranking included 768 institutions assessed for all the 17 SDGs; the last one of 2021 involves 1,117 institutions from 94 countries. Worth mentioning – since universities decide on their participation and the SDGs to be assessed voluntarily, the same university may not be participating for all three successive years and the same SDGs every year.

The overall ranking for the first time in 2021 is led by a UK university (University of Manchester), while the two previous years New Zealand dominated (University of Auckland). One can observe some territorial grouping around separate SDGs: Scandinavian universities traditionally are the best for 'quality of education – SDG4' (University of Gothenburg in 2019; Aalborg University in 2020–2021); 'climate action – SDG13' has proven to be the most successful for North American universities (University of British Columbia in 2019–2020, University at Buffalo in 2021); for 'affordable and clean energy – SDG7' winners come from south-east Asia (King Mongkut's University of Technology Thonburi in 2021, Tongji University in 2020; not included in the 2019 ranking).

Fig. 1. *Universities' contribution to the implementation of the SDGs in 2019–2021*

Fig. 1 reflects the performance of the institutions represented by the authors of this Abstract book which are included in the THE Impact ranking [11] (Lomonosov Moscow State University, Moscow Institute of Physics and Technology, Riga Technical University, Saint Petersburg Electrotechnical University, Saint Petersburg State University, University of Gothenburg, University of Latvia, University of Münster, Voronezh State University).

The survey is limited to seven entries: the overall score, the compulsory SDG 17 and five others freely chosen by the author of this paper: SDG 4 (***quality education*** **–** universities' contribution to early years and lifelong learning, pedagogical research and commitment to inclusive education), SDG 7 (***affordable and clean energy*** **–** energy use and policies, commitment to promoting of energy efficiency in the wider community), SDG 11 (***sustainable cities and communities*** **–** sustainability, the university's role in the preservation of arts and heritage, and internal approaches to sustainability), SDG 12 (***responsible consumption and production*** **–** responsible consumption and approach to sustainable use of the resources), and SDG 13 (***climate action*** **–** climate change, usage of energy and preparations for dealing with the consequences of climate change).

Since universities are not obligated to submit data for all the 17 SDGs and the participation for each of them over the years differs **–** data are presented in normalised values: merit close to 100 approves the university's high ranking for the particular SDG; rating between 20–40 reflects success below the average for the given SDG.

Due to the small set of samples and variable universities' participation, no particular trends can be determined in this overview. However, one can distinguish between universities running at the top every year and the ones with alternating success: Scandinavia represented by the University of Gothenburg is the top-runner for all three successive years; Latvian universities are in tough competition with changing leadership. Lomonosov Moscow State University performed well in 2019–2020 but has skipped the competition in 2021. Saint Petersburg Electrotechnical University being among the leaders for SDG 13 in 2019, has lost its high position later.

References

[1] Proposal for a Regulation of the European Parliament and of the Council establishing Horizon Europe **–** the Framework Programme for Research and Innovation, laying down its rules for participation and dissemination.

[2] UN Sustainable Development Goals (2015). https://sdgs.un.org/goals

[3] Aggregate Ranking of Top Universities. https://research.unsw.edu.au/artu/

[4] Academic Ranking of World Universities. http://www.shanghairanking.com/ARWU2020.html

[5] Center for World University Rankings 2019–2020. https://cwur.org/2020-21.php

[6] Quacquarelli Symonds World University rankings. https://www.topuniversities.com/university-rankings/world-university-rankings/2021

[7] The Times Higher Education World University Rankings 2021. https://www.timeshighereducation.com/world-university-rankings

[8] Reuters World's Top 100 Innovative Universities. https://www.reuters.com/innovative-universities-2019

[9] Round University Ranking. https://roundranking.com/ranking/subject-rankings.html#world-life-2020

[10] U-Multirank World University Ranking. https://www.umultirank.org/university-rankings/rankings-by-subject/

[11] Times Higher Education Impact Rankings. https://www.timeshighereducation.com/impact-rankings

Author Index